

1991

# Structure of Synthetic Oligosaccharides by Tandem Mass Spectrometry.

Eunsun Yoo Yoon

*Louisiana State University and Agricultural & Mechanical College*

Follow this and additional works at: [https://digitalcommons.lsu.edu/gradschool\\_disstheses](https://digitalcommons.lsu.edu/gradschool_disstheses)

## Recommended Citation

Yoon, Eunsun Yoo, "Structure of Synthetic Oligosaccharides by Tandem Mass Spectrometry." (1991). *LSU Historical Dissertations and Theses*. 5287.

[https://digitalcommons.lsu.edu/gradschool\\_disstheses/5287](https://digitalcommons.lsu.edu/gradschool_disstheses/5287)

This Dissertation is brought to you for free and open access by the Graduate School at LSU Digital Commons. It has been accepted for inclusion in LSU Historical Dissertations and Theses by an authorized administrator of LSU Digital Commons. For more information, please contact [gradetd@lsu.edu](mailto:gradetd@lsu.edu).

## **INFORMATION TO USERS**

**This manuscript has been reproduced from the microfilm master. UMI films the text directly from the original or copy submitted. Thus, some thesis and dissertation copies are in typewriter face, while others may be from any type of computer printer.**

**The quality of this reproduction is dependent upon the quality of the copy submitted. Broken or indistinct print, colored or poor quality illustrations and photographs, print bleedthrough, substandard margins, and improper alignment can adversely affect reproduction.**

**In the unlikely event that the author did not send UMI a complete manuscript and there are missing pages, these will be noted. Also, if unauthorized copyright material had to be removed, a note will indicate the deletion.**

**Oversize materials (e.g., maps, drawings, charts) are reproduced by sectioning the original, beginning at the upper left-hand corner and continuing from left to right in equal sections with small overlaps. Each original is also photographed in one exposure and is included in reduced form at the back of the book.**

**Photographs included in the original manuscript have been reproduced xerographically in this copy. Higher quality 6" x 9" black and white photographic prints are available for any photographs or illustrations appearing in this copy for an additional charge. Contact UMI directly to order.**

# **U·M·I**

University Microfilms International  
A Bell & Howell Information Company  
300 North Zeeb Road, Ann Arbor, MI 48106-1346 USA  
313/761-4700 800/521-0600

**Order Number 9219587**

**Structure of synthetic oligosaccharides by tandem mass  
spectrometry**

**Yoon, Eunsun Yoo, Ph.D.**

**The Louisiana State University and Agricultural and Mechanical Col., 1991**

**U·M·I**  
300 N. Zeeb Rd.  
Ann Arbor, MI 48106

**STRUCTURE OF SYNTHETIC OLIGOSACCHARIDES  
BY TANDEM MASS SPECTROMETRY**

**A Dissertation**

**Submitted to the Graduate Faculty of the  
Louisiana State University and  
Agricultural and Mechanical College  
in partial fulfillment of the  
requirements for the degree of  
Doctor of Philosophy**

**in**

**The Department of Biochemistry**

**by**

**Eunsun Yoo Yoon**

**B.S., Yonsei University, Seoul, Korea, 1983**

**M.S., Yonsei University, Seoul, Korea, 1985**

**December 1991**

## **Acknowledgements**

This work has been accomplished under the direction of Prof. Roger A. Laine, to whom I would like to express my appreciation for his guidance and continuous encouragement throughout its realization. I would also like to thank the members of my committee, Profs. E.S. Younathan, J.M. Jaynes, K.M. Morden, and R.J. Gale for reading and providing suggestions to make this work stronger. I would like to express my gratitude to Dr. A.D. French from whom I learned most of the computer calculations. Thanks are also due to Profs. Hindsgoul and Matta, whose original idea, handed to me by Prof. Laine, seeded part of this work. I would like to thank Betty Zhu, Otto Gildermeister, Shirish Dhume, Connie M. David and Jennifer Lo for helping and sharing with me their vast expertise. Thanks are also due to Thomas J. Maiher for assisting with mass spectrometry; and to Shirish Dhume for assisting with NMR spectroscopy. Also, many others, faculty, staff and students, go unnamed but not unappreciated. I would also like to thank my parents and family for their love and encouragement.

I would like to dedicate this work to my husband, Inmo Yoon, and my daughter, Suhyoung Yoon, for their love, encouragement, help and understanding which made this work possible.

## Foreword

This dissertation contains four chapters that develop tandem mass spectrometral methods to determine detailed linkage position of carbohydrate structure.

The "Introduction", as the first chapter, describes the background and objectives of this study.

The second chapter, "Non-Reducing Terminal Linkage Position Determination in Intact and Permethylated Synthetic Oligosaccharides Having a Penultimate Aminosugar: Fast Atom Bombardment Ionization, Collisional Induced Dissociation and Tandem Mass Spectrometry" was authored by Dr. Roger A. Laine, Ms. Eunsun Yoon, Mr. Thomas J. Mahier, Dr. Saeed Abbas, Mr. Brock de Lappe, Dr. Rakesh Jain, and Dr. Khushi Matta. The manuscript was submitted on May 3, 1991 and published in September 5, 1991 (*Biological Mass Spectrometry*, **20**, 505-514). In addition, some of the results reported in this chapter were presented at the 18th Annual Meeting of Society for Complex Carbohydrates in Ann Arbor, Michigan, during November 8-11, 1989 (Abstract # G155) and a revised version was presented at the Monsanto/ASMS Analytical Meeting in St. Louis, Missouri, during March 29-30, 1990. This chapter reports on the linkage determination of alkylated and permethylated synthetic trisaccharides using tandem mass spectrometry and molecular modeling.

The third chapter, "Enzyme-assisted Synthesis of four Novel Trisaccharides: Gal<sub>p</sub>(β1->4)Glu<sub>p</sub>(X)Glu where X=β1->3: β1->4: β1->6: α1->4" will be submitted for publication to Carbohydrate Research and also to Office of Technology Transfer, LSU, for obtaining a patent for the synthetic method and product trisaccharides. Also, part of the results reported in this and the following chapter were presented at the 11<sup>th</sup> International Symposium on Glycoconjugates

meeting in Toronto, Canada, June 30 - July 5, 1991 (Abstract # 14.40, Glycoconjugate Journal 8, 259, 1991). This chapter describes the synthesis of a set of trisaccharides by enzyme- assistance.

The fourth chapter, "Linkage Position Determination of Permethylated Neutral Novel trisaccharides by Collisional Induced Dissociation and Tandem Mass Spectrometry" will be submitted for publication to Biological Mass Spectrometry. This chapter reports on linkage determination of permethylated neutral synthetic trisaccharides using tandem mass spectrometry and molecular modeling.

Finally, an Appendix includes the Permethylation method of Ciucanu and Kerek and the Experimental procedure of MM2 calculation.

## Table of Contents

	page
<b>Acknowledgements</b> .....	ii
<b>Foreword</b> .....	iii
<b>List of Tables</b> .....	vii
<b>List of Figures</b> .....	viii
<b>Abbreviations</b> .....	xi
<b>Abstract</b> .....	xii
 <b>Chapter</b>	
<b>I Introduction</b> .....	1
Background: Structural Elucidation of Carbohydrates .....	1
Mass Spectrometry: A Tool for Structure Studies of Carbohydrate.....	4
Molecular Modeling and Energy Minimization.....	8
Synthesis of Carbohydrate Using an Enzyme.....	10
Objectives of This Study.....	11
References.....	12
<b>II Non-Reducing Terminal Linkage Position Determination in Intact and Permethylated Synthetic Oligosaccharides Having a Penultimate Aminosugar: Fast Atom Bombardment Ionization, Collisional Induced Dissociation and Tandem Mass Spectrometry</b> .....	14
Copyright.....	15
Abstract.....	16
Introduction.....	16
Experiment.....	19
Results and Discussion.....	20
Supplementary Material.....	39
References.....	40



<b>III Enzyme-assisted Synthesis of Four Novel Trisaccharides:</b>	
<b>Gal<sub>p</sub>(β1→4)Glu<sub>p</sub>(X)Glu where X=β1→3: β1→4: β1→6:</b>	
α1→4 .....	42
Introduction.....	42
Experimental.....	44
Results and Discussion.....	46
References.....	74
<b>IV Linkage Position Determination of Permethylated</b>	
<b>Neutral Novel Trisaccharides by Collisional Induced</b>	
<b>Dissociation and Tandem Mass Spectrometry .....</b>	<b>77</b>
Introduction.....	77
Experimental.....	79
Results and Discussion.....	80
References.....	90
<b>Future Work.....</b>	<b>92</b>
<b>Appendix.....</b>	<b>95</b>
Permethylation Method of Ciucanu and Kerek.....	95
Experimental Procedure of MM2 calculation .....	96
References.....	97
<b>Vita.....</b>	<b>98</b>

## List of tables

	page
Table 3.1 $^1\text{H}$ chemical shift (ppm) of synthetic trisaccharides, G4 (gal $\beta$ 1-4glu $\beta$ 1-4glu), G $\alpha$ 4 (gal $\beta$ 1-4glu $\alpha$ 1-4glu), G6 (gal $\beta$ 1-4glu $\beta$ 1-6glu), and G3(gal $\beta$ 1-4glu $\beta$ 1-3glu).....	66
Table 3.2 Vicinal $^1\text{H}$ coupling constants ( $J_{1,2}$ Hz) and integration intensities of synthetic trisaccharides.....	67

## List of Figures

	page
Figure 1.1 Schematic Representation of a FAB source.....	5
Figure 1.2 Schematic representation of three quadrupole rod assemblies in the TSQ70.....	7
Figure 1.3 The constitution of disaccharide, glu $\beta$ 1 $\rightarrow$ 4 glu, giving atom numbering and the torsional angles phi and psi.....	9
Figure 2.1 CAD experiments on $[M+K]^+=582$ at $-60\text{eV}$ @ $0.8\text{mTorr}$ argon gas. (F3 upper spectra, F4 middle spectra, or F6 lower spectra).....	21
Figure 2.2 CAD experiments on $[M+Li]^+=550$ at $-40\text{eV}$ @ $0.8\text{mTorr}$ argon gas. (F3 upper spectra, F4 middle spectra, or F6 lower spectra).....	23
Figure 2.3 CAD experiments on $[M+NH_4]^+=544$ at $-20\text{eV}$ @ $0.8\text{mTorr}$ argon gas. (F3 upper spectra, F4 middle spectra, or F6 lower spectra).....	24
Figure 2.4 FAB-MS-CAD-MS spectra of $m/z$ 670 for methylated L-fucosyl-( $\alpha$ 1-X)- D-N-acetylglucosaminyl-( $\beta$ 1-3)-galactosyl-( $\beta$ 1-O-methyl) at $-10\text{eV}$ where X=3 (A), 4(B), or 6(C).....	26
Figure 2.5 FAB-MS-CAD-MS spectra of $m/z$ 670 for methylated L-fucosyl-( $\alpha$ 1-X)- D-N-acetylglucosaminyl-( $\beta$ 1-3)-galactosyl-( $\beta$ 1-O-methyl) at $-60\text{eV}$ where X=3 (A), 4(B), or 6(C).....	27
Figure 2.6 FAB-MS-CAD-MS spectra of $m/z$ 700 for methylated Galactosyl-( $\beta$ 1-X)- D-N-acetylglucosaminyl-( $\beta$ 1-3)-galactosyl-( $\beta$ 1-O-methyl) at $-10\text{eV}$ where X=3 (A), 4(B), or 6(C).....	31
Figure 2.7 FAB-MS-CAD-MS spectra of $m/z$ 700 for methylated Galactosyl-( $\beta$ 1-X)- D-N-acetylglucosaminyl-( $\beta$ 1-3)-galactosyl-( $\beta$ 1-O-methyl) at $-60\text{eV}$ where X=3 (A), 4(B), or 6(C).....	32
Figure 2.8 Plot of collision offset vs. ion ratio in methylated FX: $m/z$ $(228+246+402)/670$ .....	34
Figure 2.9 Plot of collision offset vs. ion ratio in methylated GX: $m/z$ $(228+246+464)/700$ .....	35

	page
Figure 2.10 The phi and psi plots of the total energies and energy wells derived from the MM2(85) calculation. (The drawings were made with the SURF program of SURFER from Golden software).....	37
Figure 2.11 CAD experiments on $[M+Na]^+=566$ at $-40\text{eV}$ @ $0.8\text{mTorr}$ argon gas. (F3 upper spectra, F4 middle spectra, or F6 lower spectra).....	39
Figure 3.1 Thin-layer chromatography of synthesized trisaccharide, G4 (gal $\beta$ 1-4glu $\beta$ 1-4glu).....	48
Figure 3.2 Thin-layer chromatography of synthesized trisaccharide, G3 (gal $\beta$ 1-4glu $\beta$ 1-3glu).....	49
Figure 3.3 Thin-layer chromatography of synthesized trisaccharide, G6 (gal $\beta$ 1-4glu $\beta$ 1-6glu).....	50
Figure 3.4 Thin-layer chromatography of synthesized trisaccharide, G $\alpha$ 4 (gal $\beta$ 1-4glu $\alpha$ 1-4glu).....	51
Figure 3.5 Purification of synthesized trisaccharide, G4 (gal $\beta$ 1-4glu $\beta$ 1-4glu).....	53
Figure 3.6 Purification of synthesized trisaccharide, G3 (gal $\beta$ 1-4glu $\beta$ 1-3glu).....	54
Figure 3.7 Purification of synthesized trisaccharide, G6 (gal $\beta$ 1-4glu $\beta$ 1-6glu).....	55
Figure 3.8 Purification of synthesized trisaccharide, G $\alpha$ 4 (gal $\beta$ 1-4glu $\alpha$ 1-4glu).....	56
Figure 3.9 FAB MS spectra of permethylated Gal <sub>p</sub> ( $\beta$ 1-4)Glu <sub>p</sub> ( $\beta$ 1-X)Glu <sub>p</sub> where X=3(A), 4(B), or 6(C).....	57
Figure 3.10 TOF spectra of permethylated Gal <sub>p</sub> ( $\beta$ 1-4)Glu <sub>p</sub> ( $\beta$ 1-X)Glu <sub>p</sub> where X=3(A), 4(B), or 6(C).....	58
Figure 3.11 1-D $^1\text{H-NMR}$ spectra of Gal <sub>p</sub> ( $\beta$ 1-4)Glu <sub>p</sub> ( $\beta$ 1-4)Glu <sub>p</sub> at 323 K (top) and 298 K (bottom).....	61
Figure 3.12 A) Expansion of the 1-D $^1\text{NMR}$ spectrum and B) 2-D COSY $^1\text{H-NMR}$ spectrum of Gal <sub>p</sub> ( $\beta$ 1-4)Glu <sub>p</sub> ( $\beta$ 1-4)Glu <sub>p</sub> at 298 K.....	62
Figure 3.13 A) Expansion of the 1-D $^1\text{NMR}$ spectrum and B) 2-D COSY $^1\text{H-NMR}$ spectrum of Gal <sub>p</sub> ( $\beta$ 1-4)Glu <sub>p</sub> ( $\alpha$ 1-4)Glu <sub>p</sub> at 298 K.....	63

Figure 3.14 A) Expansion of the 1-D $^1\text{H-NMR}$ spectrum and B) 2-D COSY $^1\text{H-NMR}$ spectrum of $\text{Gal}_p(\beta 1-4)\text{Glu}_p(\beta 1-6)\text{Glu}_p$ at 298 K.....	64
Figure 3.15 A) Expansion of the 1-D $^1\text{H-NMR}$ spectrum and B) 2-D COSY $^1\text{H-NMR}$ spectrum of $\text{Gal}_p(\beta 1-4)\text{Glu}_p(\beta 1-3)\text{Glu}_p$ at 298 K.....	65
Figure 3.16 1-D NOE $^1\text{H-NMR}$ spectrum of $\text{Gal}_p(\beta 1-4)\text{Glu}_p(\beta 1-4)\text{Glu}_p$ at 298K..	69
Figure 3.17 1-D NOE $^1\text{H-NMR}$ spectrum of $\text{Gal}_p(\beta 1-4)\text{Glu}_p(\alpha 1-4)\text{Glu}_p$ at 298K..	70
Figure 3.18 1-D NOE $^1\text{H-NMR}$ spectrum of $\text{Gal}_p(\beta 1-4)\text{Glu}_p(\beta 1-6)\text{Glu}_p$ at 298K..	71
Figure 3.19 2-D NOESY $^1\text{H-NMR}$ spectrum of $\text{Gal}_p(\beta 1-4)\text{Glu}_p(\beta 1-3)\text{Glu}_p$ at 298K.....	72
Figure 4.1 FAB-MS-CAD-MS spectra of $m/z$ 659 for permethylated $\text{Gal}_p(\beta 1-4)\text{Glu}_p(\beta 1-X)\text{Glu}_p$ at -20eV where X=3 (A), 4(B), or 6(C)....	82
Figure 4.2 FAB-MS-CAD-MS spectra of $m/z$ 659 for permethylated $\text{Gal}_p(\beta 1-4)\text{Glu}_p(\beta 1-X)\text{Glu}_p$ at -40eV where X=3 (A), 4(B), or 6(C)....	83
Figure 4.3 Plot of collision offset vs. ion ratio in $\text{Gal}_p(\beta 1-4)\text{Glu}_p(\beta 1-X)\text{Glu}_p$ where X=3 (A), 4(B), or 6(C): $m/z$ (219+423+455)/659.....	86
Figure 4.4 The phi and psi plots of the total energies and energy wells derived from the MM2(87) calculation of permethylated $\text{Gal}_p(\beta 1-4)\text{Glu}_p(\beta 1-X)\text{Glu}_p$ where X=3 (A), 4(B), or 6(C).....	88

## Abbreviations

CAD	Collision Activated Dissociation
CI	Chemical Ionization mode of MS
COSY	Homonuclear Chemical Shift Correlated Spectrometry
EI	Electron Impact mode of MS
FAB	Fast Atom Bombardment mode of MS
FAB MS	Fast Atom Bombardment Mass Spectrometry
FAB MS/MS	Fast Atom Bombardment Tandem Mass Spectrometry
FAB MS-CID-MS	Fast Atom Bombardment-Collision- induced dissociation-Tandem mass spectrometry
GC/MS	Gas Chromatography combined with Mass Spectrometry
GlcNAc	N-acetylglucosamine
MM2	Molecular Mechanics Program 2
NMR	Nuclear Magnetic Resonance
NOE	Nuclear Overhauser Effect
X=3	1,3 linkage
X=4	1,4 linkage
X=6	1,6 linkage

## **Abstract**

Certain linkage positions in oligosaccharides can be discerned by collision-activated dissociation mass spectrometry (MS-CID-MS), rationalized by molecular modeling.

The first part of this dissertation shows that linkage-specific daughter ion spectra of synthetic amino- sugar containing oligosaccharides can be obtained from several alkylated derivatives such as sodiated, potassiated, ammoniated and lithiated derivatives. Methylated derivatives of the synthetic oligosaccharides give more useful linkage discernment product-ions, including a 3-linkage specific ion. A novel approach of relating daughter ion to parent ion ratios and collision energy is described and is predictive of linkage position in the first set of six oligosaccharides used.

In the second part, a set of trisaccharides differing only in linkage position was synthesized by enzyme assistance, reducing the time and labor. For development of tandem mass spectral methods of direct linkage determination in oligosaccharides, a set of trisaccharides differing only in one structural parameter, in this case position of linkage to the reducing-end hexose, were required. These sets of compounds would also be useful for development of high resolution separation techniques geared to resolve linkage types. Conventional organic synthesis of such a set could take as long as 2-5 months for each member of the set. Each trisaccharide would require 10-20 steps of synthesis. Instead, this dissertation utilized the loose acceptor specificity of bovine milk galactosyl transferase (lactose synthase: EC 2.4.1.22) to generate several micromoles of oligosaccharides for NMR and mass spectral studies.

Finally, the linkage positions of four novel synthetic trisaccharides were studied using low energy collision-induced-dissociation tandem mass spectrometry (FAB-MS-CID-MS) and molecular modeling. These results confirmed that the FAB-MS-CID-MS combined with molecular modeling can be used to identify the sugar linkage positions in neutral sugars as well as aminosugar- containing oligosaccharides.



## Chapter I Introduction

### Background: Structural Elucidation of Carbohydrates

Naturally occurring oligosaccharides have attracted considerable attention among scientists in the last few years, due to discovery of their biological activities. The carbohydrates possess a great variety of important biological functions, including roles as ant clotting agents, immunomodulators, tumor antigens, growth factors, genetic control elements, and so on [1.1-1.5].

Biochemists, medical scientists, and food scientists are very interested in the role of these oligosaccharides in health and nutrition. For the biotechnologists and chemists, interest arose from the desire to understand the structures of oligosaccharides as major factor which affects their biological active functions.

Both the structural elucidation and the synthesis of carbohydrates are difficult because of the complex structure. There is a very large number of possible structures for simple saccharides which have the same mass. The simplest formula for possible structures  $S^*$  for an oligosaccharide which consists of a number  $N$  of different hexoses not repeated is as follows for linear structures of one enantiomer.

$$S^* = N! \times 2_a^N \times 4^{N-1} \times 2_r^N$$

where  $N$  is the number of different hexoses,  $N!$  is the sugar epimer order,  $2_a^N$  is the anomeric configuration,  $4^{N-1}$  is the position of linkage, and  $2_r^N$  is the ring size.

For a linear string of three hexoses, the above calculation gives 6144 chemically different structures ( $S^* = 3! \times 2^3 \times 4^2 \times 2^3 = 6144$ ). Considering the branching, repeated sugars, and D and L enantiomer factors, this number enlarges greatly, producing several thousand structures. These structures not only have the same mass but also share many physical properties. It is well known that a relatively small structural change has not been ignored in the evolution of biological systems.

Especially, a variety of the glycoconjugates having an L-fucopyranosyl group  $\alpha 1 \rightarrow 3$  linked or galactopyranosyl group  $\beta 1 \rightarrow 4$  linked to a  $\beta$ -GlcNAc(N-acetyl glucosamine) glycopyranosyl residue have been reported as tumor-associated antigens [1.6]. Madiyalakan, R. *et al.* reported that only the  $1 \rightarrow 3$  linkage is related to the human cancers [1.7]. The other linkages such as the  $1 \rightarrow 4$  or  $1 \rightarrow 6$  linkage, which are found from the blood, intestine, and some normal tissues, are not related to the cancers. Although carbohydrates have been investigated for many decades, there is no comprehensive and sensitive methodology to determine all the structural parameters of carbohydrates. Structural studies of oligosaccharides have relied mainly on mass spectrometry and NMR spectrometry to elucidate one or several structural parameters.

Up till now, the methylation analysis with GC/MS [1.8] or FAB [1.9] has been used despite the tedious multi-step chemical preparation or minimal level of information. Recently, tandem mass spectrometry (MS/MS) has been applied to this field with some success [1.10].

This dissertation introduces the simplified method to determine linkage position using FAB MS/MS combined with molecular modeling. Also, a faster way for synthesis of a series of trisaccharides is reported. This time-saving, enzyme-assisted synthetic method of linkage-isomeric trisaccharides will greatly accelerate the structural studies of carbohydrates.

Reason for choosing trisaccharides as the samples:

Trisaccharides, having a reducing end, a non-reducing end and an internal monosaccharide moiety, offer minimum units to study differences between internal linkages in a linear chain of sugars. Later, this study will be extended to larger

saccharides. Low energy tandem, collision-induced dissociation mass spectrometry can be performed on compounds up to  $m/z$  2000. This limit can cover hexasaccharides to octasaccharides.

#### Biological relevance of chosen samples:

The compounds chosen for the first part of this dissertation were related to terminal groups likely to be found on polylactosamine-like glycoproteins and glycolipids which occur on the surface of mammalian cells. The samples with structures L-Fucosyl( $\alpha$ 1- $\rightarrow$ X)D- GlcNAc( $\beta$ 1- $\rightarrow$ 3)D-Galactose (FX) where X=3 and 4 have been found in nature. The series of D-Galactosyl( $\beta$ 1- $\rightarrow$ X)D- GlcNAc( $\beta$ 1- $\rightarrow$ 3)D-Galactose (GX) where X=3, 4 and 6 are also possible internal or terminal structures on mammalian glycolipids and glycoproteins [1.11, 1.12].

The second series (GX) chosen for neutral sugar sets of compounds use naturally occurring plant-derived disaccharides as starting materials, adding a sugar to the reducing end. The second set of compounds have not been found as yet. They consist of partly natural and partly undiscovered structures, related to the hemicelluloses and other cell wall components in plants [1.11, 1.12].

#### Derivatization

Several derivatives have been used to induce modification of fragmentation behavior in mass spectrometry and thereby distinguish linkage-isomeric trisaccharides. The careful choice of derivatization conditions allows labile modifying groups to be retained in their original positions.

#### Alkylation:

Several cation derivatives (Na, K, Li, and  $\text{NH}_4$ ) were tried to better understand differences in fragmentation and stability of ions when alkali metals replace hydrogen in the cationic precursors. The alkali metal ions have been proposed to

interact selectively with polar functional groups promoting local decomposition [1.13, 1.14]. The CAD spectra of the alkali adducts of sucrose [1.15] and other oligosaccharides [1.13], peptides [1.16] and nucleotides [1.17] have recently been reported to give information which is different from that obtained with the protonated ion.

#### Permethylation:

FAB MS can be used on underivatized oligosaccharides, but very little fragmentation is seen [1.18]. Proper derivatization increases the hydrophobicity [1.19] and bulkiness around the glycosidic bonds [1.20, 1.21] and enhances the FAB response. Thus, permethylation can be used to improve sensitivity and can direct the fragmentation along pathways that maximize spectral information content. Derivatives are especially important with respect to isomer distinction requiring modified fragmentation behavior.

#### **Mass Spectrometry: A Tool for Structure Studies of Carbohydrate**

Mass spectrometry provides a unique method for investigation of the type, number of sugar constituents, sequence, and sugar composition by molecular ions as well as key fragments [1.22, 1.23].

#### FAB:

FAB ionization is the most useful technique for nonvolatile and nonpolar compounds such as oligosaccharides and their derivatives [1.22]. In the FAB experiment (Fig. 1.1), an accelerated beam of atoms is fired from the gun towards the target, which has been preloaded with a liquid matrix containing the sample to be analyzed. When the atom beam collides with the matrix, kinetic energy is transferred to the surface molecules, many of which are sputtered out of the liquid

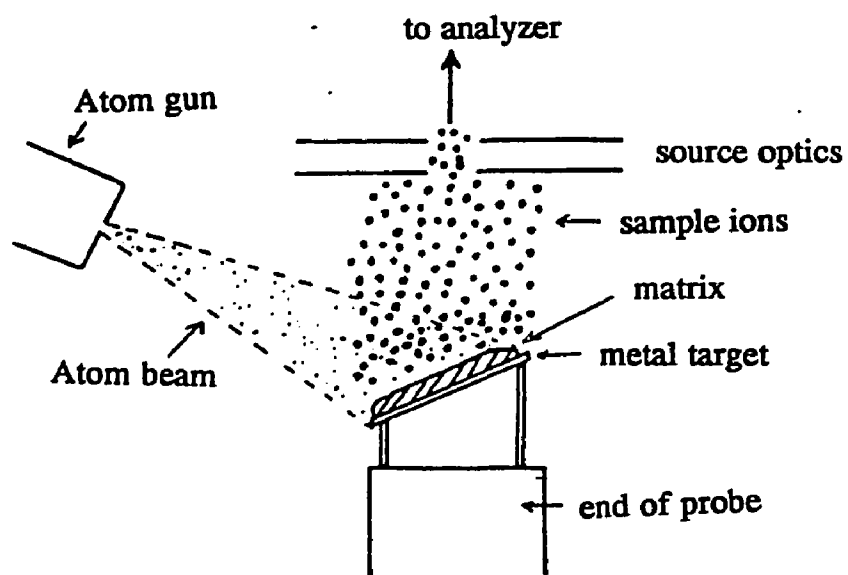


Fig. 1.1. Schematic Representation of a FAB source.

into the high vacuum of the ion source. A significant number of these molecules are ionized during the sputtering process. Thus, gas-phase ions are generated without prior volatilization of the sample [1.24]. FAB MS gives molecular ions as well as major fragments and thus generates useful structural information.

#### FAB MS/MS:

The FAB MS/MS is a more sophisticated analytical technique that involves two stages of mass analysis (Fig. 1.2). In the first stage, the ions formed in the ion source are analyzed by the first analyzer (Q1). The ions obtained from Q1 are called *parent ions*. These ions are exactly the same as those obtained from FAB MS. In the second stage, ions that have interesting mass are selected from the parent ions. These mass-selected ions are activated by collision with a neutral gas (Q2) and the resultant ionic fragments are mass analyzed by the second analyzer (Q3). The final ions are called *daughter ions* [1.25].

FAB MS/MS was used to elucidate the carbohydrate structure due to the ability to dissociate the carbohydrates into constituent building blocks upon collisional activation. This feature is probably because the bonds between the building blocks are the weakest chemically. The ions from FAB MS/MS have entirely originated from the mass-selected ions. Therefore, FAB MS/MS data can be used to reconstruct the original structure and to distinguish between linkage positions of saccharides.

The MS/MS spectra were simplified by selecting a single molecular ion or fragment ion in the analysis of mixtures, and interference by background signals from the liquid matrix could be avoided.

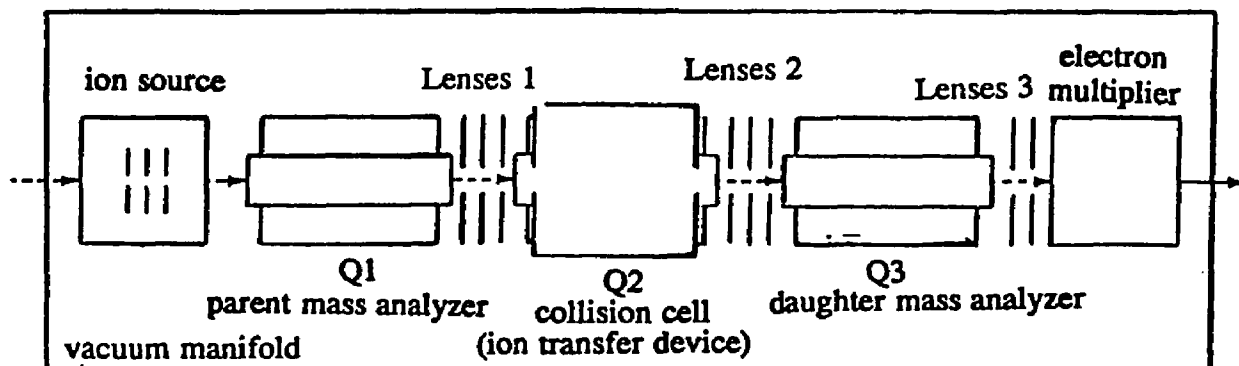


**Fig. 1.2. Schematic representation of three quadrupole rod assemblies in the TSQ70.** The collision offset can be changed by changing the negative voltage on Lenses 2. As negative voltage increases, the positively charged ions generated in ion source are accelerated. In Q2 (collision cell), the accelerated ions collide with neutral gas to produce fragments.

## **Molecular Modeling and Energy Minimization**

The molecular modeling study is used to rationalize the observed FAB MS/MS fragmentation ratios. The hypothesis of combining FAB MS/MS with molecular modeling is as follows: Threshold energies imparted to oligosaccharide ions in collision cells of tandem mass spectrometers may give different patterns of fragmentation based on the differential ability of isomers to absorb and dissipate vibrational energy. Linkage position, among other structural parameters of a carbohydrate, may be the most sensitive to variance in vibrational freedom, particularly rotation, due to the different steric hindrance and degrees of freedom of motion between sugars.

### Nomenclature

The constitution of disaccharide, glu  $\beta$ 1- $\rightarrow$ 4 glu, giving atom numbering and the torsional angles phi and psi, are shown in Fig. 1.3. Phi and psi are defined by atoms H1'-C1'-O4-C4 and H4-C4-O4-C1', respectively. The definition of a torsional angle follows the IUPAC convention [1.26].

### MM2

The computer program used herein, MM2, is one of the molecular mechanics programs that optimize the atomic coordinates of a molecule to produce a structure at a local minimum on a multidimensional hypersurface of potential energy [1.27, 1.28]. It includes potentials for bond stretching, bending, and stretch-bending, 3-fold torsional potentials, van der Waals interactions, and dipole-dipole interactions [1.29]. The program MM2 (87) was chosen for this work for the following reasons:

First, a carbohydrate has a number of possible ring conformers such as  ${}^4C_1$ ,  ${}^1C_4$ ,  ${}^1S_5$ , etc [1.30] that the MM2 program can alter to a low energy form for a



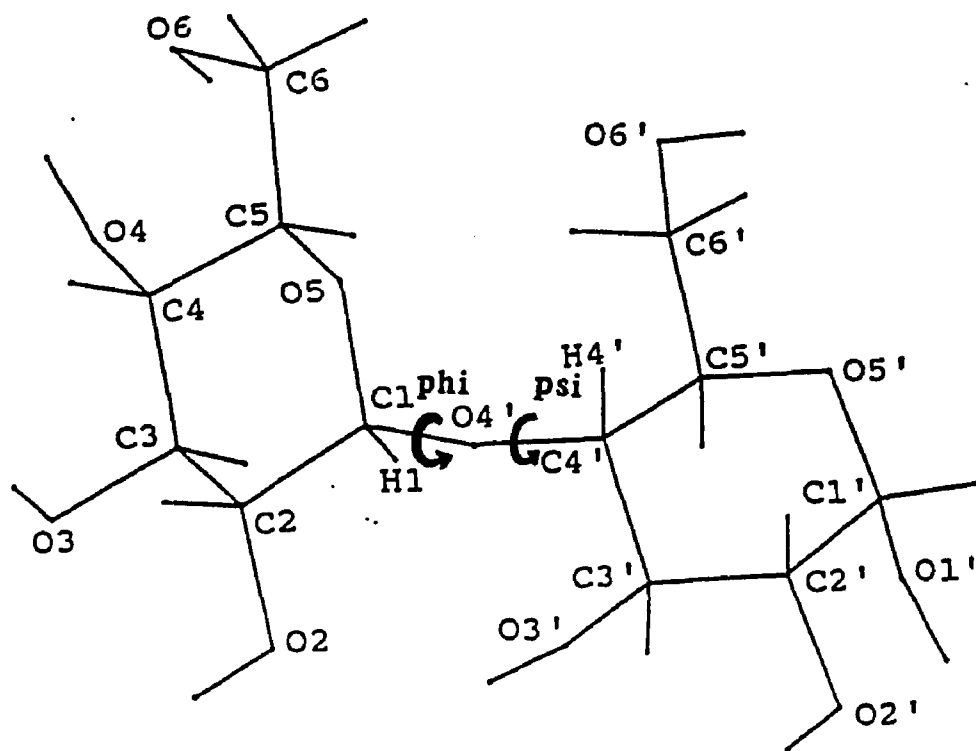


Fig. 1.3. The constitution of disaccharide, glu  $\beta$ 1->4 glu, giving atom numbering and the torsional angles phi and psi. Phi and psi are defined by atoms H1-C1-O4'-C4' and H4'-C4'-O4'-C1, respectively.

particular saccharide shape. Second, the MM2(87) version, automatically provides the anomeric effects that are important for sugars. Also, the lone pairs are treated as if they are atoms because MM2 requires lone pairs of electrons on all ether and hydroxyl oxygen atoms to fit the data on alcohols and ethers which are major components of carbohydrates. Finally, this version (87) has a "dihedral driver" facility which accepts the initial, final, and increment size values of two torsional angles and energy-minimization at each increment of these torsion angles. This permits conformational analysis of a disaccharide by rotating the glycosidic bond.

MM2 (87) was further modified by A.D. French [1.31] to contain a rigid dihedral driver option that starts with the same intra-residue geometry at each increment of the driven torsion angles. This avoids the propagation of residue distortions from one conformation to the next.

The MM2 calculations have previously produced results in good accord with the conformational properties of oligosaccharides in solution as reflected from NMR data [1.30-1.32].

### **Synthesis of Carbohydrate Using an Enzyme**

Carbohydrates have inherently complicated structures for which there is no comprehensive high sensitivity analytical methodology available. Furthermore, the biosciences are increasingly confronted with minute amounts of this material which can only be obtained from natural or biological systems.

Methods for the syntheses of such structures in amounts sufficient for study are important. Chemical syntheses require multi-step procedures [1.32]. It would not be possible to examine all of the carbohydrate structural parameters by the combined use of synthetic oligosaccharide sets and analytical methods such as mass

spectrometry and NMR. The organic synthesis of sets of carbohydrates differing in only one parameter is time consuming, labor intensive and difficult.

This dissertation introduces the faster synthetic method of linkage-isomeric trisaccharides using altered reaction condition to induce a loose acceptor specificity for bovine milk galactosyl transferase (lactose synthase: EC 2.4.1.22).

The advantage of this method is that milligrams of trisaccharides can be synthesized within 4-5 days using EC 2.4.1.22 without complicated blocking, coupling, and unblocking steps. The use of an enzyme facilitates synthesis of oligosaccharides with a minimum of reaction steps. Also, syntheses with enzymes are advantages because of their stereospecificity and regioselectivity.

#### **Objectives of This Study**

The purpose of this research is to develop tandem mass spectrometral methods to determine detailed carbohydrate structure on cationized and derivatized oligosaccharides for future applications on biologically active glycoconjugates and to exploit the faster synthetic method to make a series of structural isomeric oligosaccharides for further mass spectrometry and NMR study.

## References

- 1.1 S. Dube, J.W. Fisher and J.S.Powell, *J.B.C.* **263**, 17516 (1988).
- 1.2 J.J. Feige and A. Baird, *J.B.C.* **263**, 14023 (1988).
- 1.3 C.A. Wilson, A.J. Leigh and A.J. Chapman, *J. Endocrinol.* **125**, 3 (1990).
- 1.4 K.B.Lee, D. Loganathan, Z.M. Merchant and R.J. Linhardt, *Appl. Biochem. Biotechnol.* **23**, 53 (1990).
- 1.5 M. Tsujisaki, K. Imai, S. Tokuchi, Y. Hanzawa, T. Ishida, H. Kitagawa, Y. Hinoda and A. Yachi, *Cancer Res.***51**, 2599 (1991).
- 1.6 K.J. Rakesh et al. *Carbohydr. Res.* **17**, 27 (1988).
- 1.7 R. Madiyalakan et al. *Carbohydr. Res.* **152**, 22 (1986).
- 1.8 B. Lindberg and J. Lonngren, *Methods in Enzymology* **50**, 3 (1978).
- 1.9 H. Egge and J. Peter-Katalinic J., *Mass Spectrometry Review* **6**, 331 (1987).
- 1.10 S.A. Carr, V.N. Reinhold, B.N. Green and Hass *Biomed. Mass Spectrom.* **12**, 288 (1985).
- 1.11 C.C. Sweeley and N.A. Nunez, *Annu. Rev. Biochem.* **54**, 756 (1985).
- 1.12 K. Kobata, K. Yamashita and S. Takasaki, *Methods in Enzymol.* **138**, 884 (1987)
- 1.13 R. Orlando, C.A. Bush and C.Fenselau (1990) *Biomedical and Environmental Mass Spectrometry*, **19**, 747.
- 1.14 J. Adams and M.L. Gross *J. Am. Chem. Soc.* **108**, 6915 (1986).
- 1.15 R.L. Cerney, K.B. Tomer and M.L. Gross *Org. Mass Spectrometry*, **21**, 655 (1986).
- 1.16 L.M. Mallis and D.H. Russell *Anal. Chem.*, **58**, 1076 (1986).
- 1.17 M.L. Gross, K.B. Tomer, R.L. Cerny, and D.E. Gilbin in *Mass Spectrometry In the Analysis of Large Molecules.* ed. by McNeal C.J. (1986) Wiley, New York, 171.
- 1.18 A. Angel, F. Lindh and B. Nilsson, *Carbohydrate Res.* **168**, 15 (1987).
- 1.19 B.M. Domon, D.R. Mueller, and W.J. Richter, *Biomed. Environ. Mass Spectrom.* **19**, 390 (1990).

- 1.20 R.A. Laine, K.M. Pamidimukkala, A.D. French, R.W. Hall, S.A. Abbas, R.K. Jain, and K.L. Matta, *J. Am. Chem. Soc.* **110**, 6931 (1988).
- 1.21 R.A. Laine, E. Yoon, T.J. Mahier, S.A. Abbas, B. de Lappe, R.K. Jain, and K.L. Matta, *Biological Mass Spectrometry*, **20**, 505 (1991).
- 1.22 R.A. Laine, *Methods in Enzymol.* **179**, 157 (1989).
- 1.23 H. Egge, and J. Peter-Katalinic, *Mass Spectrometry Review* **6**, 331 (1987).
- 1.24 A. Dell *Adv. Carbohydr. Chem. Biochem.* **45**, 19 (1987).
- 1.25 TSQ 70 Operator's manual, Finnigan Mat, San Jose, CA (1986).
- 1.26 IUPAC Tentative Rules for the Nomenclature of Organic Chemistry, *Eur. J. Biochem.* **18** 151 (1971).
- 1.27 T. Clark, *A Handbook of Computational Chemistry: A Practical Guide to Chemical Structure and Energy Calculations.* 12-92, John Wiley & Sons (1985).
- 1.28 U. Burkert and N.L. Allinger, *Molecular Mechanics.* 23-50, American Chemical Society, Washington D.C. (1982).
- 1.29 J.-H. Lii and N.L. Allinger, MM2 Program (QCPE 543), University of Georgia (1987).
- 1.30 A.D French, V.H. Tran and S. Perez, *Computer Modeling Carbohydrate Molecules*, 191-212, (ed. by A.D. French and J.W. Brady), American Chemical Society, Washington D.C. (1989).
- 1.31 A.D French, *Carbohydr. Res.* **188** 206 (1989).
- 1.32 A.D. French, *Biopolymer*, **27** 1519 (1988).
- 1.33 H. Paulson, *Chem. Soc. Rev.* **13** 15 (1984).

## Chapter II.

### **Non-Reducing Terminal Linkage Position Determination in Intact and Permethylated Synthetic Oligosaccharides Having a Penultimate Aminosugar: Fast Atom Bombardment Ionization, Collisional Induced Dissociation and Tandem Mass Spectrometry.**

Roger A. Laine\*<sup>@+</sup>, Eunsun Yoon\*, Thomas J. Mahier\*  
Departments of \*Biochemistry and @Chemistry  
Louisiana State University  
and  
The LSU Agricultural Center  
Baton Rouge, LA 70803

Saeed Abbas, Brock de Lappe#  
#Glycomed Inc.  
860 Atlantic Avenue  
Alameda, CA 94501

Rakesh Jain% and Khushi Matta%,  
%Department of Obstetrics and Gynecology,  
Roswell Park Memorial Institute  
666 Elm Street  
Buffalo, New York 14263.

+ Author to whom correspondence should be addressed.

\* This work was supported, in part, by NIH Grants R1DK33755 and R1GM32594 to R.A.L. and Grant No. 35329 and CH419 to K.M..

Published in Biol. Mass Spec.20, 505-514 (1991).



Department of Biochemistry  
 LOUISIANA STATE UNIVERSITY AND AGRICULTURAL AND MECHANICAL COLLEGE  
 BATON ROUGE • LOUISIANA 70803-1806

(504) 388-1556  
 FAX # (504) 388-5321

October 8, 1991

14 OCT 1991

Copyright Administrator  
 John Wiley & Sons Limited  
 Baffins Lane, Chichester  
 Sussex PO19 1UD  
 England

Dear Sir:

I am writing to you in reference to the article "Non-reducing Terminal Linkage Position Determination in Intact and Permethylated Synthetic Oligosaccharides Having a Penultimate Amino Sugar: Fast Atom Bombardment Ionization, Collisional-induced Dissociation and Tandem Mass Spectrometry" published in *Biological Mass Spectrometry* (Vol. 20, 505-514, 1991). I am an author of this manuscript and I would like to use a reprint in my Ph.D. dissertation.

Please forward permission to reprint the manuscript. I will appreciate your prompt reply.

Sincerely,

*Eunsun Yoon*

Eunsun Yoon  
 Department of Biochemistry  
 Louisiana State University  
 Baton Rouge, LA 70803  
 USA

Permission granted  
 Proper credit must be given to our publication  
*Diana Southern 17-10-91*  
 DIANA SOUTHERN  
 Permissions Department  
 For John Wiley & Sons Ltd.

If material appears in our work with credit to another source, authorization from that source is required.

Credit should include the following components: Title, author(s) and/or editor(s), Copyright ( ) (date and owner). Reprinted by permission of John Wiley & Sons, Ltd.

*17-10-91*

## Abstract

Certain linkage positions in oligosaccharides can be discerned by collision-activated dissociation mass spectrometry (MS-CID-MS) and rationalized by molecular modeling. Previous work on synthetic oligosaccharides has suggested that daughter ion patterns can distinguish among intact compounds which terminate in  $\alpha$ -*L*-fucose and have a penultimate aminosugar (Laine, *et al.*, Journal of The American Chemical Society, **110**, 6931, 1988). The current study indicates that these observations can be extended to oligosaccharides terminating in  $\beta$ -*D*-galactose. In addition, we have observed that protonated, ammoniated and lithiated molecular ions all produce linkage-specific daughter ion spectra in these two sets of oligosaccharides. Sodiated molecular ions could be fragmented usefully under high collision energy offset conditions (18), and potassiated ions were stable, not dissociable under conditions available in a triple quadrupole instrument. We also show linkage discernment among the permethylated set of these six synthetic oligosaccharides. Methylated derivatives of this set of compounds give more useful product-ions, including a 3-linkage specific ion. A novel relationship was noted by a plot of collision energy vs. [daughter ion/parent ion] ratio which gave an unique slope for each of the non-reducing terminal linkage positions 3, 4 and 6 in the set of six compounds. The slope of this plot is related to the ability of each linkage position in the oligosaccharide to absorb collisional energy. Rotational freedom of the individual glycosidic linkage is hypothesized to play a role in this phenomenon.

## Introduction

Collision-induced dissociation (CID) of Fast Atom Bombardment (FAB) ionization-generated ions of carbohydrates was first attempted by Carr, *et al.* [2.1]



using high energy collision in a four-sector magnetic instrument with major fragmentation occurring at the glycosidic linkages. Previous work on collision of disaccharide ions had suggested that MS-MS could be useful for some aspects of carbohydrate structure, (de Jong *et al.*, [2.2]). Subsequent work by Domon and Costello [2.3], Costello and Vath [2.4], Gillece-Castro and Burlingame [2.5] and Domon *et al.* [2.6] have shown that some position- of-linkage information in oligosaccharides and disaccharides and glycoconjugates may be derived from high energy collision by linkage-specific, through-the-ring cleavages. Mueller *et al.* [2.7-2.9] have demonstrated that non-reducing end epimers can be identified by ion fragmentation from low energy collision experiments. Other workers have also shown isomer differentiation of larger oligosaccharides [2.10, 2.11] and significant structural information derived from FAB MS-CID-MS experiments with oligosaccharides and glycoconjugates [2.12-2.16]. A set of 19 oligosaccharides was examined by negative ion FAB and linked scanning for terminal linkage position assignment [2.17]. Rationale for most of the fragmentation (daughter ion) assignments of glycoconjugates and oligosaccharides has come from traditional organic ionic mechanisms. Using low energy CID experiments and molecular modeling, we have suggested that significant differences in glycosidic bond cleavage may occur due not only to ionic considerations but also may have contributions from steric hindrance of the absorbance of collision energy [2.18, 2.19], leading to a statistically higher bond cleavage for sterically crowded linkages.

In the present extension of the previous study, collision-induced dissociation mass spectrometry (MS-CID-MS), in conjunction with suitable cationization or derivatization procedures, and justified with molecular modeling yielded a sensitive method to analyze the non-reducing terminal linkage position in a set of six

synthetic, linkage-isomeric trisaccharides. Low energy collision FABMS-CID-MS on a triple quadrupole instrument gave fragmentation data that allow differentiation among the three possible linkage positions of either terminal fucose or galactose to N-acetylglucosamine in intact or permethylated versions of the following otherwise identical structures:

Set I, the FX series

(Methylated FX are called MFX, where X=3,4 or 6)

L-fucosyl-( $\alpha$ 1->X)-D-N-acetylglucosaminyl-( $\beta$ 1->3)-D-galactosyl-( $\beta$ 1-O-methyl):FX

Set II, the GX series

(Methylated GX are termed MGX, where X = 3,4 or 6)

D-galactosyl-( $\beta$ 1->X)-D-N-acetylglucosaminyl-( $\beta$ 1->3)-D-galactosyl-( $\beta$ 1-O-methyl):GX

In addition to traditional ionic mechanisms, we hypothesize [2.18,2.19] that differences in internal, non-bonding free energy, and in entropic parameters such as degrees of freedom of motion near minimum energy conformations could allow threshold CID experiments to distinguish among the linkage-positions of the various sugar isomers. In a preliminary report, Laine *et al.* suggested [2.18] that ion patterns obtained from fast atom bombardment mass spectra (FABMS), and MS-CID-MS studies of the above FX series could distinguish among the three possible linkage positions of the terminal fucose by comparison of the relative intensities of the daughter ions. In the present investigation, several approaches were used to further study the linkage-dependent sensitivity of CID spectra of these trisaccharide moieties. A related set of compounds (GX) containing D-galactose at the non-

reducing terminus was synthesized and examined in parallel with the FX set previously mentioned. Experiments were conducted on the intact trisaccharides using several different cationized species (K, Li, and  $\text{NH}_4$ ) resulting in spectra having a better correlation of linkage with fragmentation patterns than our earlier studies on protonated and sodiated molecular ions. Also, sodiated ions gave very useful spectra at high collision offset values. Permethylated derivatives of the above FX and GX series were prepared, which gave even more discriminating fragmentation patterns along with enhanced sensitivity. Recently, several laboratories have studied trimethylsilyl, acetyl, and methyl derivatives [2.17, 2.20-2.26] of some free saccharides and of the corresponding alditols to distinguish linkage-positions of glycosidic bonds. Also, a recent study of cationized oligosaccharides recommended the lithiated ions for collision experiments [2.27].

To rationalize the observed results in the MS-CID-MS studies, SYBYL and MM2(87) molecular modeling programs were modified for use on an IBM 3090 and were also used on DEC MicroVAX equipment to calculate minimum energy structures and freedom of motion volumes near the minima but below the bond-breaking energy for the permethylated fucosyl-GlcNAc series [2.18]. Structures with more freedom of motion would more readily dissipate energy absorbed from collision events due to lowered probability of populating the reaction coordinate for glycosidic bond cleavage.

### **Experiment**

Oligosaccharides were synthesized as described previously [2.28] and characterized by  $^{13}\text{C}$  NMR. For preparing cationized species, each oligosaccharide (3 $\mu\text{g}$ /1 $\mu\text{l}$  of water) was dissolved in 1  $\mu\text{l}$  of glycerol on a copper FAB probe tip. Samples contained 0.1-0.5  $\mu\text{g}$  of KCl, NaCl, LiCl and  $\text{NH}_4\text{Cl}$ . The trisaccharides

were permethylated by the method of Ciucanu and Kerek [2.29] and dissolved in chloroform. The FABMS spectra were obtained on a Finnigan TSQ-70 triple quadrupole instrument using Xenon gas and an Ion Tech Saddle-Field FAB gun, or an ANTEK cesium gun at 8-9 KeV.

The CID studies were performed using 0.8 mTorr of argon as collision gas and varying the collision energy offset from -10 to -60 eV at 10 eV increments. Each permethylated oligosaccharide (3ug) was dissolved in 1 ul of glycerol on a copper probe tip and the spectra were scanned during 3 sec from m/z 50 to 800. For CID measurements four to eight spectra from m/z 50 to 750 were averaged taken as 5 second scans at each 10 eV collision energy increment. Molecular calculations were performed on a DEC MicroVAX 3500 or an IBM-3090 using SYBYL (Tripos. Associates Inc., 1989) and MM2 (Indiana Univ., 1987) software. Energy contour maps were made with TOPO and SURF programs from the SURFER package (Golden Software, Inc., Golden Co.).

## **Results and Discussion**

### **Cationized Oligosaccharides**

Cationized (Na, Li, NH<sub>4</sub>) molecular ions gave linkage dependent fragment patterns superior to our original observations with protonated molecular ions [2.18, 2.19] and cationized molecular ions exhibited decreasing stability under collision-induced dissociation in the series K > Na > Li > NH<sub>4</sub> using 0.8 mTorr argon pressure in the collision cell. Figure 2.1 shows the potassiated molecular ion at m/z 582 for the F3 and F4 compounds collided at -60 eV collision energy offset. Potassium cationized trisaccharides were so stable that they would not yield fragment ions under conditions of collision available in the triple quadrupole. Potassium is the

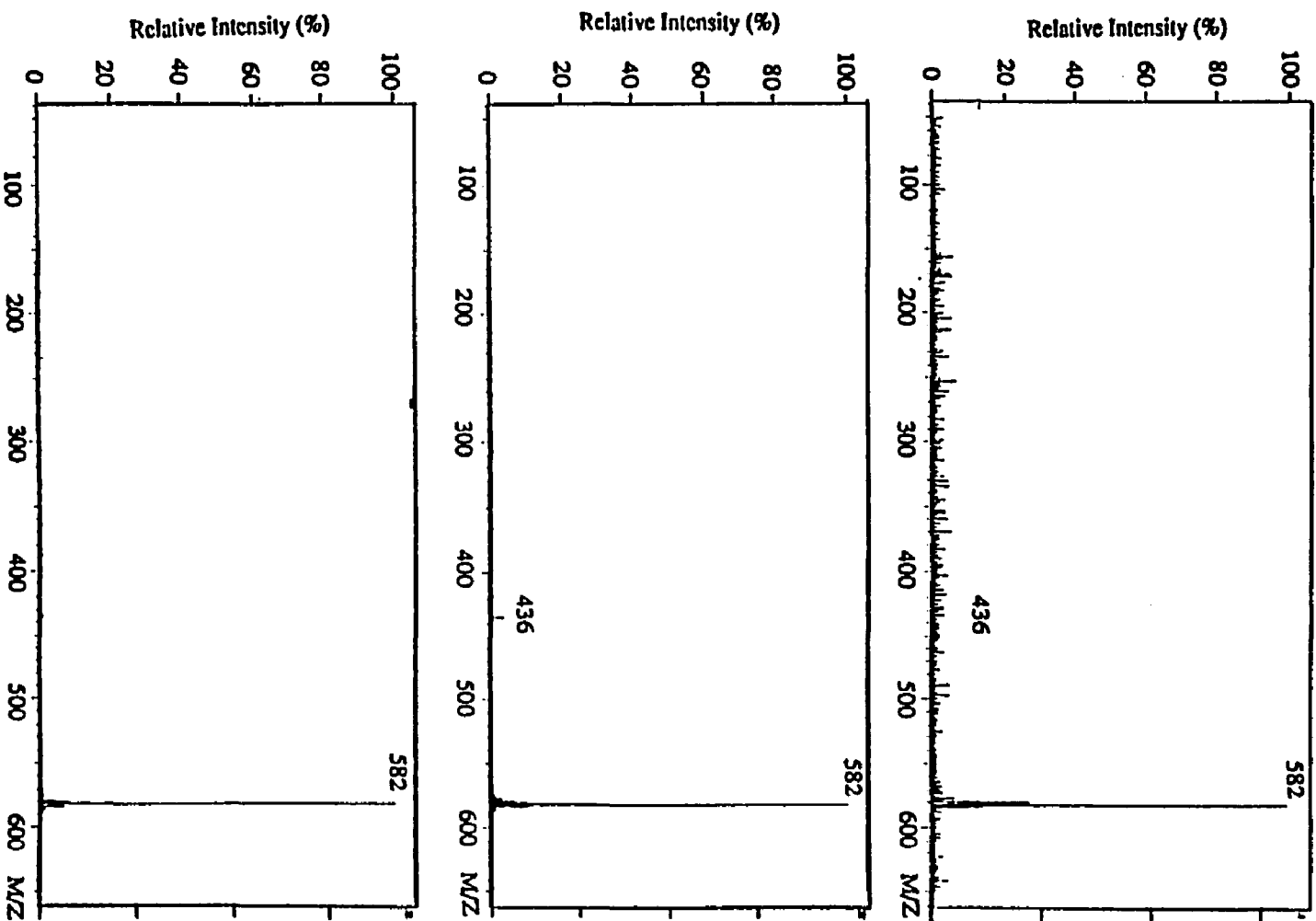


Fig. 2.1 CAD experiments on  $[M+K]^+ = 582$  at  $-60\text{eV}$  @  $0.8\text{ mTorr}$  argon gas. (F3 upper spectra, F4 middle spectra, or F6 lower spectra).

cation of choice for production of molecular ions absent of ambiguity in the spectrum caused by an oligomer sugar mixture series. Previously reported sodium cationized species [2.19] could be fragmented at higher energies (- 60 eV offset), but not at -10 eV offset which easily fragmented either lithiated (Fig. 2.2) or protonated molecular ions [2.18,2.19]. Thus, the sodiated molecular ion was quite versatile, displaying only molecular ions at low collision energy offsets and diagnostic fragmentation at higher energies. The most useful lithiated molecular ion CID spectra were recorded at a medial collision offset, -40 eV as shown in Figure 2.2. Argon pressure of 0.8 mTorr was used in all of the studies for comparative purposes. The m/z 550 lithiated molecular ion was much more stable in F4 than F3, yielding ions from the loss of fucose at m/z 404, from the aminosugar remnant ion at m/z 210 (GlcNAc+Li) and from lithiated O-methylated galactose ion at m/z 201. The ratios of m/z 201 and 210 were switched when comparing F3 and F4, tending toward a predominance of lower mass ions in the F3 compound. The lithiated  $[M+Li]^+$  ion for F6 was more stable than either F3 or F4 (not shown) just as in the protonated molecular ion [2.18,2.19]. Figure 2.3 shows that the ammoniated molecular ion is not visible in the spectrum of F3 at -20eV collision offset, where the differences were most apparent, while a small amount was seen in F4. The ratio of  $[M+H]^+$  ion at m/z 544 [2.19] with daughter ions in the ammoniated molecular ions showed a great difference among the FX linkage set I with the m/z 544 and m/z 398 ions from loss of fucose significantly different among the three test FX compounds. Also the m/z 350 ion which contains the linkage in question [2.19], when collisionally activated was much more stable in the series  $F6 > F4 > F3$ . The remnant GlcNAc ion at m/z 204 similarly showed prominence in the more unstable oligosaccharides.

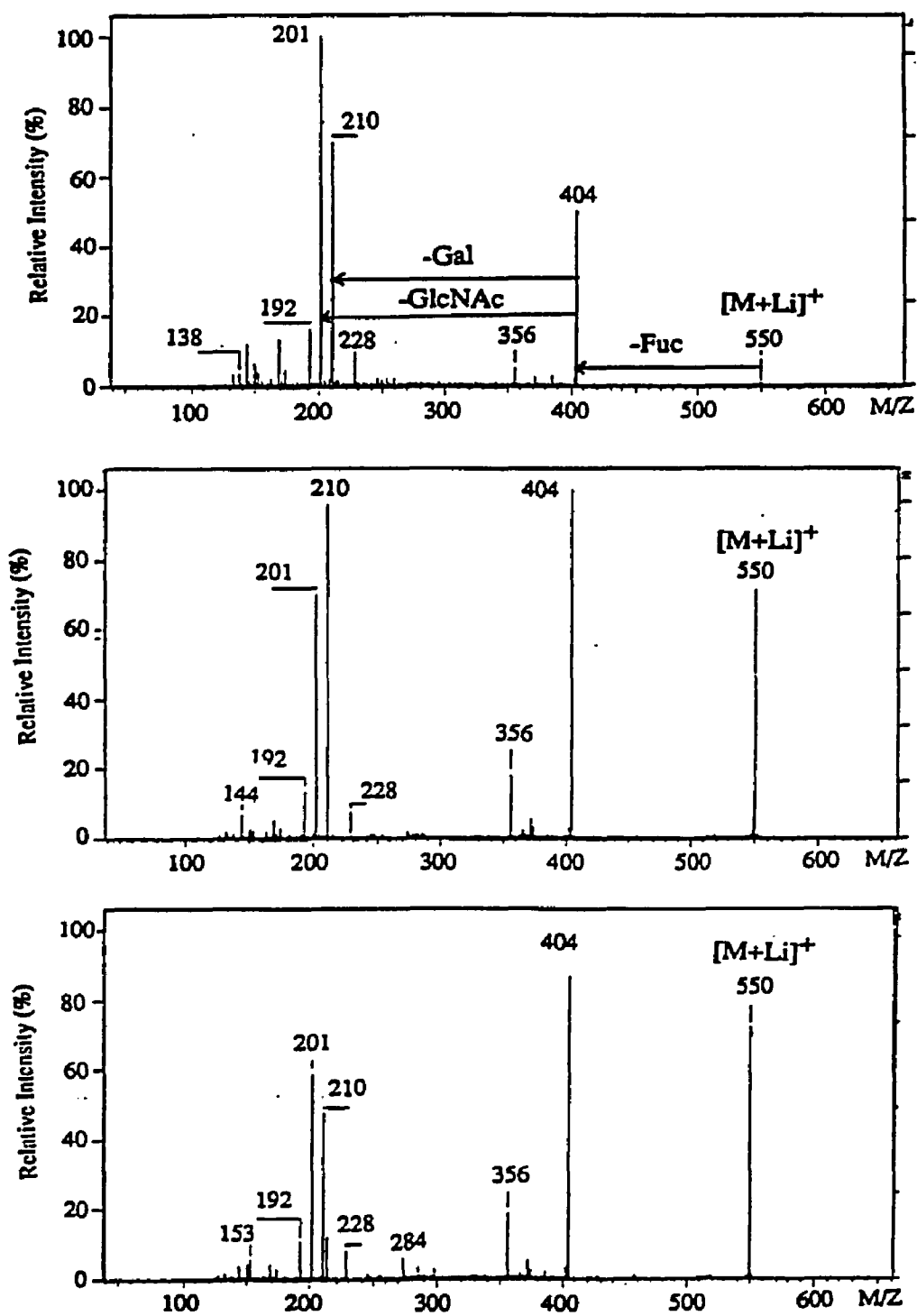


Fig. 2.2 CAD experiments on  $[M+Li]^+ = 550$  at  $-40\text{eV}$  @  $0.8\text{ mTorr}$  argon gas. (F3 upper spectra, F4 middle spectra, or F6 lower spectra).

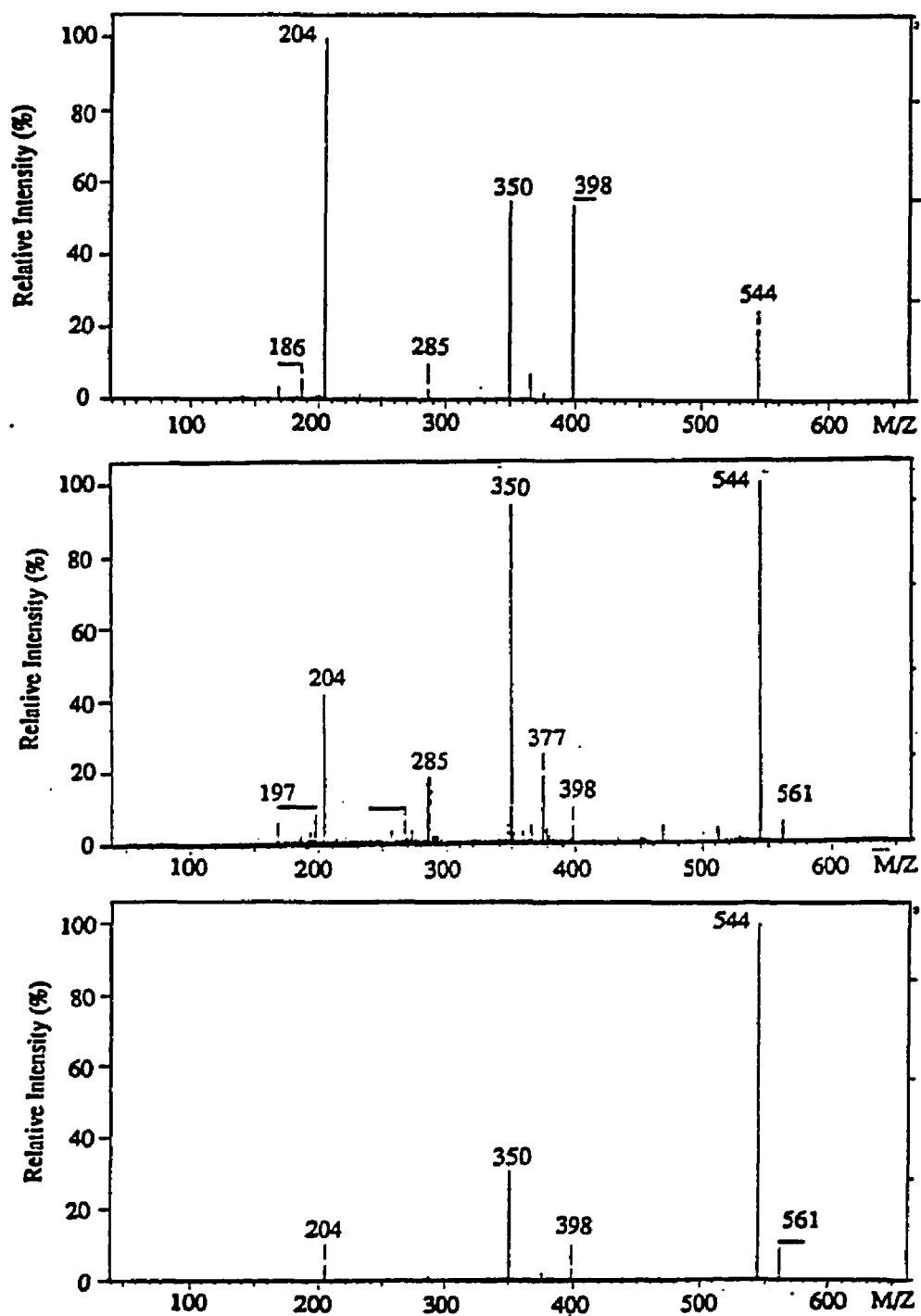


Fig. 2.3 CAD experiments on  $[M+NH_4]^+ = 544$  at  $-20\text{eV}$  @  $0.8$  mTorr argon gas. (F3 upper spectra, F4 middle spectra, or F6 lower spectra).



Permethyated Fucose series: Set I, MF3, MF4 and MF6

The FAB MS-CID-MS spectra of methylated isomeric trisaccharides, MF3 [2,3,4-tri-O-methyl-*L*-fucosyl-( $\alpha$ 1- > 3)-2-*N*-acetyl-2-*N*-methyl-4,6-di-O-methyl-*D*-glucosaminyl- ( $\beta$ 1- > 3)-2,4,6-tri-O-methyl-*D*-galactosyl-( $\beta$ 1- > O-methyl)], MF4, and MF6 are shown in Figures 2.4 and 2.5 at both -10 eV and -60 eV collision energy offset, respectively. The spectra all show the same  $[M+H]^+$  ion at  $m/z$  670 as expected, as well as common fragment ions at  $m/z$  434 and  $m/z$  482. The survival rate (relative intensity of collided ion) of the molecular ion ( $m/z$  670) in compounds decreases differently according to linkage as the collision offset increases, and methylated MF6 has the highest survival  $m/z$  670 ion at -60 eV among the set of three methylated trisaccharides (Figure 2.5). The relative intensity of the molecular ions with respect to the daughter ions in the MFX methylated series at -60 eV collision offset and 0.8 mTorr argon was as follows: Methylated F6(80%) > Methylated F4(45%) > Methylated F3(30%).

The major fragment ion at  $m/z$  434 is formed by loss of methylated galactose with cleavage of the glycosidic bond between GlcNAc and galactose according to the *a*-type pathway [2.30], which is characterized by a hydrogen transfer from the amino-containing sugar to the methylated galactose, generating an oxonium ion on the methylated GlcNAc (Scheme 2.1). Loss of the methylated fucose moiety from the molecular ion ( $m/z$  670) by cleavage of the fucose C1-O glycosidic bond with a hydrogen transfer to methylated-GlcNAc results in an ion at  $m/z$  482 (*b*-type pathway). These bond scissions result in a loss of one sugar from either end of the oligosaccharide, but only the non-reducing end  $m/z$  434 ion contains the linkage in question.

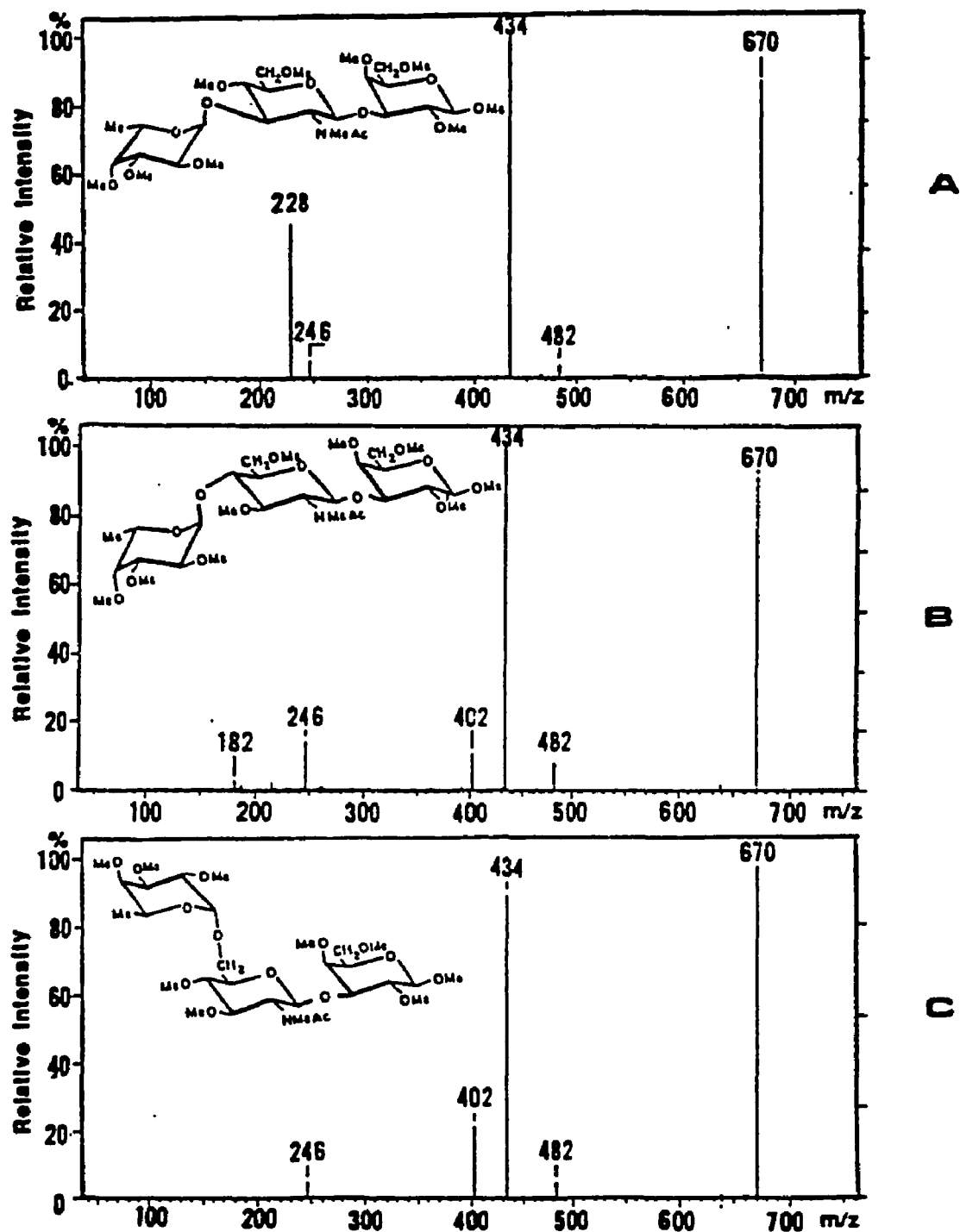


Fig. 2.4 FAB-MS-CAD-MS spectra of m/z 670 for methylated L-fucosyl-( $\alpha$ 1-X)-D-N-acetylglucosaminyl-( $\beta$ 1-3)-galactosyl-( $\beta$ 1-O-methyl) at -10eV where X=3 (A), 4(B), or 6(C).

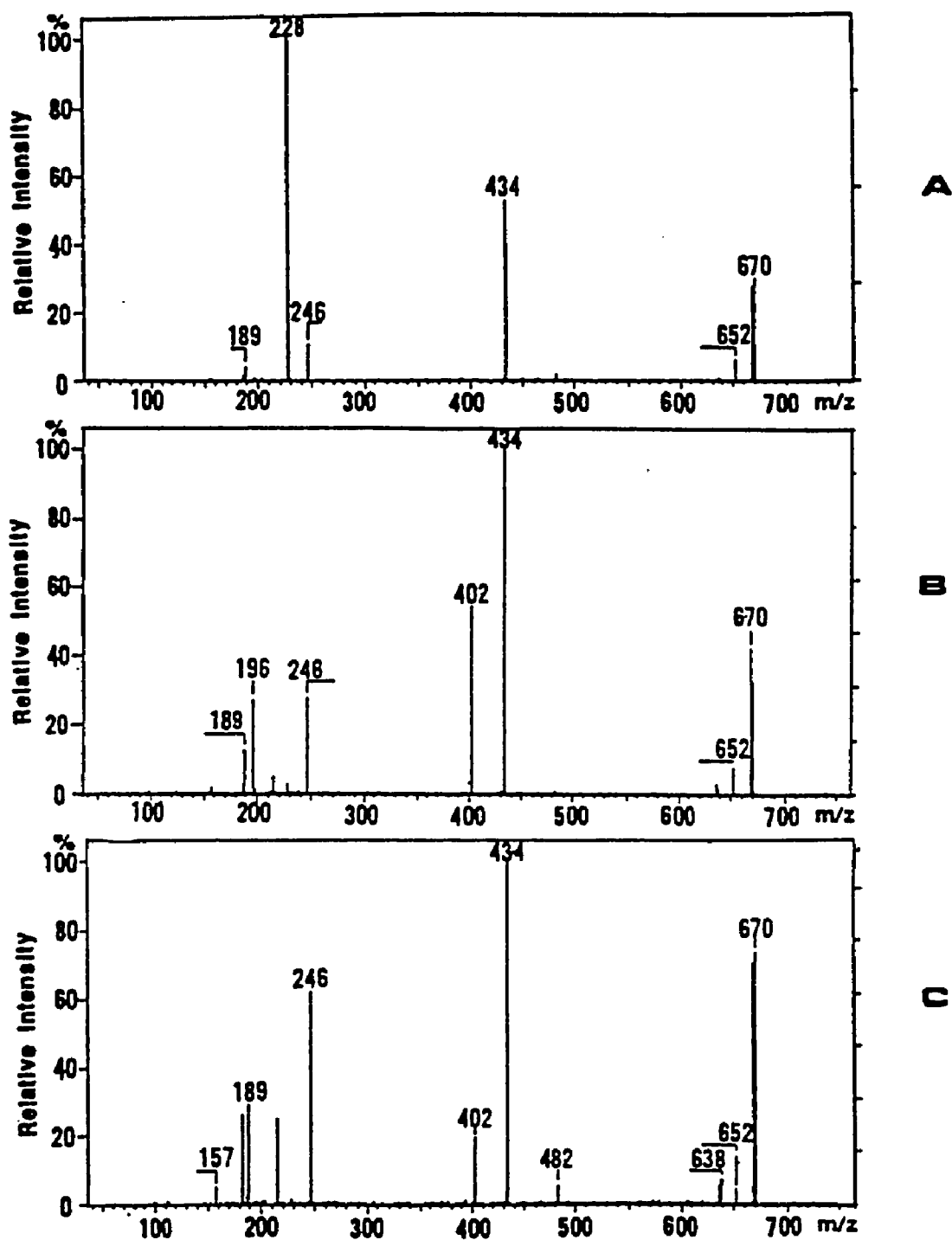
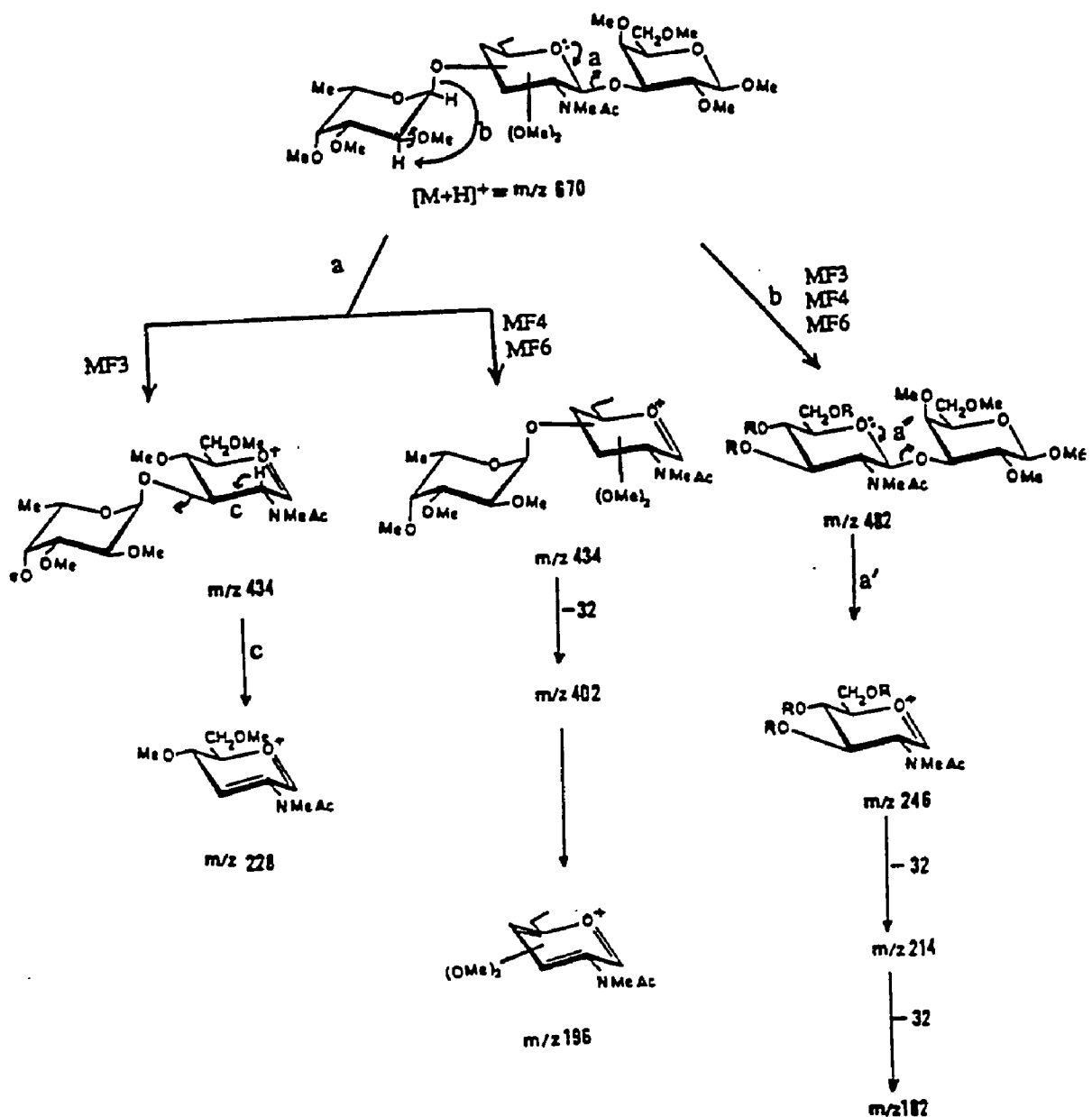


Fig. 2.5 FAB-MS-CAD-MS spectra of m/z 670 for methylated L-fucosyl-( $\alpha$ 1-X)-D-N-acetylglucosaminyl-( $\beta$ 1-3)-galactosyl-( $\beta$ 1-O-methyl) at -60eV where X=3 (A), 4(B), or 6(C).

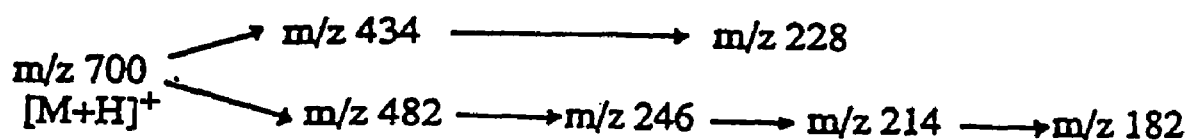


Scheme 2.1 Fragment pathway of methylated F3 (MF3), methylated F4 (MF4) and methylated F6 (MF6) where R=H or  $CH_3$ .

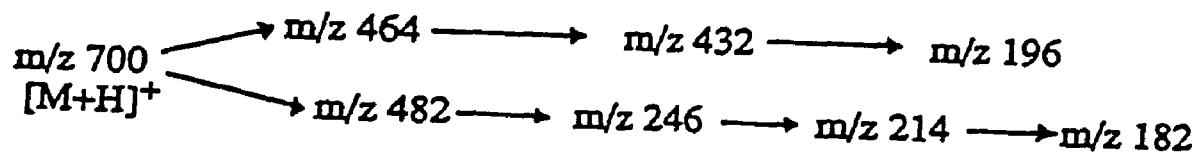
Compared with the spectra of the other methylated saccharides those of MF3 (which contains the  $\alpha 1 \rightarrow 3$  linkage) at each collision energy level exhibits a relatively intense peak at  $m/z$  228 that is diagnostic for the remnant penultimate aminosugar moiety from the non-reducing terminal loss of 3-linked methylated sugars. Dell [2.24] has proposed a structure for this ion similar to our results. Similar observation for a 3-specific ion has been made by Domon *et al.* and Egge *et al.* [2.25,2.26]. The (*a*-type) fragment ion at  $m/z$  402 is diagnostic for  $\alpha 1 \rightarrow 4$  or  $\alpha 1 \rightarrow 6$  linkages in the same class of molecules, and is due to the loss of reducing end methylated galactose with cleavage of the glycosidic bond between galactose and GlcNAc moieties and consecutive losses of methanol. Further loss of the methylated fucose moiety yields an unsaturated, partially methylated GlcNAc ion at  $m/z$  196.

Permethylated Galactose series: Set II, MG3, MG4 and MG6.

The FAB MS-CID-MS spectra of methylated G3 [MG3; 2,3,4,6-tetra-O-methyl-4,6-di-O-methyl-*D*-galactosyl-( $\beta 1 \rightarrow X$ )-*N*-acetyl-*N*-methyl-X,X-di-O-methyl-*D*-glucosaminyl-( $\beta 1 \rightarrow 3$ )-2,4,6-tri-O-methyl-*D*-galactosyl-( $\beta 1$ -O-methyl)], MG4, and MG6 at -10 eV are shown in Figure 2.6. Figure 2.7 shows the CID spectra of the same compounds at -60 eV. MFX and MGX sets exhibited the same cleavage fragment pattern according to the position of linkage. A significant diagnostic ion for the 3 linkage at  $m/z$  228 appeared in the CID spectrum of MG3 at -10 eV collision offset and increased its relative abundance at higher collision offsets. Methylated F6 and G6 have identical cleavage pathways as those of the 1- $\rightarrow$ 4 linkage-containing methylated F4 and G4, respectively (Schemes 2.2,2.3). Significant differences in the fragment ratios contribute to discernment between 1- $\rightarrow$ 4 and 1- $\rightarrow$ 6 linkages.



Scheme 2.2 Fragment pathway of methylated G3.



Scheme 2.3 Fragment pathway of methylated G4 and G6.

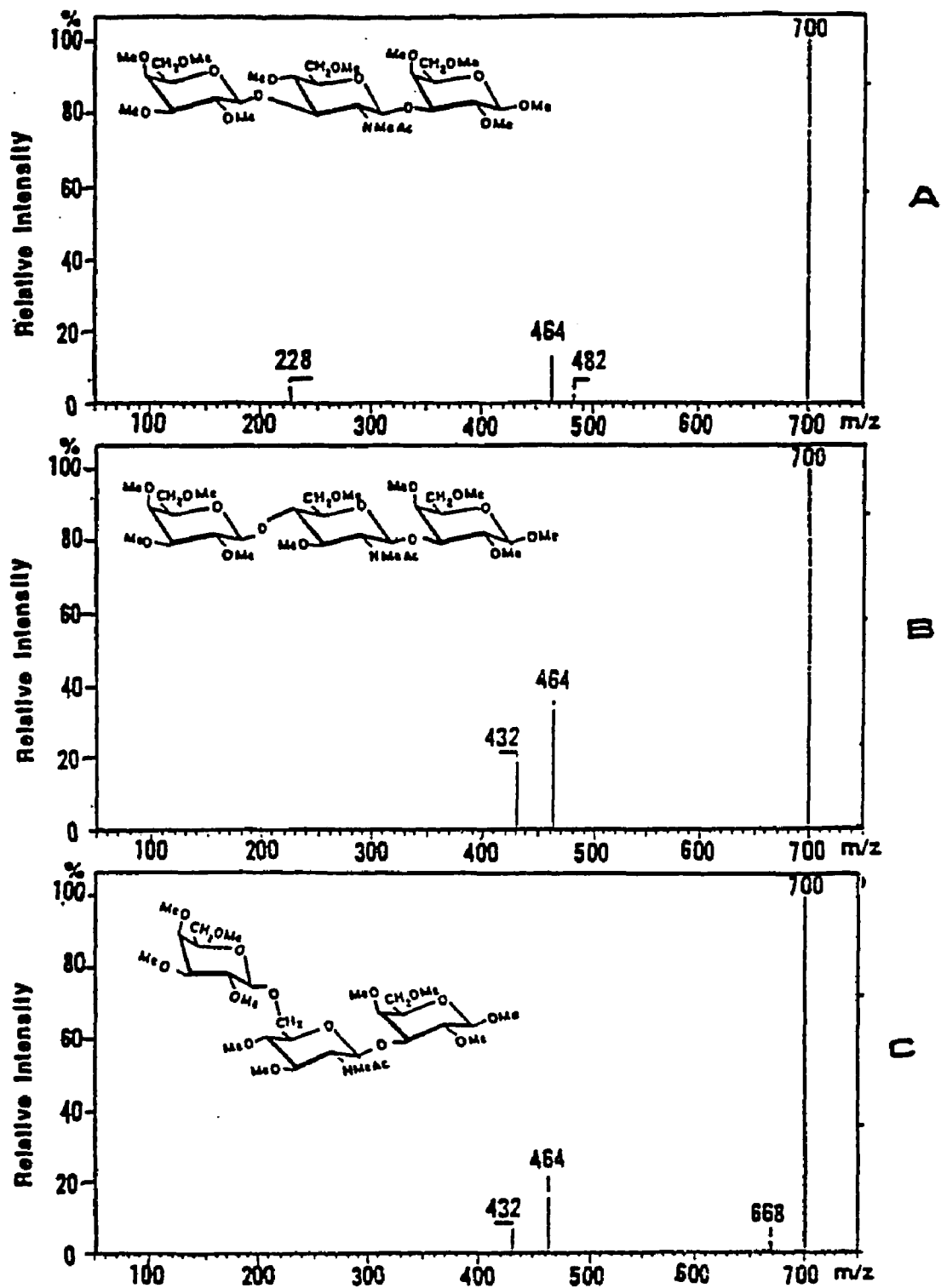


Fig. 2.6 FAB-MS-CAD-MS spectra of m/z. 700 for methylated Galactosyl-(β1-X)-D-N-acetylglucosaminyl-(β1-3)-galactosyl-(β1-O-methyl) at -10eV where X=3 (A), 4(B), or 6(C).

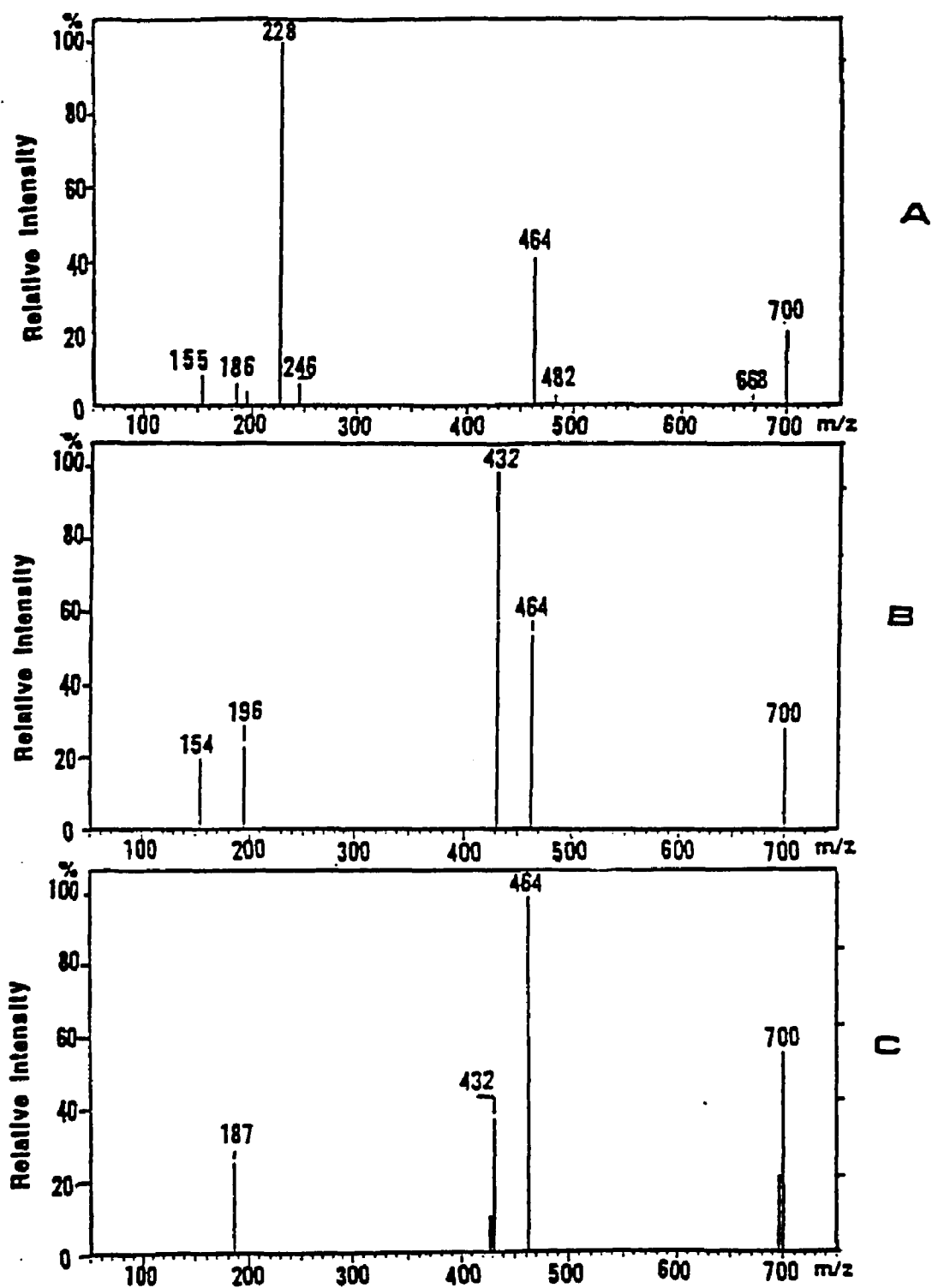


Fig. 2.7 FAB-MS-CAD-MS spectra of m/z 700 for methylated Galactosyl-( $\beta$ 1-X)-D-N-acetylglucosaminyl-( $\beta$ 1-3)-galactosyl-( $\beta$ 1-O-methyl) at -60eV where X=3 (A), 4(B), or 6(C).



Observation of the molecular similarity between the  $\alpha$ -L-fucose and  $\beta$ -D-galactose terminating sets of compounds reveals that the molecular parameters of the glycosidic linkages from C1-O (Phi) bonds and the sugar rings are very closely related. This is due to the peculiarity of the nomenclature which relates the epimer of the highest chiral carbon to the assignment of the anomer. Therefore the present study does not directly address possible differences in spectra that may arise solely from differences in spatial orientations of the sugar rings which result from anomeric configuration.

Plot of Collision energy vs. Parent/Daughter ratio:

A particularly interesting relationship was found between physical parameters of the analysis and the linkage position in the methylated versions of oligosaccharide Sets I and II. A plot of collision offset energy vs. parent/daughter ratios (Figure 2.8) gave a unique linkage-related slope across a gradient of collision energy, another way to depict the relative stability among the three linkage positions. This relationship broke down above collision offset energies of -60 eV. The ratio of  $m/z$  (228+246+402)/670 was considered to be particularly useful (Figures 2.8 and 2.9), among other ratios examined (e.g.  $m/z$  434(228+246+402)/670) in the MFX series, Set I. Parent ion survival vs. daughter ion ratios in the fragmentations of the FX, GX and MFX, MGX in each collision energy set is a strong indicator of linkage position in FABMS-CID-MS spectra [2.18, 2.19 and the present study] in which the order of bond stability was  $1 \rightarrow 6 > 1 \rightarrow 4 > 1 \rightarrow 3$ . This was especially clear in the plot of collision offset vs. relative intensity of ion ratio, (e.g.  $m/z$  (228+246+464)/700 in MGX, Set II). In both the methylated MFX and MGX series, the compound containing the  $1 \rightarrow 3$  linkage was always more labile because

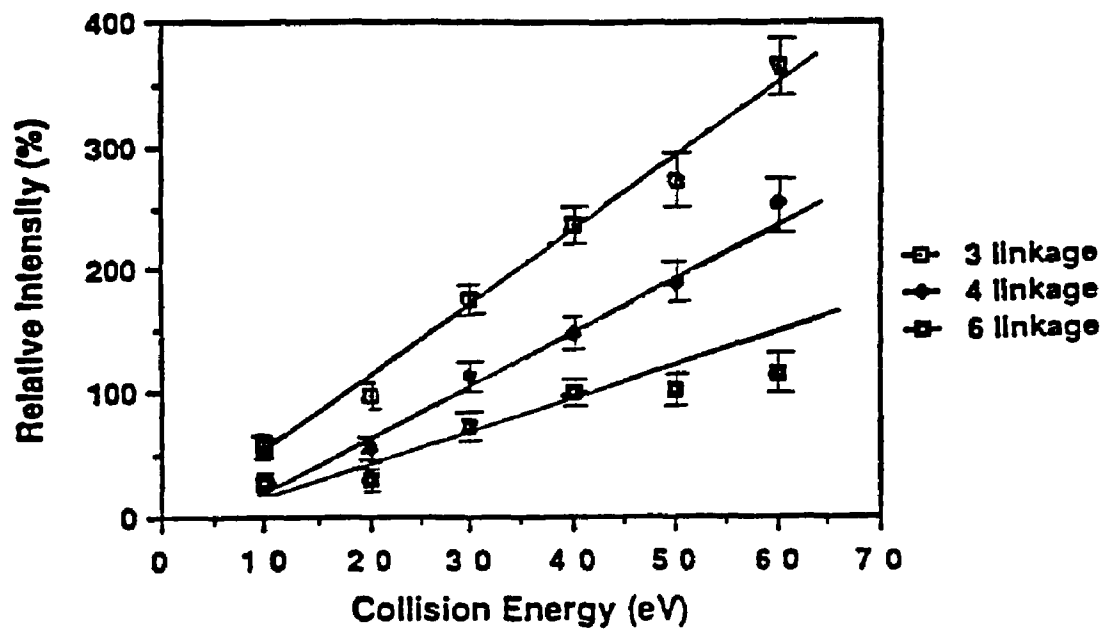


Fig. 2.8 Plot of collision offset vs. ion ratio in methylated FX:  $m/z (228+246+402)/670$ .

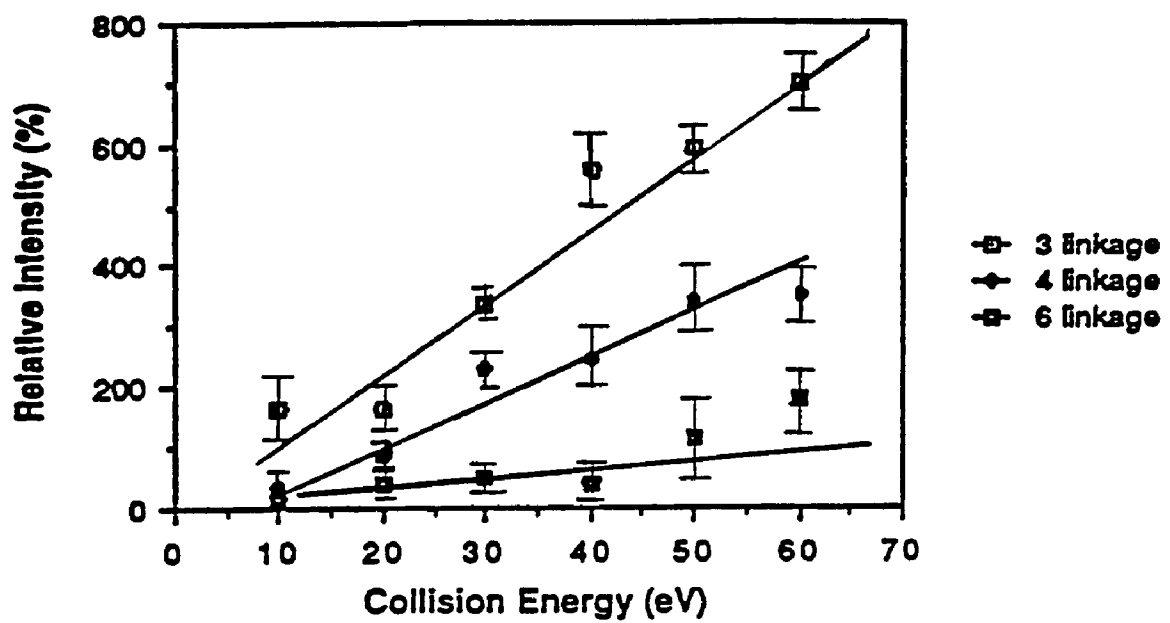


Fig. 2.9 Plot of collision offset vs. ion ratio in methylated GX:  $m/z (228+246+464)/700$ .

of the propensity for charge retention on the nearby amino group on GlcNAc. In this comparison, the 1- >4 linkage compound was always intermediate in stability and the 1->6 linkage-containing compound the most stable. The intensity ratio of major fragments reflects variations in the internal energy of the precursor ions with fragmentation of the methylated 1->6 linkage-containing compound requiring higher energy.

#### Molecular Modeling:

Molecular modeling of the permethylated derivatives supported the rationale for the above-described order of stability by examining the degree of rotational freedom (number of available vibronic states) around the isomeric linkage [2.18]. Figure 2.10 shows energy wells [2.18] derived from the MM2(87) calculations on neutral, uncharged molecules which depict degrees of phi-psi rotational freedom. MF3, the most rigid isomer, generates a volume which we will depict as 1.0, while MF4 generates an intermediate volume of 1.3. MF6, being the most flexible with its three rotational bonds generates a much larger well (1.8). Comparison of the volumes of rotational freedom wells for intact [2.18] and methylated derivatives of Set I, showed much smaller volumes (about 5 times smaller than intact saccharides) for the latter due to greater steric hindrance caused by the methyl groups. Concurrently, the methylated compounds, unable to absorb as much collision energy as the intact oligosaccharide, tended to fragment at lower energies in CID. Pioneering efforts have yet to be made in molecular modeling of ionized, charged oligosaccharides, and we have not yet attempted such a study. Calculations with regard to charge localization may more clearly define and predict fragmentation pathways.

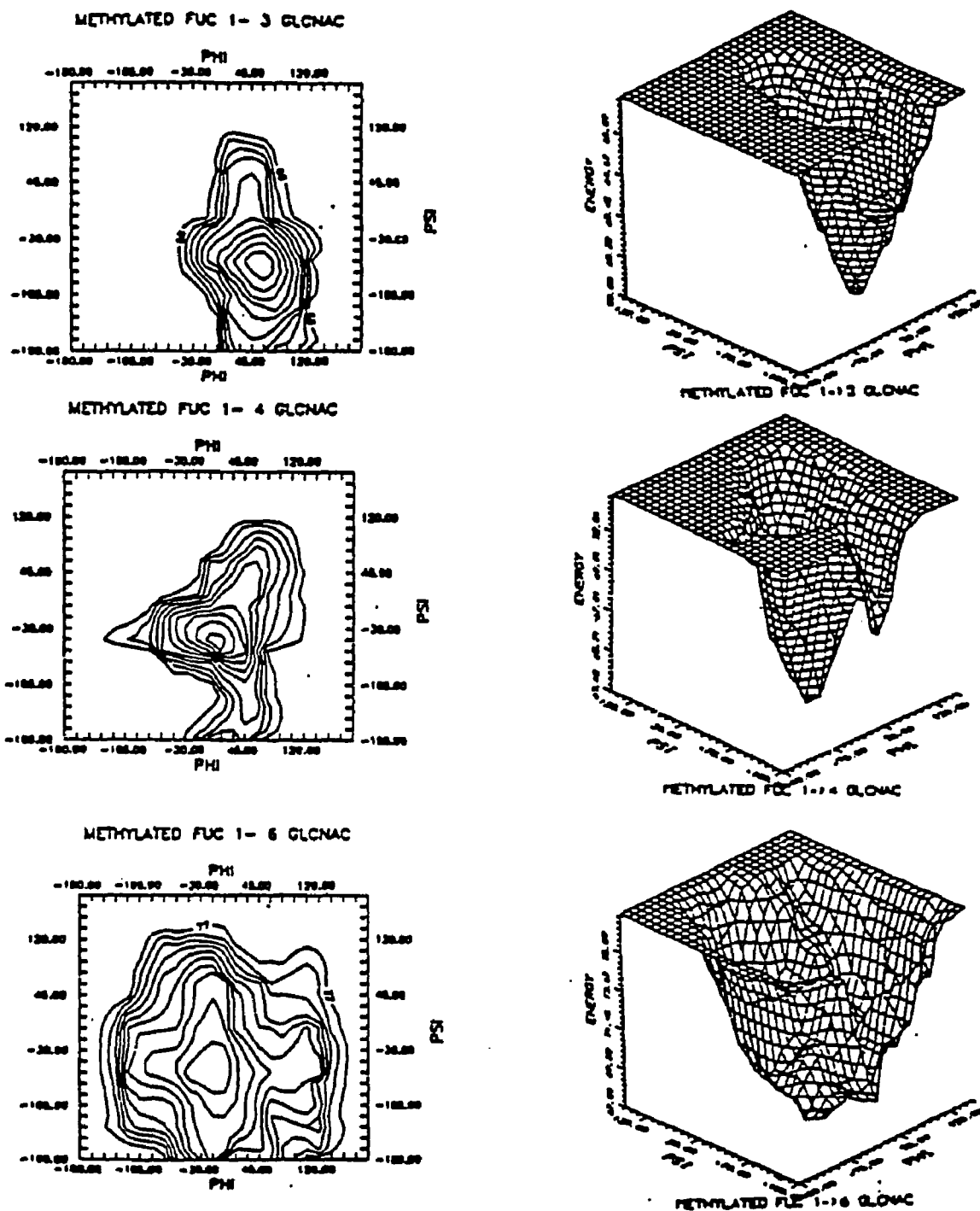


Fig. 2.10 The phi and psi plots of the total energies and energy wells derived from the MM2(85) calculation. (The drawings were made with the SURF program of SURFER from Golden software.)

FABMS-CID-MS in combination with molecular modeling may lead to useful procedures to recognize linkage position in oligosaccharide structures with much less effort than conventional methylation linkage analysis.

## Supplementary Material (not included in original paper)

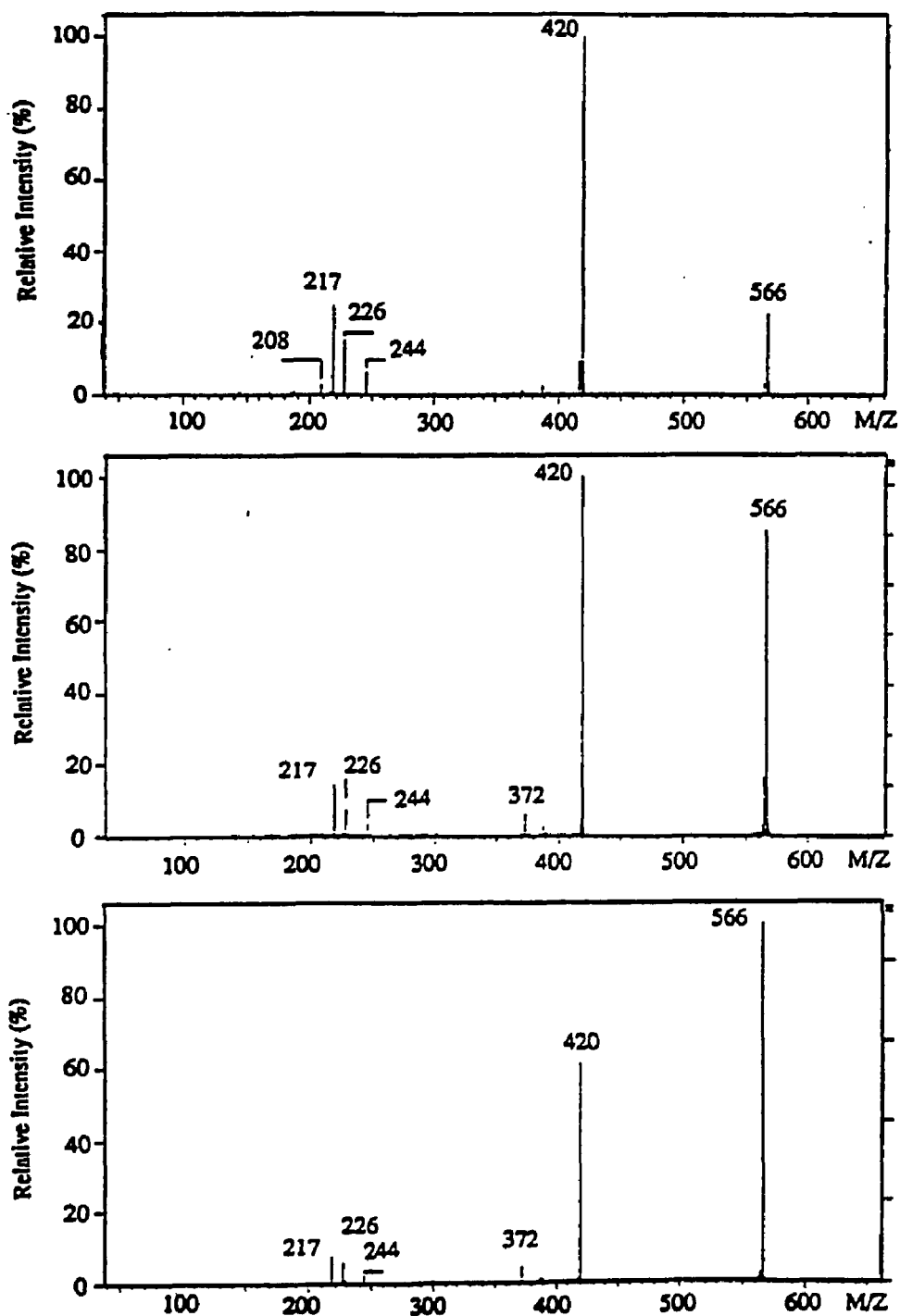


Fig. 2.11 CAD experiments on  $[M+Na]^+ = 566$  at  $-40\text{eV}$  @  $0.8\text{ mTorr}$  argon gas. (F3 upper spectra, F4 middle spectra, or F6 lower spectra).

## References

- 2.1 S.A. Carr, V.N. Reinhold, B.N. Green, and J.R. Hass, *Biomed. Environ. Mass Spectrom.* **12**, 288 (1985).
- 2.2 E.G. de Jong, W. Heerma and G. Dijkstra, *Biomedical Mass Spectrometry*, **7**, 127 (1980).
- 2.3 B. Domon and C.E. Costello, *Biochemistry*, **27**, 1534 (1988).
- 2.4 C.E. Costello, and J.E. Vath, *Methods in Enzymology*, **193**, 738 (1990).
- 2.5 B.L. Gillece-Castro and A.L. Burlingame, *Methods in Enzymology*, **193**, 689 (1990).
- 2.6 B.M. Domon, D.R. Mueller, W. Blum, and W.J. Richter, *Org. Mass Spectrom.* **24**, 357 (1989).
- 2.7 D.R. Mueller, B.M. Domon, W. Blum, F. Rashdorf, and W.J. Richter, *Biomed. Environ. Mass Spectrom.* **15**, 441 (1988).
- 2.8 D.R. Mueller, B. Domon, W.J. Richter, *Adv. in Mass Spectrom.* **118**, 1309 (1989).
- 2.9 D.R. Mueller, B. Domon, and W.J. Richter, *Methods in Enzymology*, **193**, 607 (1990).
- 2.10 B.M. Domon, D.R. Mueller, and W.J. Richter, *Biomed. Environ. Mass Spectrom.* **19**, 390 (1990).
- 2.11 R. Orlando, C.A. Bush, and C. Fenseleau, *Biomed. Environ. Mass Spectrom.* **19**, 747 (1990).
- 2.12 K. Hirayama, S. Akashi, T. Ando, and I. Horino, *Biomed. Environ. Mass Spectrom.* **14**, 305 (1987).
- 2.13 Y. Chen, N. Chen, M. Li, F. Zhao, N. Chen, *Biomed. Environ. Mass Spectrom.* **14**, 9 (1987).
- 2.14 J.P. Kamerling, W. Heerma, F.G. Vliegthart, N.B. Green, J.A.S. Lewis, G. Strecker, G. Spik, *Biomed. Mass Spectrom.* **10**, 420 (1983).
- 2.15 Z. Lam, M.V. Comisarow, G.G.S. Dutton, D.A. Weil, A. Biarnson, *Rapid Commun. Mass Spectrom.* **1**, 83 (1987).
- 2.16 J.C. Prome, M., Aurelle, D. Prome, D. Savagnac, *Org. Mass Spectrom.* **22**, 6 (1987).



- 2.17 D. Garozzo, K.M. Giuffrida, G. Impallomeni, A. Ballistreri, and C. Montaudou, *Anal. Chem.* **62**, 279 (1990).
- 2.18 R.A. Laine, K.M. Pamidimukkala, A.D. French, R.W. Hall, S.A. Abbas, R.K. Jain, and K.L. Matta, *J. Am. Chem. Soc.* **110**, 6931 (1988).
- 2.19 R.A. Laine, *Methods in Enzymol.* **179**, 157 (1989).
- 2.20 A. Dell and C.E. Ballou, *Biomedical Mass Spectrometry*, **10**, 50 (1983).
- 2.21 W. Heerma, C. Versluis, W. Kulik, R.R. Contreras, and J.P. Kamerling, *Biomed. Environ. Mass Spectrom.* **17**, 257 (1988).
- 2.22 Dell, J.E. Oates, H.R. Morris, H. Egge, *Int. J. Mass Spectrom. Ion Phys.*, **465**, 415 (1983).
- 2.23 J.E. Thomas-Oates, and A. Dell, *Biochem. Soc. Trans.* **17**, 243 (1989).
- 2.24 A. Dell *Adv. Carbohydr. Chem. Biochem.* **45**, 19 (1987).
- 2.25 B. Domon, and Costello, C.E., *Glycoconjugate J.* **5**, 397 (1988).
- 2.26 H. Egge, and J. Peter-Katalinic, *Mass Spectrometry Review* **6**, 331 (1987).
- 2.27 Z. Zhou, S. Ogden, and J.A. Leary, *J. Org. Chem.* **55**, 5444 (1990).
- 2.28 R.K. Jain, K. Kohata, S.A. Abbas, and K.L. Matta, *Carbohydr. Res.* **131**, 209 (1984).
- 2.29 I. Ciucanu, and F. Kerek, *Carbohydr. Res.* **131**, 209 (1984).
- 2.30 N.K. Kochekov and O.S. Chizhov, *Adv. Carbohydr. Chem. Biochem.* **21**, 39 (1966).

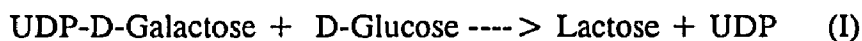
### Chapter III.

#### Enzyme-assisted Synthesis of Four Novel Trisaccharides: Gal<sub>p</sub>(β1->4)Glu<sub>p</sub>(X)Glu where X=β1->3: β1->4: β1->6: α1->4

##### Introduction

Development of tandem mass spectral methods for direct linkage determination in oligosaccharides requires sets of trisaccharides differing only in one structural parameter. In this case, we chose the position of linkage to be the reducing-end hexose. These sets of compounds would also be useful for the development of high resolution separation techniques geared to resolve linkage types. Conventional organic synthesis of such a set could take as long as 2-5 months for each member of the set. Each trisaccharide would require 10-20 steps of synthesis. Instead, we utilized low pH to induce a loose acceptor specificity for bovine milk galactosyl transferase (lactose synthase: EC 2.4.1.22) and by this method, generated several micromoles of four novel oligosaccharides for NMR and mass spectral studies. The disaccharides cellobiose (β1->4), laminaribiose (β1->3), and gentiobiose (β1->6) and maltose (α1->4) acted as acceptors for EC 2.4.1.22 activity under these conditions. The β1->2 linked disaccharide, sophorose, was not commercially available. The alpha-linked disaccharides were also examined but were very poor acceptors under a variety of conditions, only the α1->4 disaccharide, maltose, showing activity as an acceptor for galactose transfer by EC 2.4.1.22. From these four acceptors, 4 novel trisaccharides were synthesized in micromole amounts, suitable for studies of linkage position using low energy collision-induced-dissociation tandem mass spectrometry (FAB-MS-CID-MS), and for NMR. These new saccharides are gal<sub>p</sub>(β1->4)glu<sub>p</sub>(β1->3)glu, gal<sub>p</sub>(β1->4)glu<sub>p</sub>(β1->4)glu, gal<sub>p</sub>(β1->4)glu<sub>p</sub>(β1->6)glu, and gal<sub>p</sub>(β1->4)glu<sub>p</sub>(α1->4)glu.

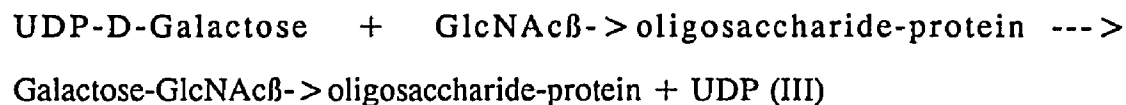
Lactose Synthase (UDP-D-Galactose: D-Glucose 1- Galactosyl(1->4)-transferase: EC 2.4.1.22) catalyzes the biosynthesis of lactose (reaction I) in the presence of  $\alpha$ -lactalbumin [3.1-3.5].



In the absence of  $\alpha$ -lactalbumin, free N- acetylglucosamine serves as an excellent acceptor for galactose leading to the formation of N-acetyllactosamine [3.5-3.8] according to reaction (II).



Our laboratory [3.9] and others [3.6-3.8, 3.10] have shown that EC 2.4.1.22 also catalyzes incorporation of galactose into  $\beta$ 1->4 linkage with glycosidically linked GlcNAc in the oligosaccharide prosthetic groups of certain glycoproteins according to reaction (III).



Under normal assay conditions,  $\alpha$ -lactalbumin inhibits reaction (II) and allows synthesis of lactose in the presence of glucose by reaction (I). Thus,  $\alpha$ -lactalbumin modifies the acceptor specificity and broadens the possible substrates of EC 2.4.1.22 from GlcNAc to glucose. Among many groups investigating [3.6,3.10-3.15] the acceptor specificity of EC 2.4.1.22, Berliner and Robinson [3.13] suggested that the structural requirements of the UDP-galactose binding site were as follows: an axial 4'-hydroxyl group and an equatorial 6'CH<sub>2</sub>OH on the pyranosyl moiety, necessary for precise substrate alignment. Lambright *et al.* [3.6] found EC 2.4.1.22 had a strong anomeric preference for  $\beta$ -D-glucose, and  $\beta$ - glucosides were

much better substrates than corresponding  $\alpha$ -analogs. Substitution of the hydrogen on the  $\beta$ -1-OH in glucose with bulky hydrophobic groups such as  $\beta$ -methyl,  $\beta$ -phenyl and  $\beta$ -indoxyl group generated more effective galactosyl acceptors than glucose in the absence of  $\alpha$ -lactalbumin [3.14]. Our study now extends the limited known specificity of EC 2.4.1.22 to a few disaccharide acceptors. The resulting synthetic trisaccharide compounds are expected to be useful in linkage studies using mass spectrometry and NMR. Compounds like these may also be possible core structures for novel carbohydrate-based neutrophil and lymphocyte homing receptor antagonists such as sialyl-LeX [3.35-3.39].

### **Experimental**

*Materials* - Laminaribiose, cellobiose, gentiobiose, maltose, UDP-galactose,  $\alpha$ -lactalbumin, and lactose synthase (UDP-galactose:D-glucose 4- $\beta$ -galactosyltransferase: EC 2.4.1.22) were purchased from Sigma Co.. All other chemicals were of reagent grade quality.

*Synthesis of trisaccharides* - The reaction mixture contained 10 mM  $\text{MnCl}_2$ , 20 mM disaccharide (laminaribiose, cellobiose, gentiobiose, or maltose) as substrate, 0.63mM UDP-galactose and 0.2 mg/ml  $\alpha$ -lactalbumin with 1 unit of EC 2.4.1.22 (one unit will transfer 1.0 micromole of galactose from UDP-galactose to D-glucose per minute at pH 8.4 at 30 °C, in the presence of 0.2 mg  $\alpha$ -lactalbumin per ml reaction mixture) in 50 mM sodium cacodylate buffer, pH 6.0 in a total volume of 500 ul. Assay mixtures were prepared in ice and the reaction started by the addition of disaccharide. After incubation (3hrs, at 37°C), the reaction was stopped by cooling to 0°C.

*Purification* - The incubated sample was applied to a 1X100 cm Bio-Gel P2 (100-200 mesh) and eluted with water containing 10% acetic acid. Fractions of 1 ml were collected and the saccharide content in 6 ul aliquots was determined by the phenol-sulfuric acid method [3.16].

*TLC* - Synthetic trisaccharides, isolated by Bio-Gel P-2 (BioRad. Inc.) gel permeation chromatography, were analyzed by thin-layer chromatography on Anal Tech Silica gel G Uniplates (scored 10X20 cm, 250 microns thickness), developed in n-butanol: ethanol: water (2:1:1 by vol). Saccharides were visualized with 2% orcinol- 95% sulfuric acid spray after heating 120°C.

*MS* - Each trisaccharide was permethylated by Ciucanu and Kerek's method [3.18] and dissolved in chloroform. The FAB MS spectra were obtained on a Finnigan TSQ-70 using Xenon gas and an Ion Tech Saddle-Field FAB gun at 8-9 KeV. Each permethylated oligosaccharide (10ug) was dissolved in 1 ul of glycerol on a copper tip and the spectra were scanned at 3 sec from m/z 50 to 700.

*NMR* -  $^1\text{H}$  NMR spectra of synthetic trisaccharides were recorded on a Bruker AM-400 equipped with an Aspect 3000 computer. Approximately 700 ug of the sample was used for the NMR studies. Prior to the NMR experiment, the sample was dissolved in  $\text{D}_2\text{O}$  (99.9 atom% from Sigma Chemical Company), and lyophilized to remove exchangeable hydroxyl protons. This procedure was repeated 3 times, the last time the sample was placed in the NMR tube (Wilmad tube number 528pp). The sample was dissolved in 99.96 atom %  $\text{D}_2\text{O}$  from MSD Isotopes to give a final conc. of about 31 mM. Both one- and two-dimensional NMR experiments were performed at 298K. Higher temperature experiments (323 K) were performed as needed, to shift the solvent (HDO) peak away from one of the anomeric resonances. Acetone at 2.225 ppm was used as

an internal reference, indirectly referenced to 2,2-dimethyl-2-silapentane-5-sulfonic acid. The homonuclear chemical shift correlated spectrometry (COSY) is obtained using 2048 data points in the t<sub>2</sub>- domain and a spectral width of 2200 Hz. In the t<sub>1</sub> domain, 1024 data points were acquired and zero-filled to 2048 points before Fourier transformation to give a digital resolution of about 2.2 Hz/point.

Nuclear Overhauser experiments were performed as described by Bax H. *et al.* [3.19] with a three second presaturation pulse and a one second delay between successive pulses. The 2-D NOESY experiment was performed as described by Kumar A. *et al.* [3.20]. The spectral width was 1200 Hz. 512 data points were used in each value of t<sub>1</sub>. The mixing time was 300 msec. The total accumulation time was 6 hrs.

## Results and Discussion

Work by K.Matta [3.11] and O. Hindsgaul [3.12] suggesting exploitation of the loose donor specificity of enzymes (the use of alternative sugar nucleotides) led us to try variance in acceptors as a method to generate test compounds. We found that EC 2.4.1.22 transfers galactose from UDP-galactose to the β-linked disaccharides laminaribiose, cellobiose, and gentiobiose, and one alpha-linked disaccharide, maltose under altered reaction conditions.

Using UDP-Galactose: D-Glucose-4-β-Galactosyl transferase (EC 2.4.1.22), the product trisaccharides were gal<sub>p</sub>(β1->4)glu<sub>p</sub>(β1->3)glu, gal<sub>p</sub>(β1->4)glu<sub>p</sub>(β1->4)glu, gal<sub>p</sub>(β1->4)glu<sub>p</sub>(β1->6)glu and gal<sub>p</sub>(β1->4)glu<sub>p</sub>(α1->4)glu. All of the above trisaccharides have the same molecular weight, the only difference being linkage- position or anomeric configuration between the second glucose and the third

glucose. Previously reported substrates of EC 2.4.1.22 were glucose [3.1-3.5], GlcNAc [3.5-3.8], and a few glycoprotein oligosaccharide which have GlcNAc at their non-reducing terminus [3.6-3.10].

UDP-gal + linkage-specific disaccharide  
 laminaribiose (glu $\beta$ 1->3glu)  
 cellobiose (glu $\beta$ 1->4glu)  
 gentiobiose (glu $\beta$ 1->6glu)  
 maltose (glu $\alpha$ 1->4glu)

-----> linkage-specific trisaccharide  
 gal $\beta$ 1->4glu $\beta$ 1->3glu  
 gal $\beta$ 1->4glu $\beta$ 1->4glu  
 gal $\beta$ 1->4glu $\beta$ 1->6glu  
 gal $\beta$ 1->4glu $\alpha$ 1->4glu

Based on TLC data, EC 2.4.1.22 transfers galactose from UDP-galactose to the non-reducing terminal glucose of disaccharides at a moderate velocity during 1 hr incubation at 37°C, pH 6.0. Figure 3.1 shows thin-layer chromatography of the synthetic trisaccharide, gal $\beta$ 1->4glu $\beta$ 1->4glu. Lane A shows the reaction mixture spots before incubation. After 1 hour incubation, 2 new spots appeared from the reaction mixture (Lane B) which were UDP-galactose and trisaccharide product spots. Lane C has no UDP-galactose spots after 3 hours incubation. Lane D has darker product spots after 3 days incubation than those of 3 hours incubation. The TLC of the synthetic trisaccharide, gal $\beta$ 1->4glu $\beta$ 1->3glu, is shown in Figure 3.2. Lane A contains UDP-galactose and cellobiose spots but not product spots before incubation. After a 3 hour incubation, Lane B contains light spots of product and dark cellobiose and UDP-galactose spots. Lane C has more dense product spots after 3 days incubation than those in Lane B. Likewise, Figure 3.3 shows the TLC of the synthetic trisaccharide, gal $\beta$ 1->4glu $\beta$ 1->6glu. At each incubation time, the results are similar to those shown in Figure 3.2. After 3 days incubation, more abundant product spots appeared.

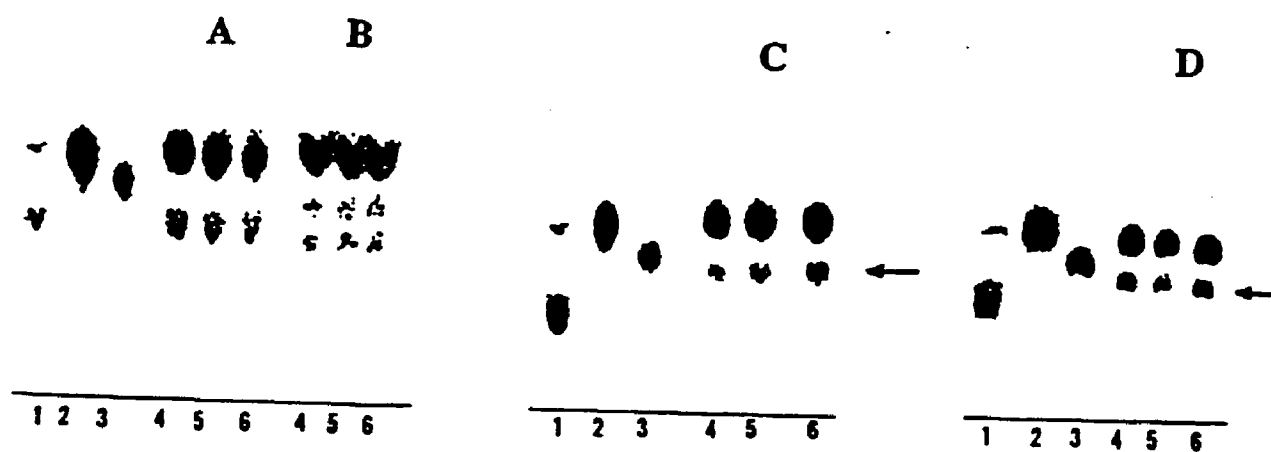


**Fig. 3.1 Thin-layer chromatography of synthesized trisaccharide, G4 (gal $\beta$ 1-4glu $\beta$ 1-4glu).** The thin-layer plate was developed with n-butanol-ethanol-water (2:1:1 v/v/v) and the compounds were visualized with orcinol- sulfuric acid reagent. A) No incubation, B) 1hr incubation C) 3hr incubation, D) 3 days incubation at 37°C. Arrows show trisaccharide product spots. Lanes 1-3 on each plate are as follows: (1) standard UDP-galactose, (2) standard cellobiose, (3) standard cellotriose, (4)(5)(6) synthesized trisaccharide from reaction mixture.



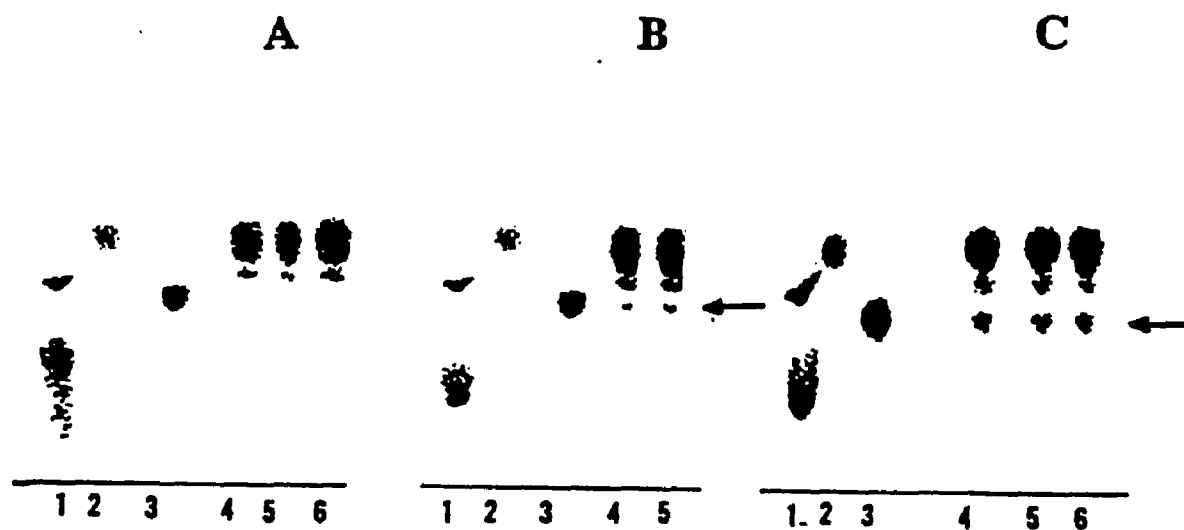


**Fig. 3.2 Thin-layer chromatography of synthesized trisaccharide, G3(gal $\beta$ 1-4glu $\beta$ 1-3glu).** The thin-layer plate was developed with *n*-butanol-ethanol-water (2:1:1 v/v/v) and the compounds were visualized with orcinol- sulfuric acid reagent. A) No incubation, B) 3hr incubation, C) 3days incubation at 37°C. Arrows show trisaccharide product spots. Lanes 1-3 on each plate are as follows: (1) standard UDP-galactose, (2) standard laminaribiose, (3) standard cellotriose, (4)(5)(6) synthesized trisaccharide from reaction mixture.



**Fig. 3.3 Thin-layer chromatography of synthesized trisaccharide, G6 (gal $\beta$ 1-4glu $\beta$ 1-6glu).** The thin-layer plate was developed with n-butanol-ethanol-water (2:1:1 v/v/v) and the compounds were visualized with orcinol- sulfuric acid reagent. A) No incubation, B) 3hr incubation, C) 3days incubation at 37°C. Arrows show trisaccharide product spots. Lanes 1-3 on each plate are as follows: (1) standard UDP-galactose, (2) standard gentiobiose, (3) standard cellotriose, (4)(5)(6) synthesized trisaccharide from reaction mixture.

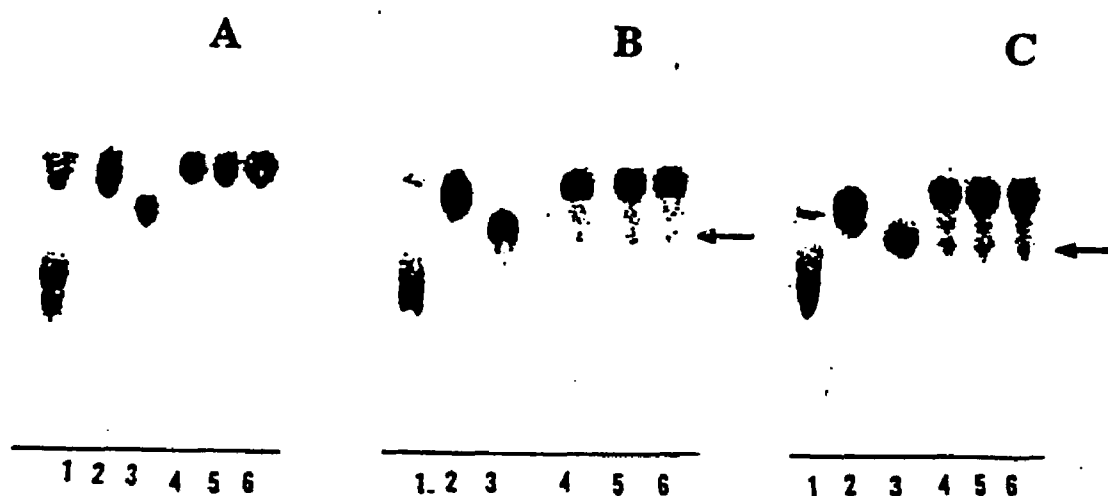


**Fig. 3.4 Thin-layer chromatography of synthesized trisaccharide,  $G\alpha 4$  (gal $\beta$ 1-4glu $\alpha$ 1-4glu).** The thin-layer plate was developed with n-butanol-ethanol-water (2:1:1 v/v/v) and the compounds were visualized with orcinol- sulfuric acid reagent. A) No incubation, B) 3hr incubation, C) 3days incubation at 37°C. Arrows show trisaccharide product spots. Lanes 1-3 on each plate are as follows: (1) standard UDP-galactose, (2) standard maltose, (3) standard cellotriose, (4)(5)(6) synthesized trisaccharide from reaction mixture.

The TLC of synthetic trisaccharide, gal $\beta$ 1- >4glu $\alpha$ 1- >4glu, is shown in Figure 3.4. Product spots after 3 days incubation (Lane B) were much weaker than  $\beta$ -linked trisaccharides we synthesized. This result agrees with the strong  $\beta$ -anomeric preference of EC 2.4.1.22 suggested by Lambright *et al.* [3.6]. Biogel P-2 chromatography was used to purify product trisaccharides from reaction mixtures. Each fraction of reaction mixture passed through the P-2 column was analyzed using sulfuric acid [3.17] and phenol-sulfuric acid colorimetrically detected at 490 nm (Fig. 3.5-3.8) [3.16]. Fig. 3.5A shows each fraction of  $\beta$ 1- >4 linked reaction mixture from the P-2 column spotted on TLC. Fraction numbers 79-83 contain the product trisaccharide, gal $\beta$ 1- >4glu $\beta$ 1- >4glu (Fig. 3.5B). Fraction numbers 85-91 contain substrate disaccharide, cellobiose (Fig. 3.5B). Other synthetic trisaccharides were purified (Fig. 3.6-3.8) in the same way. From phenol-sulfuric acid colorimetric data, the  $\beta$ 1- >4 linked disaccharide, cellobiose, was the best substrate for EC 2.4.1.22 among the  $\beta$ -disaccharides examined (laminaribiose, gentiobiose).

To our knowledge, none of these four trisaccharides have been previously synthesized. After methylation of purified product trisaccharides, molecular ions of trisaccharides were obtained from synthetic product using both Finnigan TSQ70 Triple quadrupole (Fig.3.9) and Bio-Ion  $^{252}\text{Cf}$  TOF (Time Of Flight)(Fig. 10) instruments. Figure 3.9 shows molecular ions ( $m/z$  659) for  $\beta$ 1- >3 linked trisaccharide (Fig. 3.9A), the  $\beta$ 1- >4 linked trisaccharide (Fig. 3.9B), and  $\beta$ 1- >6 linked trisaccharide (Fig. 3.9C). In Figure 3.10, strong sodium-adduct molecular ions ( $m/z$  681) were shown from gal $\beta$ 1- >4glu $\beta$ 1- >3glu (Fig. 3.10A), gal $\beta$ 1- >4glu $\beta$ 1- >4glu (Fig. 3.10B), gal $\beta$ 1- >4glu $\beta$ 1- >6glu (Fig. 3.10C).

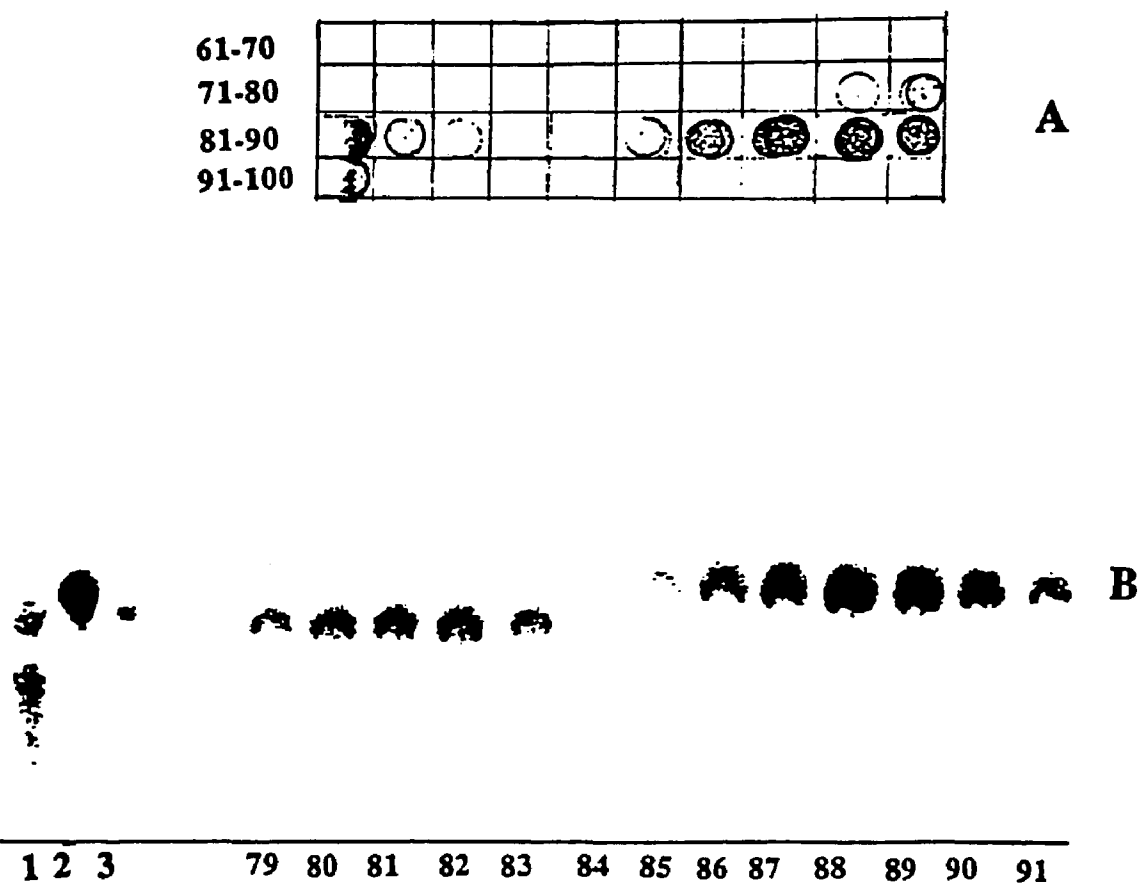
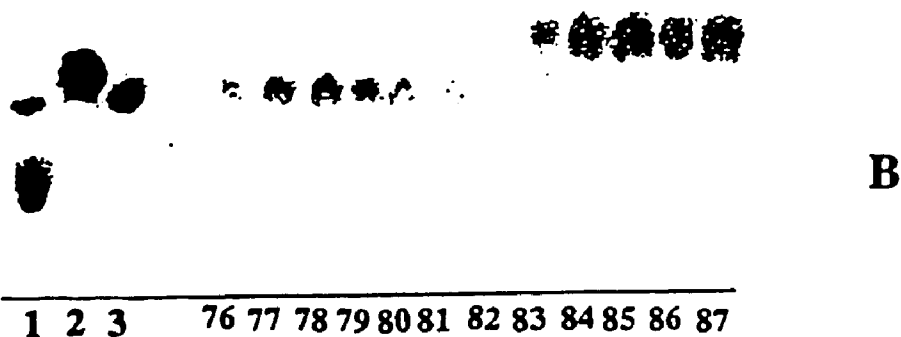
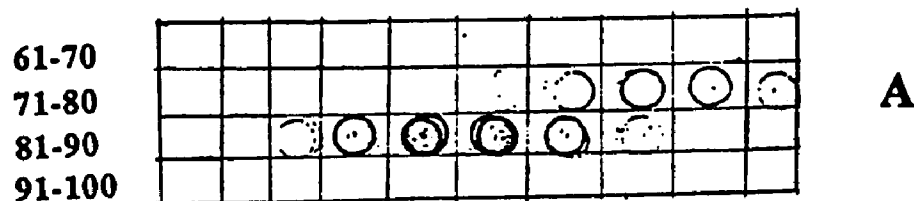


**Fig. 3.5 Purification of synthesized trisaccharide, G4 (gal $\beta$ 1-4glu $\beta$ 1-4glu).**  
 A. 3 ul of each fraction (Tube No. 61-100) purified by P- 2 chromatography was spotted on Anal Tech Silica Gel G Uniplates (scored 10X20 cm, 250 micron), and the saccharide was determined by sulfuric acid spray method, B. Each spot that contained saccharide on the thin-layer plate was developed with n-butanol-ethanol-water (2:1:1 v/v/v) and the compounds were visualized with orcinol- sulfuric acid reagent. (1) standard UDP-galactose, (2) standard cellobiose, (3) standard cellotriase, (79-91) Tube No. of synthesized trisaccharide, G4 (gal $\beta$ 1-4glu $\beta$ 1- 4glu) and cellobiose obtained from Bio-Gel P2 chromatography.



1 2 3      76 77 78 79 80 81 82 83 84 85 86 87

**Fig. 3.6 Purification of synthesized trisaccharide, G3 (gal $\beta$ 1-4glu $\beta$ 1-3glu).** A. 3  $\mu$ l of each fraction (Tube No. 61-100) purified by P-2 chromatography was spotted on Anal Tech Silica Gel G Uniplates (scored 10X20 cm, 250 micron), and the saccharide was determined by sulfuric acid spray method, B. Each spot that contained saccharide on the thin-layer plate was developed with n-butanol-ethanol-water (2:1:1 v/v/v) and the compounds were visualized with orcinol-sulfuric acid reagent. (1) standard UDP-galactose, (2) standard laminaribiose, (3) standard cellotriose, (76-87) Tube No. of synthesized trisaccharide, G3 (gal $\beta$ 1-4glu $\beta$ 1-3glu) and laminaribiose obtained from Bio-Gel P2 chromatography.

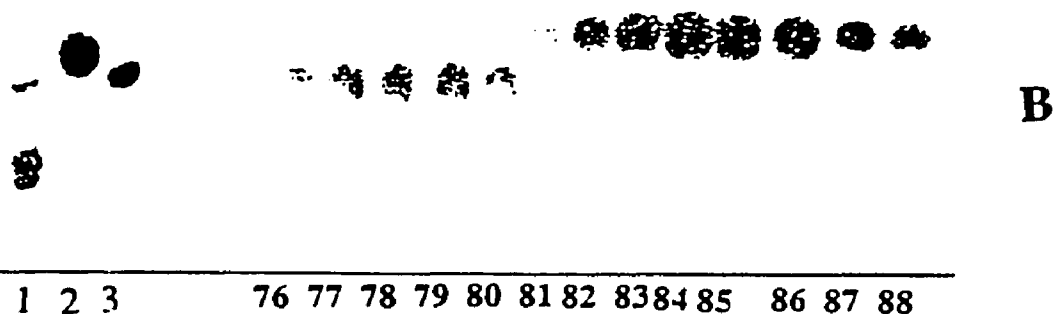
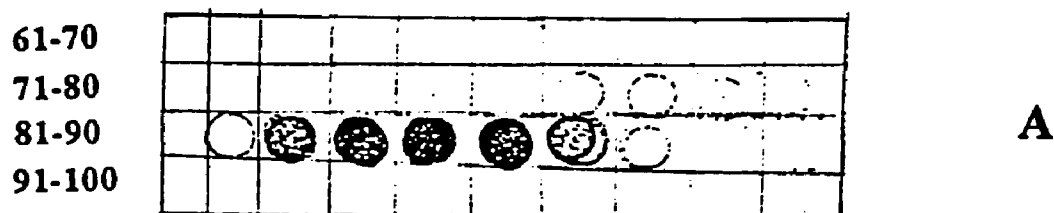
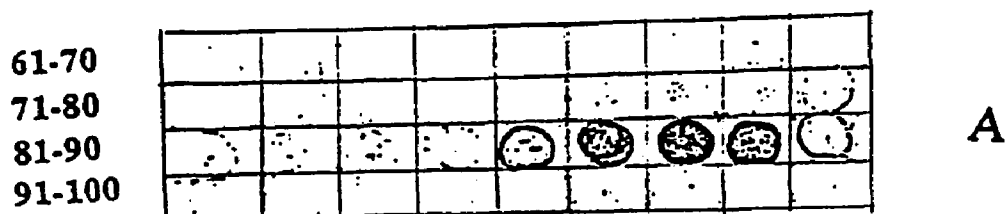
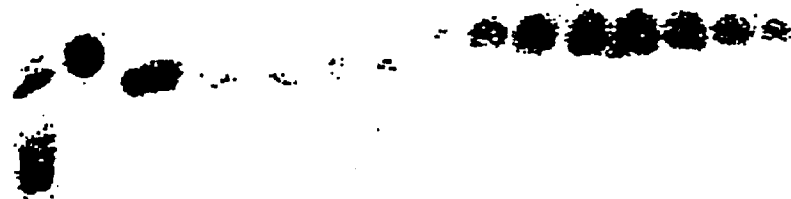


**Fig. 3.7 Purification of synthesized trisaccharide, G6 (gal $\beta$ 1-4glu $\beta$ 1-6glu).**  
 A. 3  $\mu$ l of each fraction (Tube No. 61-100) purified by P-2 chromatography was spotted on Anal Tech Silica Gel G Uniplates (scored 10X20 cm, 250 micron), and the saccharide was determined by sulfuric acid spray method, B. Each spot that contained saccharide on the thin-layer plate was developed with n-butanol-ethanol-water (2:1:1 v/v/v) and the compounds were visualized with orcinol-sulfuric acid reagent. (1) standard UDP-galactose, (2) standard gentiobiose, (3) standard cellotriose, (76-88) Tube No. of synthesized trisaccharide, G6 (gal $\beta$ 1-4glu $\beta$ 1-6glu) and gentiobiose obtained from Bio-Gel P2 chromatography.



A



B

---

A B C 80 81 82 83 84 85 86 87 88 89 90 91

**Fig. 3.8 Purification of synthesized trisaccharide,  $G\alpha 4$  ( $gal\beta 1-4glu\alpha 1-4glu$ ).**  
 A. 3  $\mu$ l of each fraction (Tube No. 61-100) purified by P- 2 chromatography was spotted on Anal Tech Silica Gel G Uniplates (scored 10X20 cm, 250 micron), and the saccharide was determined by sulfuric acid spray method, B. Each spot that contained saccharide on the thin-layer plate was developed with n-butanol-ethanol-water (2:1:1 v/v/v) and the compounds were visualized with orcinol- sulfuric acid reagent. (1) standard UDP-galactose, (2) standard maltose, (3) standard cellotriose, (80-91) Tube No. of synthesized trisaccharide,  $G\alpha 4$  ( $gal\beta 1-4glu\alpha 1-4glu$ ) and maltose obtained from Bio-Gel P2 chromatography.



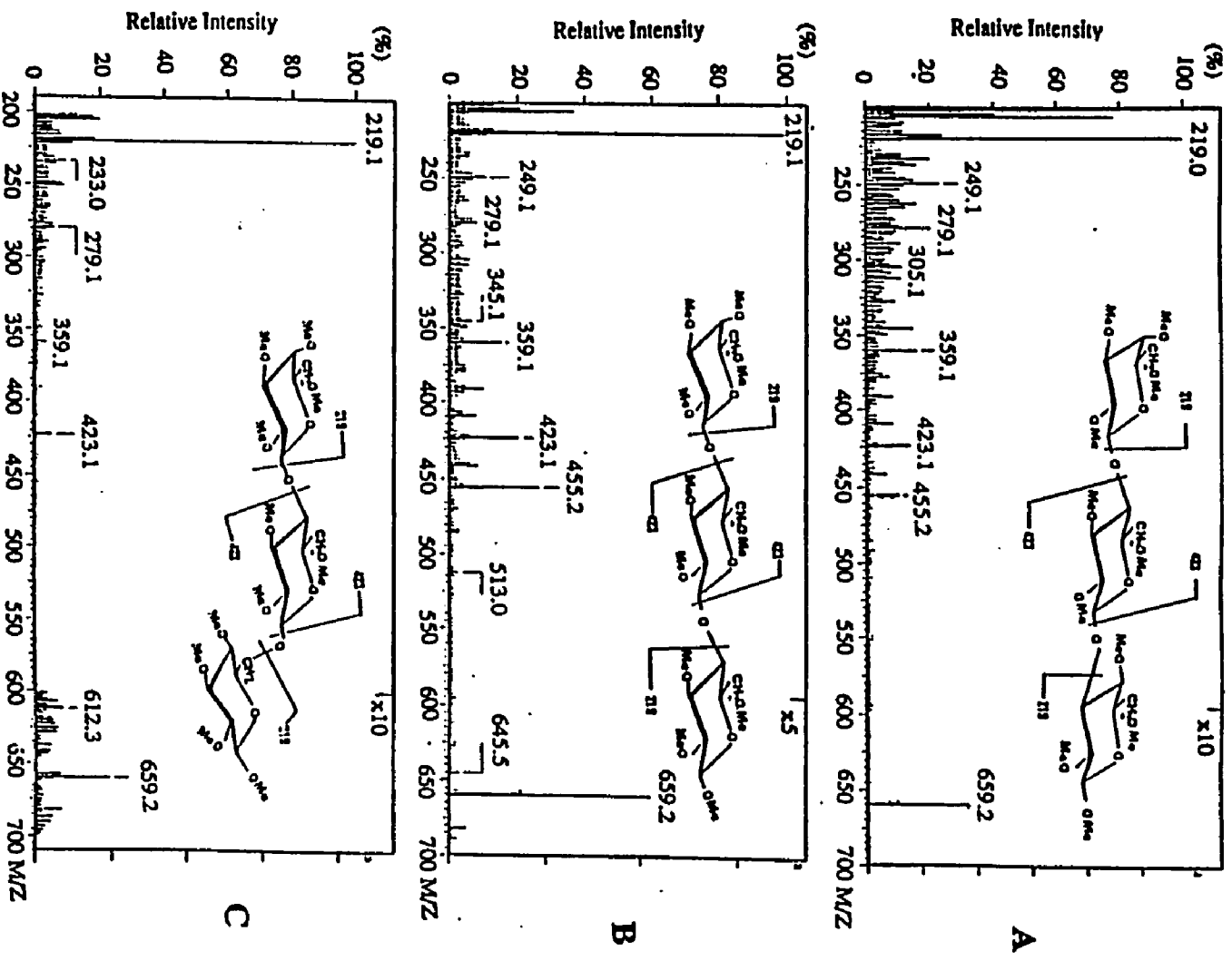


Fig. 3.9 FAB MS spectra of permethylated Gal<sub>p</sub> (β1-4)Glu<sub>p</sub> (β1-X)Glu<sub>p</sub> where X=3(A), 4(B), or 6(C).

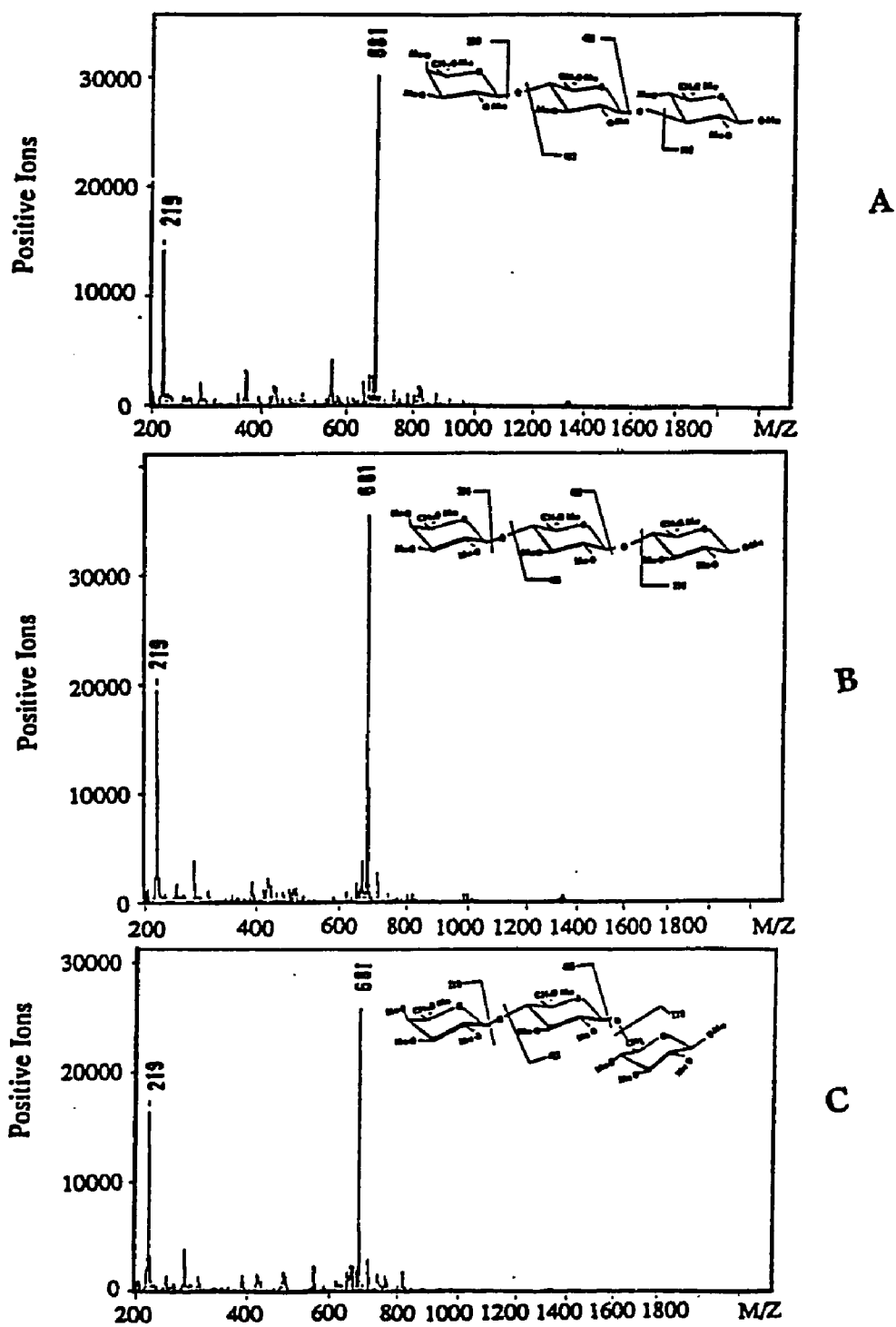


Fig. 3.10 TOF spectra of permethylated Gal<sub>p</sub>(β1-4)Glu<sub>p</sub>(β1-X)Glu<sub>p</sub> where X=3(A), 4(B), or 6(C).

Further details of the structure of synthetic trisaccharides were established by NMR. Significantly, both anomers of the compounds gave good signal/noise ratios in both the 1- and 2-D spectra. One of the anomers (the  $\alpha$ ) was only 30-40 % of the total concentration and each anomer have their own independent set of resonances. Anomeric configuration and the number of sugar residues were determined by measuring the coupling constants and integral intensities of the H-1 doublets. Figure 3.11 shows the one-dimensional  $^1\text{H}$  NMR spectrum of the synthetic trisaccharide, gal $\beta$ 1- $\rightarrow$ 4glu $\beta$ 1- $\rightarrow$ 4glu, in  $\text{D}_2\text{O}$  at 298 K (bottom) and 323 K (top). From the anomeric region ( $\delta$ 4.0 - 5.3 ppm), it is possible to estimate the number of sugar residues. There are doublets corresponding to three  $\beta$  anomeric protons and one small doublet for the reducing end  $\alpha$ -anomeric proton. By increasing the temperature from 298 K to 323 K, the HDO peak shifted upfield to reveal that there are only three  $\beta$ -anomeric protons. From the 1-D NMR spectra, the synthetic product was confirmed as a trisaccharide. The anomeric protons were at  $\delta$ 4.45, 4.55, 4.66 and 5.23 ppm with coupling constants of 7.84, 7.94, 7.99 and 3.72 Hz, respectively (Fig. 3.11; Table 3.2). From coupling constant information [3.25 and 3.26], peak B ( $\delta$ 4.55 ppm) and C ( $\delta$ 4.66 ppm) are assigned to glucose and peak A ( $\delta$ 4.45 ppm) to galactose. Usually, integration rate of protons from monosaccharides is about 0.7-0.8 [3.27 and 3.28]. According to the integration rate, the peak at  $\delta$ 4.45 ppm was galactose H1, peak at  $\delta$ 4.55 ppm was assigned to the penultimate glucose and peak at  $\delta$ 4.66 ppm and the small  $\alpha$ -doublet ( $\delta$  5.23 ppm) together were assigned to the reducing end glucose.

The linkage position between galactose and the internal glucose was established by the glycosylation shift of H-4 of the internal glucose [3.25-3.31] and by

interresidue NOE [3.30]. Figures 3.12-3.15 are the 2-D COSY spectra of gal $\beta$ 1->4glu $\beta$ 1->4glu, gal $\beta$ 1->4glu $\alpha$ 1->4glu, gal $\beta$ 1->4 glu $\beta$ 1->6glu and gal $\beta$ 1->4glu $\beta$ 1->3glu, respectively. In the expansion of the 1-D spectra of gal $\beta$ 1->4glu $\alpha$ 1->4glu (Fig. 3.13), gal $\beta$ 1->4 glu $\beta$ 1->6glu (Fig. 3.14) and gal $\beta$ 1->4glu $\beta$ 1->3glu (Fig. 3.15) on the top of their 2-D COSY spectra, the H-1 peaks of internal glucoses of the above three trisaccharides apparently resonate as triplets instead of doublets. However, this is because the two forms of the reducing end glucose in these trisaccharides influence the H-1 of the adjacent glucose. Hence, the H-1 of internal glucose that apparently resonates as a triplet, is actually overlapping doublet. Interestingly, this happens only in the  $\beta$ 3,  $\alpha$ 4 and  $\beta$ 6 linked compounds, pointing to the fact that the 4 $\beta$ -linked internal glucose is shielded from this "anomeric effect".

From the 2-D COSY spectra, each proton of the internal glucose and of the non-reducing terminal galactose was assigned by cross peaks starting from assignments of the anomeric protons. By comparing several reference spectra [3.27, 3.28 and 3.31], the chemical shifts of all protons of gal $\beta$ 1->4glu $\beta$ 1->4glu (Fig. 3.12) were slightly changed except the internal glucose H-4 which shows a much larger shift (Table 3.1). The chemical shift of the internal glucose H-4 ( $\delta$ 3.67 ppm) of gal $\beta$ 1->4glu $\beta$ 1->4glu shifted towards lower field than an earlier reference spectrum of glucose H-4 ( $\delta$ 3.39 ppm). Each internal glucose H-4 of all four synthetic trisaccharides shows a glycosylation shift which was the diagnostic signal for the gal( $\beta$ 1->4)glu linkage position (Figs. 3.12-3.15; Table 3.1). Further evidence for a 1->4 linkage between galactose and the penultimate glucose can be obtained from the 1-D NOE or 2-D NOESY experiment.

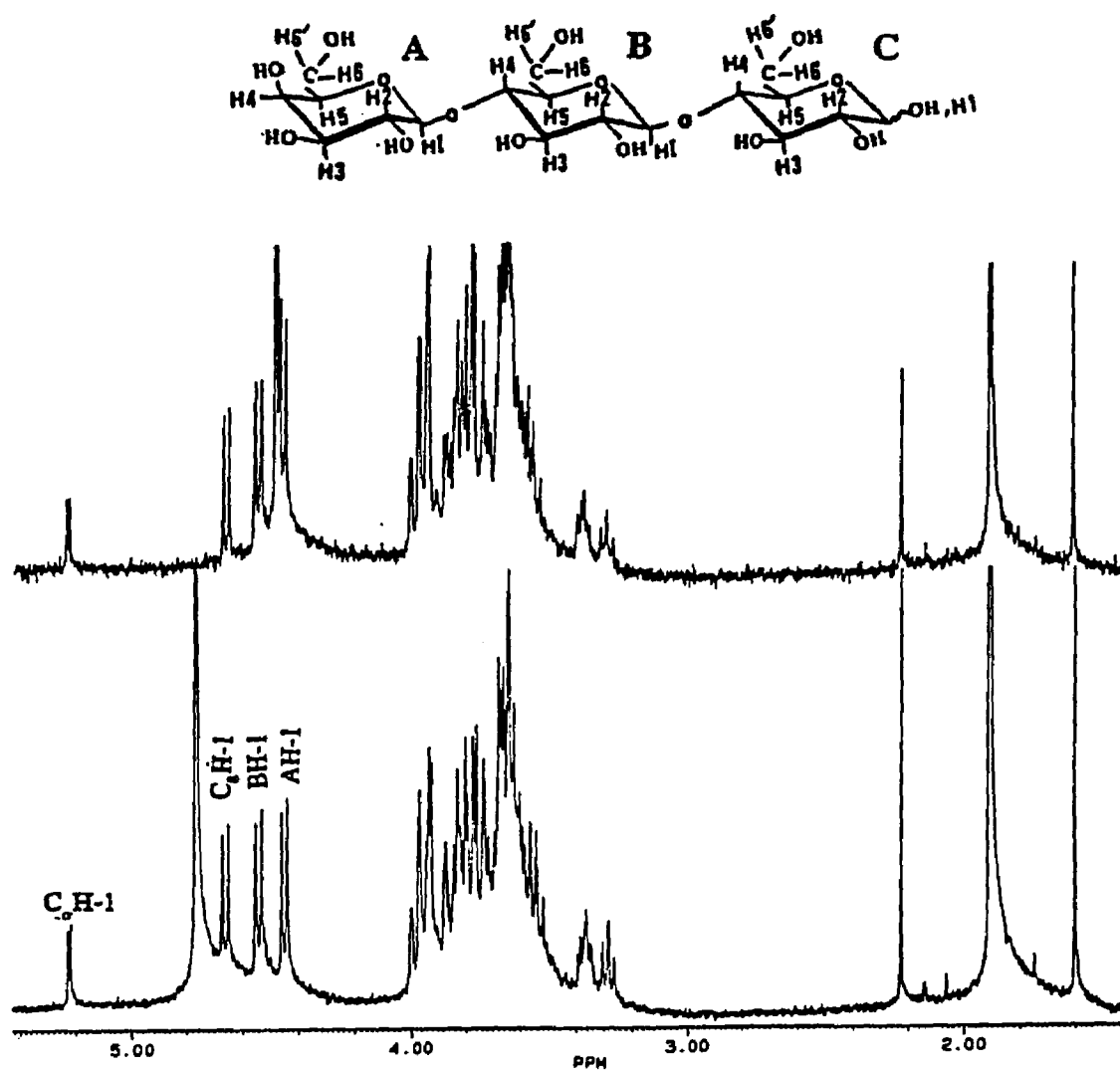


Fig. 3.11 1-D <sup>1</sup>H-NMR spectra of Gal<sub>p</sub>(β1-4)Glu<sub>β</sub>(β1-4)Glu<sub>β</sub> at 323 K (top) and 298 K (bottom).

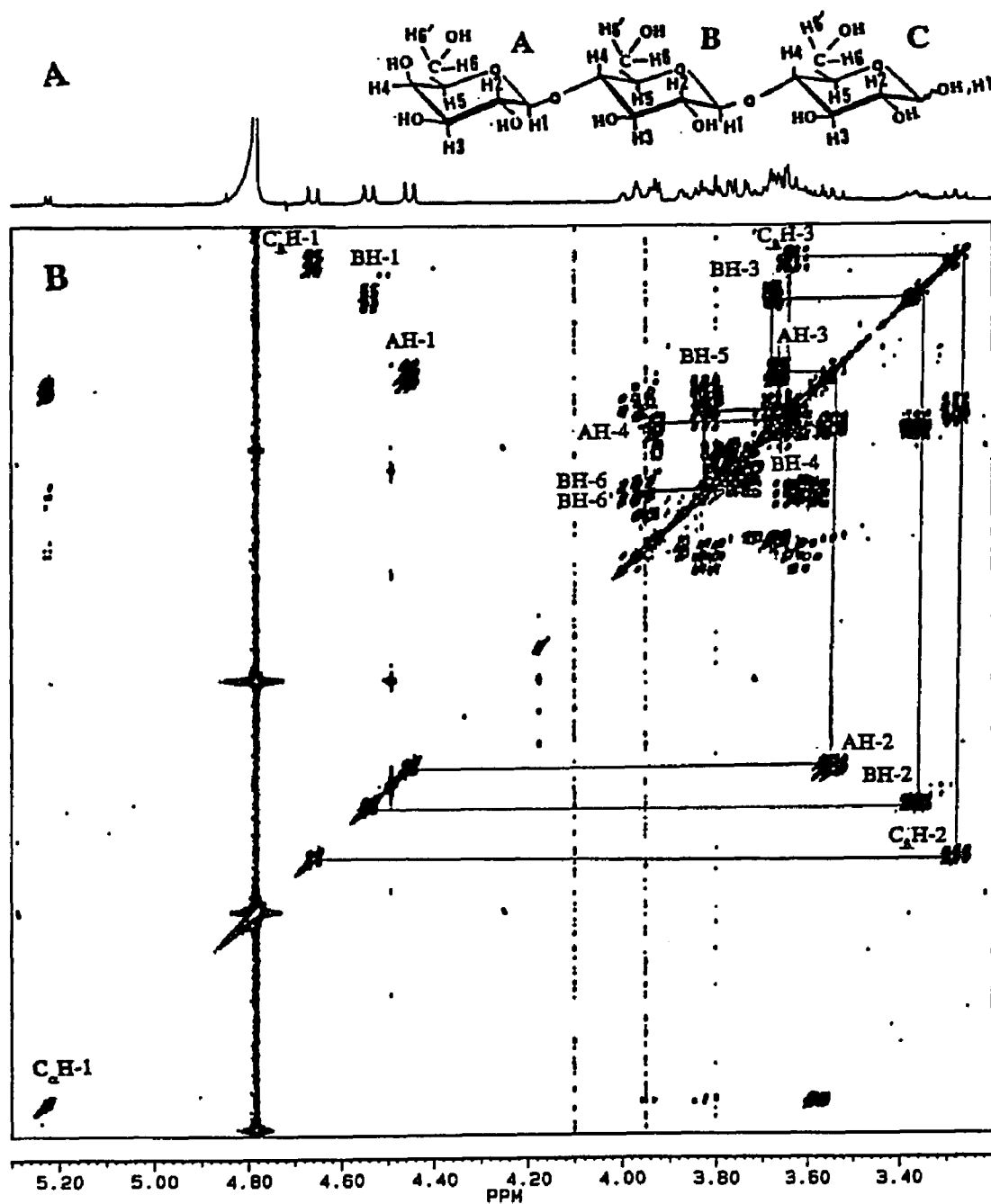


Fig. 3.12 A) Expansion of the 1-D <sup>1</sup>H NMR spectrum and B) 2-D COSY <sup>1</sup>H-NMR spectrum of Gal<sub>p</sub>(β1-4)Glu<sub>p</sub>(β1-4)Glu<sub>p</sub> at 298 K.

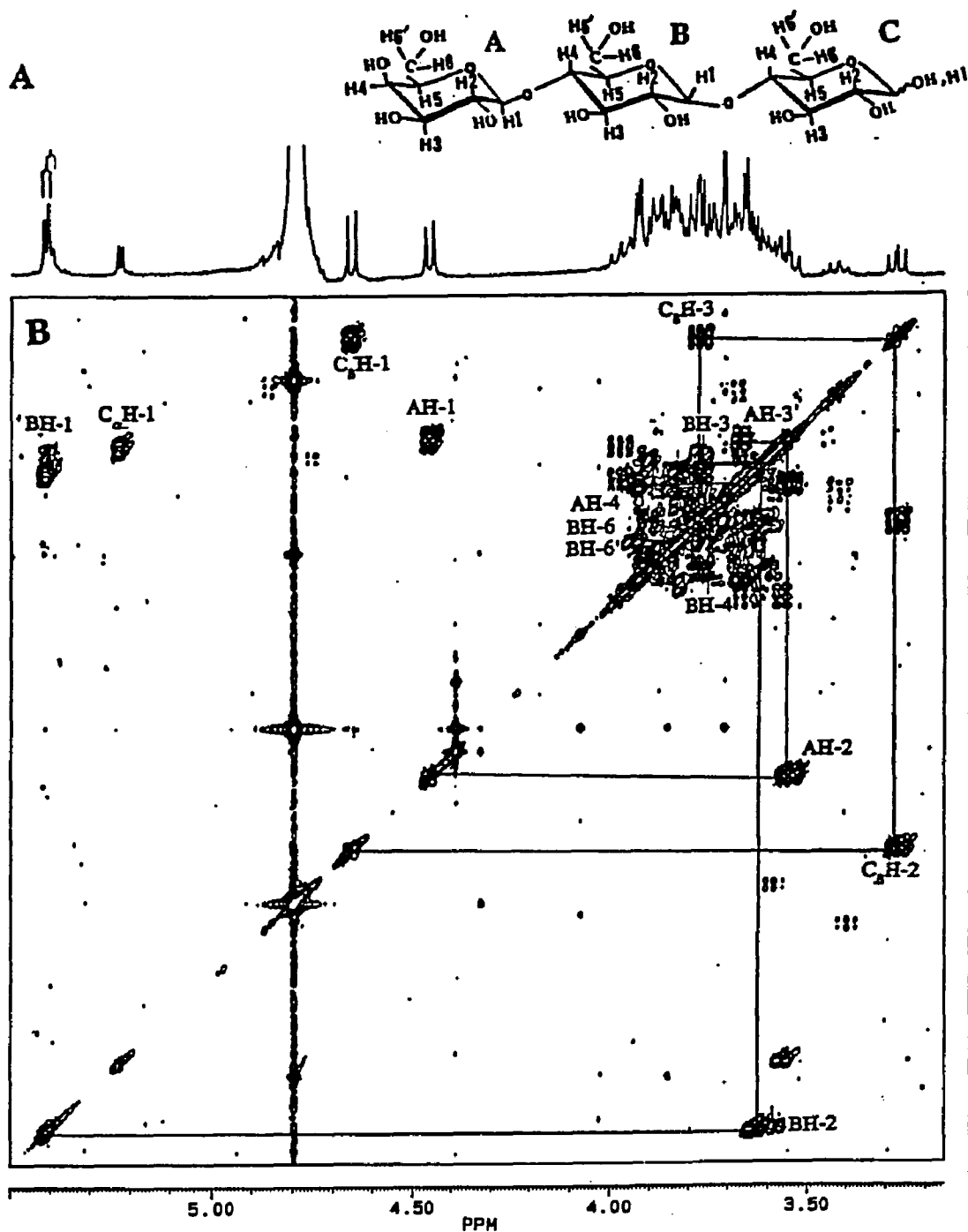


Fig. 3.13 A) Expansion of the 1-D  $^1\text{H}$  NMR spectrum and  
 B) 2-D COSY  $^1\text{H}$ -NMR spectrum of  $\text{Gal}_p(\beta 1-4)\text{Glu}_p(\alpha 1-4)\text{Glu}_p$  at 298 K.

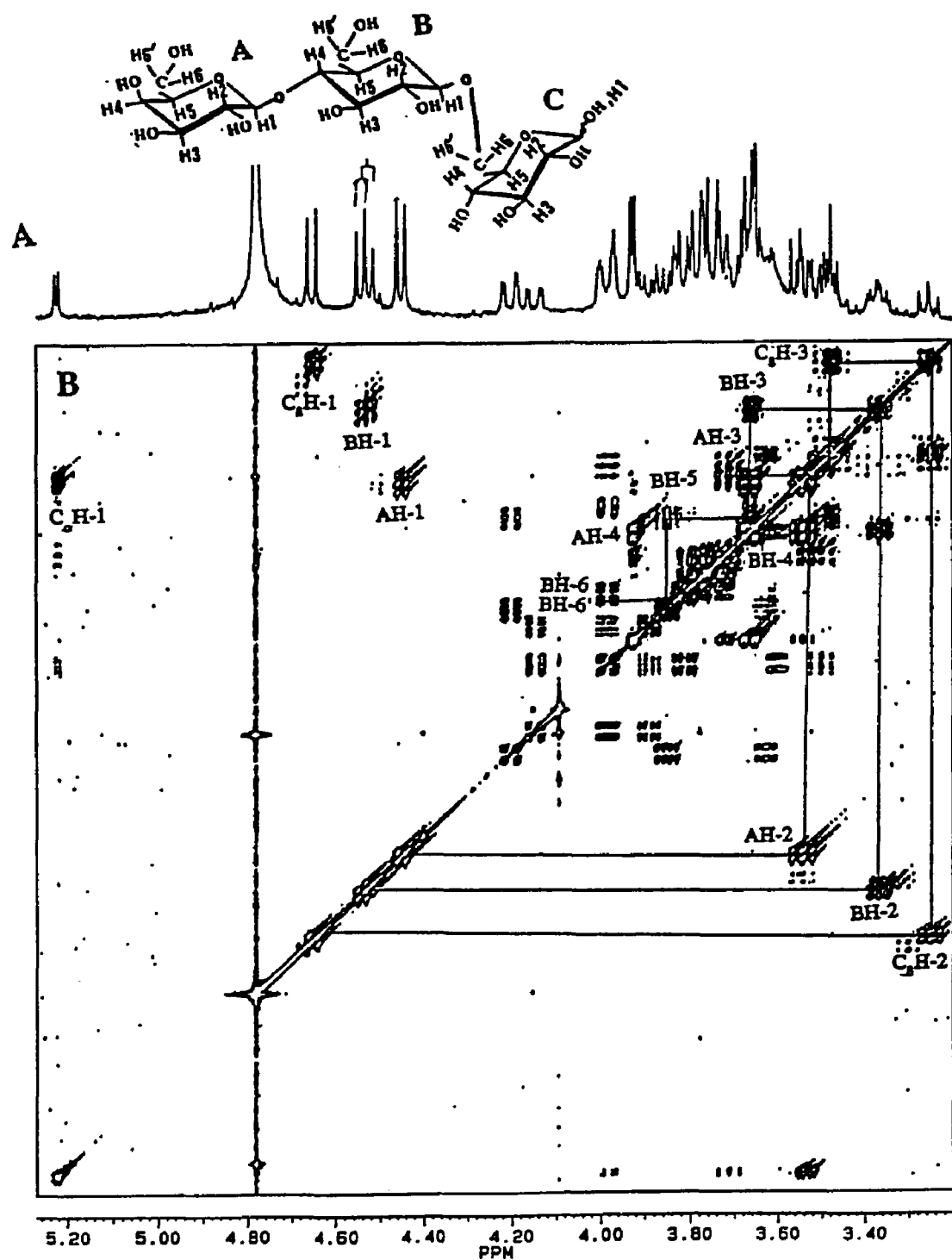


Fig. 3.14 A) Expansion of the 1-D  $^1\text{H}$  NMR spectrum and  
 B) 2-D COSY  $^1\text{H}$ -NMR spectrum of Gal<sub>p</sub>(β1-4)Glu<sub>p</sub>(β1-6)Glu<sub>p</sub> at 298 K.



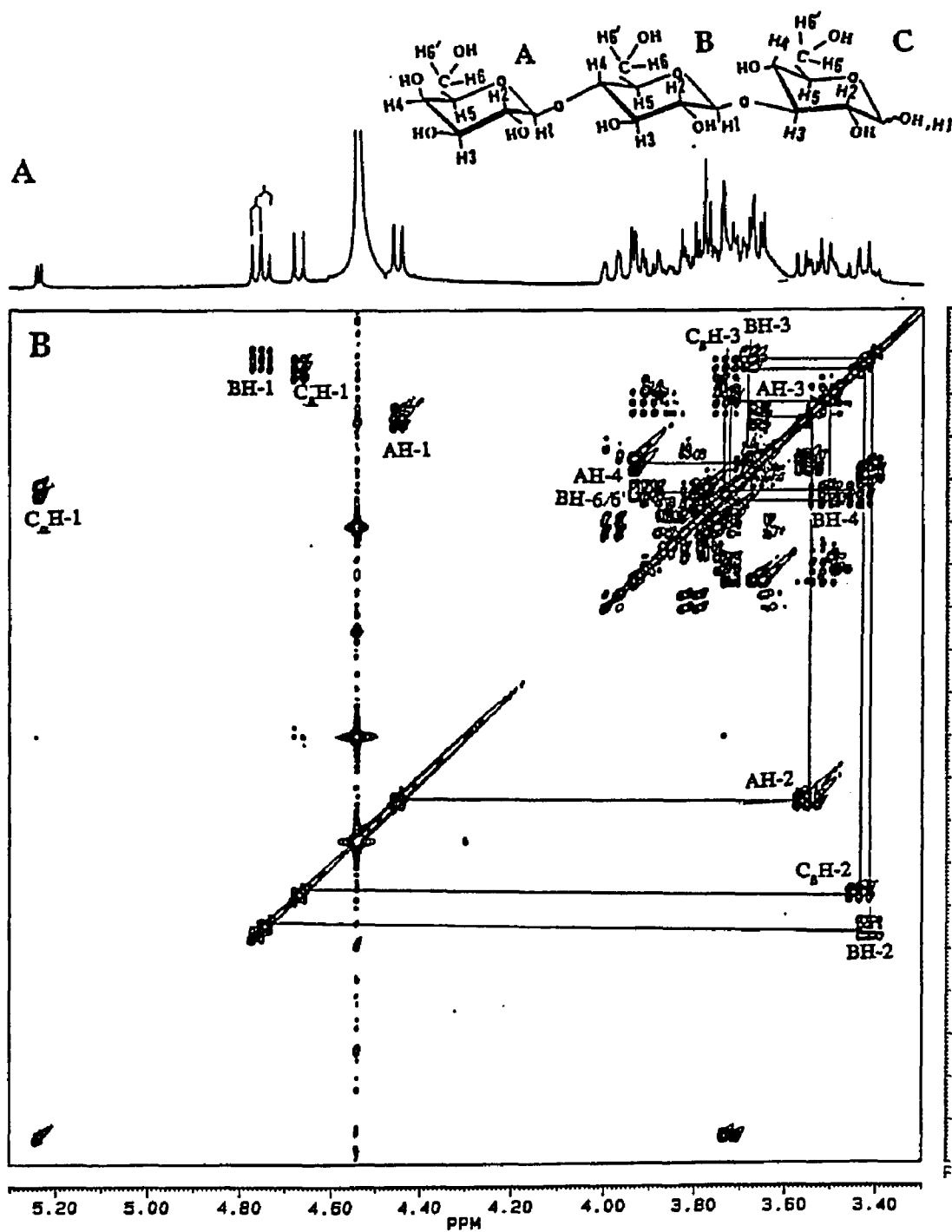


Fig. 3.15 A) Expansion of the 1-D <sup>1</sup>H NMR spectrum and B) 2-D COSY <sup>1</sup>H-NMR spectrum of Gal<sub>p</sub>(β1-4)Glu<sub>p</sub>(β1-3)Glu<sub>p</sub> at 298 K.

Table 3.1  $^1\text{H}$  chemical shift (ppm) of synthetic trisaccharides, G4 (gal $\beta$ 1-4glu $\beta$ 1-4glu), G $\alpha$ 4 (gal $\beta$ 1-4glu $\alpha$ 1-4glu), G6 (gal $\beta$ 1-4glu $\beta$ 1-6glu), and G3 (gal $\beta$ 1-4glu $\beta$ 1-3glu).

residue	proton	$^1\text{H}$ chemical shift (ppm)		
		A (gal)	B (internal glc)	C (glc)
G4	H-1	4.45	4.55	4.66 (B)/5.23 ( $\alpha$ )
	H-2	3.55	3.36	3.28
	H-3	3.68	3.71	3.66
	H-4	3.95	3.67	3.64
	H-5	--	3.84	--
	H-6/6'	--	3.96	--
G $\alpha$ 4	H-1	4.45	5.42 ( $\alpha$ )	4.65 (B)/5.25 ( $\alpha$ )
	H-2	3.56	3.60	3.27
	H-3	3.68	3.75	3.79
	H-4	3.98	3.66	3.64
	H-5	3.85	3.84	--
	H-6/6'	--	3.93	--
G6	H-1	4.45	4.53	4.65 (B)/5.23 ( $\alpha$ )
	H-2	3.55	3.39	3.25
	H-3	3.74	3.67	3.50
	H-4	3.90	3.64	--
	H-5	--	3.86	--
	H-6/6'	--	3.96	--
G3	H-1	4.45	4.54	4.66 (B)/5.23 ( $\alpha$ )
	H-2	3.55	3.42	3.43
	H-3	3.67	3.71	3.74
	H-4	3.95	3.51	--
	H-5	--	3.72	--
	H-6/6'	--	3.93	--

Table 3.2 Vicinal  $^1\text{H}$  coupling constants ( $J_{1,2}$  Hz) and integration intensities of synthetic trisaccharides.

residue	coupling constant (integration intensity)		
	A (gal)	B (internal glc)	C (glc <sub><math>\beta</math></sub> , $\alpha$ )
G4	7.84 (.652)	7.94 (.707)	7.99 (.393), 3.72 (.166)
G $\alpha$ 4	7.72 (.737)	3.95 (.849)	8.00(1.121), 3.79 (.319)
G6	7.78 (1.27)	7.76 (.748)	7.96 (.999), 3.74 (.479)
G3	7.78	8.19	8.00

Figures 3.16-3.18 are the 1-D NOE spectra of gal $\beta$ 1- $\rightarrow$ 4glu $\beta$ 1- $\rightarrow$ 4glu, gal $\beta$ 1- $\rightarrow$ 4glu $\alpha$ 1- $\rightarrow$ 4glu and gal $\beta$ 1- $\rightarrow$ 4 glu $\beta$ 1- $\rightarrow$ 6glu, respectively. Figure 3.19 is the 2-D NOESY spectrum of gal $\beta$ 1- $\rightarrow$ 4glu $\beta$ 1- $\rightarrow$ 3glu. In Figure 3.16, preirradiation of galactose H-1 ( $\delta$ 4.45 ppm), generates three NOE difference signals which are the interresidue signals of internal glucose H-4 ( $\delta$ 3.67 ppm) and of internal glucose H-3 ( $\delta$ 3.71 ppm) and an intraresidue signal from galactose H-2 ( $\delta$ 3.55 ppm).

The largest NOE signal at  $\delta$ 3.67 ppm among others indicates the 1- $\rightarrow$ 4 linkage between galactose and internal glucose (Fig.3.16). The interresidue signal of internal glucose H-3 ( $\delta$ 3.73 ppm) and intraresidue signal from galactose H-2 ( $\delta$ 3.55 ppm) appeared because of proximity. Figure 19 shows a proton 2-D NOESY spectrum of gal $\beta$ 1- $\rightarrow$ 4glu $\beta$ 1- $\rightarrow$ 3glu. The H-1 peak of galactose ( $\delta$ 4.55 ppm) is dipole-dipole coupled with H-4 peak of internal glucose ( $\delta$ 3.51 ppm). This intense signal indicates the 1- $\rightarrow$ 4 linkage position between galactose and internal glucose. Other NOE's obtained from 1-D and 2-D spectra, just confirm the purity and linkage positions of starting compounds and need not be discussed further.

The enzyme, EC 2.4.1.22 lactose synthase, therefore, transfers galactose from UDP-galactose to the  $\beta$ 4-position of the nonreducing glucose of the acceptor disaccharides laminaribiose, cellobiose, gentiobiose, and maltose.

This study increases the knowledge of the substrate flexibility for EC 2.4.1.22 and points to a useful expansion of the capabilities of enzyme-assisted synthesis by manipulation of the acceptor specificity. Also, four novel compounds resulted from the enzyme synthesis and will be used for models to determine whether linkage position can be determined in neutral oligosaccharides and their permethyl and other proton replacement derivatives by FAB-MS-CID-MS [3.32] without the usual

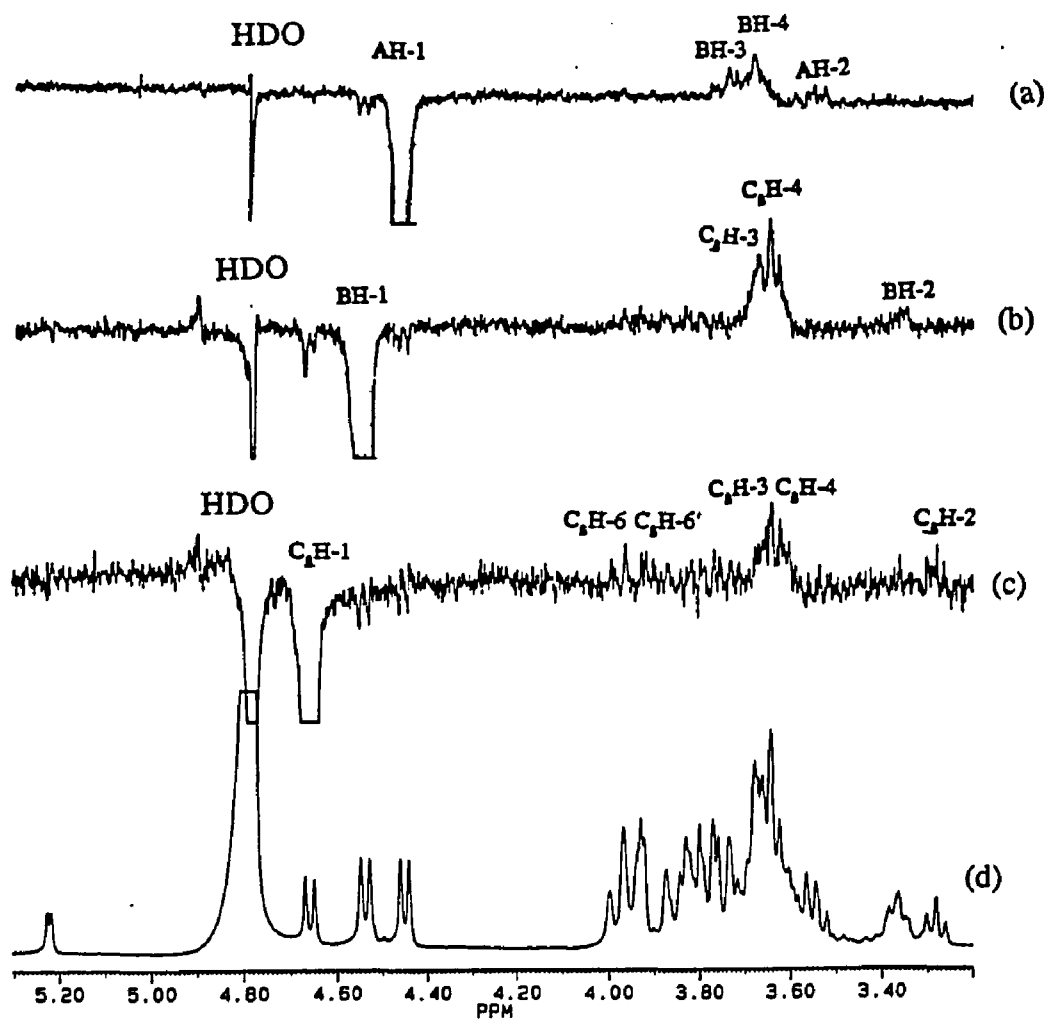


Fig. 3.16 1-D NOE  $^1\text{H-NMR}$  spectrum of Gal ( $\beta 1-4$ )Glu ( $\beta 1-4$ )Glu at 298 K, (a) preirradiation of AH-1, (b) preirradiation of  $^p\text{BH-1}$ , (c)  $^p$ preirradiation of CH-1 and (d) control spectrum.

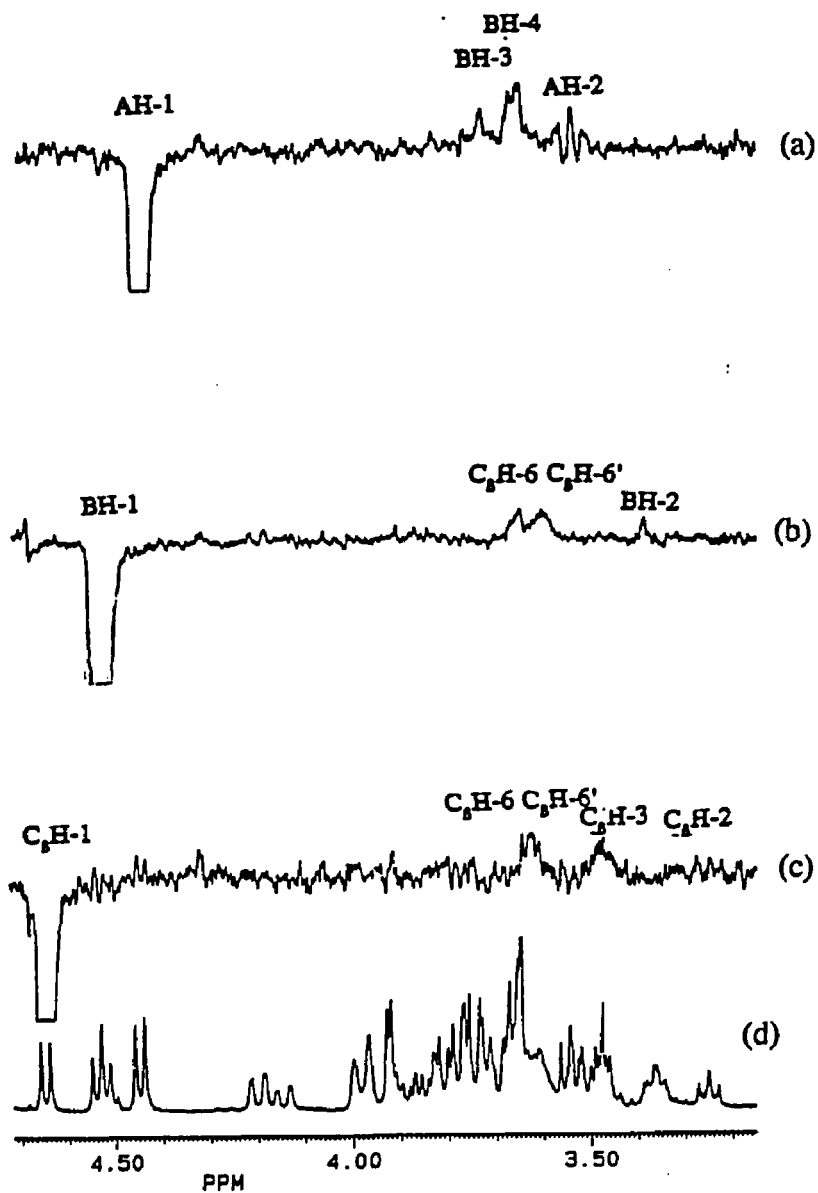


Fig. 3.17 1-D NOE  $^1\text{H-NMR}$  spectrum of Gal( $\beta$ 1-4)Glu( $\alpha$ 1-4)Glu at 298 K, (a) preirradiation of AH-1, (b) preirradiation of BH-1 and (c) control spectrum.

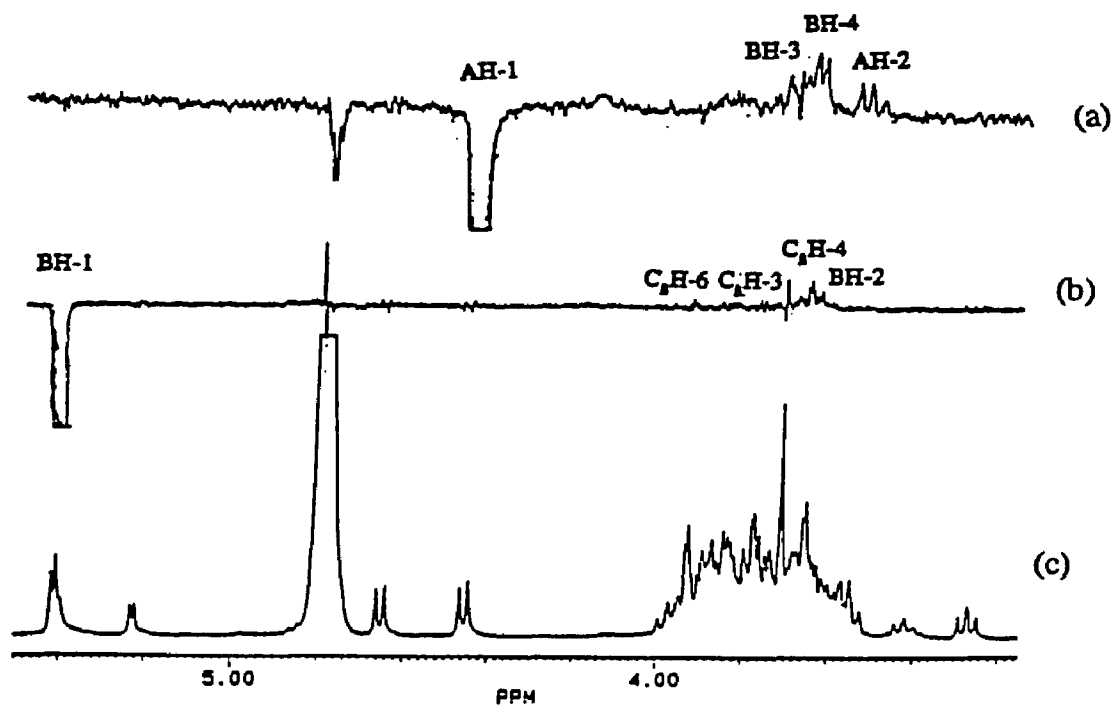


Fig. 3.18 1-D NOE  $^1\text{H-NMR}$  spectrum of Gal ( $\beta 1-4$ )Glu ( $\beta 1-6$ )Glu, at 298 K, (a) preirradiation of AH-1, (b) preirradiation of BH-1, (c) preirradiation of CH-1 and (d) control spectrum.

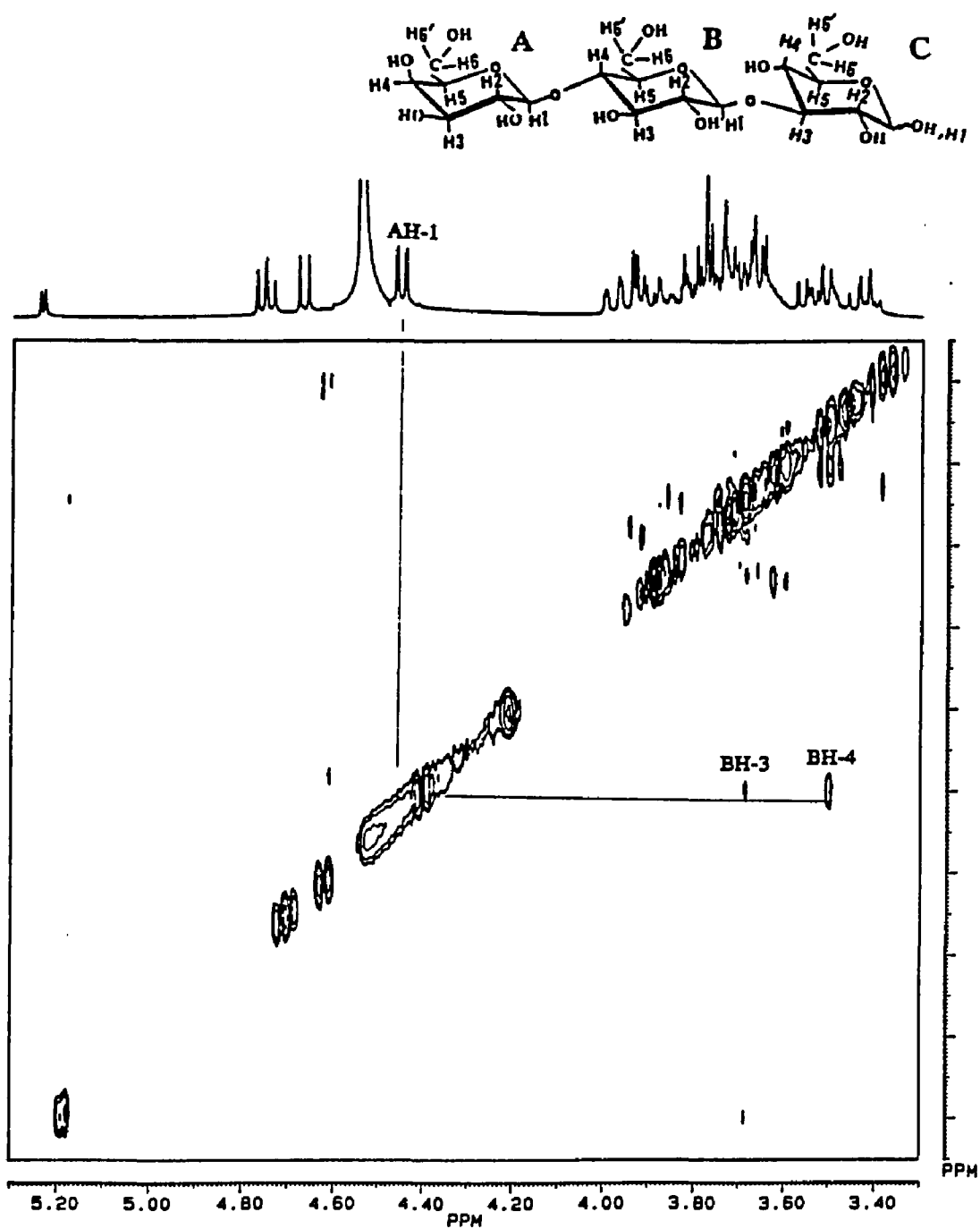


Fig. 3.19 2-D NOESY <sup>1</sup>H-NMR spectrum of Gal<sub>p</sub>(β1-4)Glu<sub>p</sub>(β1-3)Glu<sub>p</sub> at 298 K.



lengthy methylation linkage analysis [3.33]. We have previously studied two synthetic trisaccharide sets synthesized by conventional methods contain that aminosugars [3.23 and 3.24]. The four novel compounds we synthesized may be interesting acceptors for fucosyl  $\alpha$ 1- $\rightarrow$ 3 transferase and sialyl  $\alpha$ 2- $\rightarrow$ 3 transferase enzymes as core structures for sialyl Lewis-X [3.34-3.37] which are putative receptors for the neutrophil-binding factors, Elam 1 or E-selectin [3.37 and 3.38] and for L-selectin [3.39].

## References

- 3.1 R.L. Hill and K. Brew, *Adv. Enz. Relat. Area Mol. Biochem.* 43 (1975) 411-490.
- 3.2 E.C. Heath, *Ann. Rev. Biochem.* 40 (1971) 29-56.
- 3.3 T.A. Beyer, J.E. Sadler, J.I. Rearick, J.C. Paulson and R.L. Hill, *Adv. Enzymol.* 51 (1981) 23-175.
- 3.4 F.L. Schanbacher and K.E. Ebner, *J.B.C.* 245 (1970) 5057-5061.
- 3.5 D.R. Johnson, D.G. Lambright and S.S. Wong, *Biochim. Biophys. Acta* 832 (1985) 373-377.
- 3.6 D.G. Lambright, T.K. Lee and S.S. Wong, *Biochemistry* 24 (1985) 910-914.
- 3.7 K. Brew, T.C. Vanaman and R.L. Hill, *Proc. Natl. Acad. Sci.* 59 (1968) 491-497.
- 3.8 S.P. Yadav and K. Brew, *J.B.C.* 266 (1991) 698-703.
- 3.9 K.J. Kaur, S.J. Turco and R.A. Laine, *Biochemistry International* 4 (1982) 345-351.
- 3.10 H. Schachter, I. Jabbal, R.L. Hudgin and L. Pinteric, *J.B.C.* 245 (1970) 1090-1100.
- 3.11 K.L. Matta, personal communication.
- 3.12 O. Hindsgaul, personal communication.
- 3.13 L.J. Berliner and R.D. Robinson, *Biochemistry* 21 (1982) 6340-6343.
- 3.14 K. Takase and K.E. Ebner, *Current Topics In Cellular Regulation* 24 (1984) 51-62.
- 3.15 M.M. Palcic, O.P. Srivastava and O. Hindsgaul, *Carbohydr. Res.* 159 (1987) 315-324.
- 3.16 M. Dubios, K.A. Gilles, J.K. Hamilton, P.A. Revers, and F. Smith, *Anal. Chem.* 28 (1956) 350-356.
- 3.17 J.C. Touchston and M.F. Dobbins, *Practice of Thin Layer Chromatography.* (1978) John Wiley & Sons.
- 3.18 I. Ciucanu and F. Kerek, *Carbohydr. Res.* 131 (1984) 209-217.
- 3.19 A. Bax, W. Eagan, and P. Kovac, *J. Carbohydr. Chem.* 3 (1984) 593-611.

- 3.20 A. Kumar, R.R. Ernst and K. Wuthrich, *Biochim. Biophys. Acta* 95 (1980) 1.
- 3.21 B. Domon, D.R. Mueller and W.J. Ritcher, *International Journal of Mass Spectrometry and Ion Processes* 100 (1990) 301-311.
- 3.22 W.J. Ritcher D.R. Mueller and B. Domon, *Methods Enzymol.* 193 (1990) 607-623.
- 3.23 R.A. Laine, K.M. Pamidimukkala, A.D. French, R.W. Hall, S.A. Abbas, R.K. Jain, and K.L. Matta, *J. Am. Chem. Soc.* 110 (1988) 6931-6939.
- 3.24 R.A. Laine, E. Yoon, T.J. Mahier, S.A. Abbas, B. de Lappe, R.K. Jain and K.L. Matta, *Biological Mass Spectrometry*, 20 (1991) 505-514.
- 3.25 N.R. Krishna, B. Choe, M. Prabhakaran, G.C. Ekborg, L. Roden and S.C. Harvey, *J.B.C.* 265 (1990) 18256-62.
- 3.26 A. Gamlan, E. Ramanowska, U. Dabrowski and J.Dabrowski, *Biochemistry* 30 (1991) 5032-5038.
- 3.27 J. Dabrowski, P. Hanfland, H. Egge and U. Dabrowski, *Arch. Biochem. Biophys.* 210 (1981) 405.
- 3.28 J. Dabrowski, P. Hanfland and H. Egge, *Methods in Enzymology* 83 (1982) 69-86.
- 3.29 Y.T. Li, B.Z. Carter, B.N. Rao, H. Schweingruber and S.C. Li, *J.B.C.* 266 (1991) 10723-10726.
- 3.30 H. Egge, J. Dabrowski and P. Hanfland, *Pure and Appl. Chem.*, 56 (1984) 807-819.
- 3.31 S.W. Homans, R.A. Dwek and T.W. Rademachek, *Biochemistry* 26 (1987) 6571-6578.
- 3.32 E. Yoon and R.A. Laine, will be submitted for publication (1991).
- 3.33 C.G. Hellerqvist, *Methods in Enzymology* 193 (1990) 554-573.
- 3.34 Y. Fukushi, S. Hakomori, E. Nudelman and N. Cochran, *J.B.C.* 259 (1984) 4681-4685.
- 3.35 K. Fukushima, M. Hirota, P.I. Terasaki, A. Wakisaka, H. Togashi, D. Chia, N. Suyama, Y. Fukushi, E. Nudelman and S. Hakomori, *Cancer Res.* 44 (1984) 5279-5285.
- 3.36 R. Kannagi, Y. Fukushi, T. Tachikawa, A. Noda, S. Shin, K. Shigeta, K. Hiraiwa, N. Fukuda, T. Inamoto, S. Hakomori, and H. Imura, *Cancer Res.* 46 (1986) 2619- 2626.

3.37 J.B. Lowe, L.M. Stoolman, R.P. Nair, R.D. Larsen, T.L. Berhend and R.M. Marks, *Cell* 63 (1990) 475-482.

3.38 E. Larsen, A. Celi, G.E. Gilbert, B.C. Furie, J.K. Erban, R. Bonfanti, D.D. Wagner and B. Furie, *Cell* 59 (1989) 305-312.

3.39 Tiemeyer M., Swiedler S.J., Ishihara, M., Moreland M., Schweingruber H., Hirtzer P., and Brandley, B.K. *Proc. Natl. Acad. Sci.* 88 (1991) 1138-1142.

## Chapter IV.

### Linkage Position Determination of Permethylated Neutral Novel Trisaccharides by Collisional Induced Dissociation and Tandem Mass Spectrometry

#### Introduction

Sets of neutral trisaccharides having different internal and terminal linkages have been synthesized to develop a sensitive method for analysis of the reducing terminal linkage position. The trisaccharides, gal( $\beta$ 1->4)glu( $\beta$ 1->X)glu, where X=3, 4 and 6, were synthesized [4.1] and examined using Fast Atom Bombardment (FAB)-Collision-induced dissociation (CID)-Tandem mass spectrometry. Results have been rationalized using molecular modeling. We have previously reported results with synthetic trisaccharides containing aminosugars [4.2,4.3]. A novel approach of relating daughter ion to parent ion ratios and collision energy offset has been used to generate a slope to predict linkage position.

Fast atom bombardment (FAB) ionization combined with tandem mass spectrometry (MS/MS) and collision-induced dissociation (CID) has been used as a method to identify linkage positions in intact [4.3-4.7], alkylated [4.2], permethylated [4.2,4.8] and peracetylated [4.9-4.13] oligosaccharides. Aminosugar-containing oligosaccharides give specific fragmentation patterns due partly to charge retention [4.14-4.16] and partly due to steric hindrance to vibronic degree of motion around glycosidic bonds [4.2,4.3,4.17]. Extensions of these studies should include investigation of derivatized neutral oligosaccharides via FAB MS and FAB MS/MS in order to better understand carbohydrate fragmentation mechanisms resulting from different linkage positions. Neutral oligosaccharides are generally difficult to study using mass spectrometry because of polar and neutral characteristics [4.18].

Some oligosaccharides derived from bacterial polysaccharides and plant cell walls do not have the regularly spaced HexNAc residues found in many mammalian glycosphingolipids [4.19] and glycoproteins [4.20]. Without modification, neutral oligosaccharides may not produce sufficient glycosidic bond cleavage ions to allow complete sequence assignment .

Kochekov and Chizhov [4.21] initially introduced permethylation to several disaccharides in order to increase the EI spectra signals of neutral disaccharides. Later, Karkkainen discussed the CI mass spectrometry of permethylated trisaccharide-alditols [4.22]. Other permethylated neutral disaccharides were also studied to identify the linkage position of glycosidic bond using EI [4.23] and CI [4.24].

More recently, several laboratories have introduced chromophores or flurophore-tagging [4.25-4.27] or several derivatives such as oximes [4.28.4.29] to block the reducing end and TMAPA (trimethyl *p*-aminophenyl ammonium chloride) to incorporate a permanent positive charge into the reducing end. Dell *et al.* [4.18] also used the TMAPA derivatives in conjunction with peracetylation to obtain useful fragmentation.

In order to develop a more generally applicable discrimination method for reducing as well as non-reducing carbohydrates, FAB CID MS/MS combined with molecular modeling has been investigated using synthetic trisaccharide sets [4.2-4.4]. Our previously reported [4.2-4.4], rationale for most of the fragmentation (daughter ion) assignment was suggested to be due to steric factors. Differences in ratios (statistics) of glycosidic bond cleavage may occur due not only to ionic

considerations but also to steric hindrance of the absorbance of collision energy, leading to a higher statistical bond cleavage rate for sterically crowded linkages.

This study shows how the reducing end linkage position of different isomeric neutral trisaccharide can be distinguished when the permethylated trisaccharides undergo CID after FAB ionization. Our lab already has reported that FAB MS/MS combined with molecular modeling is a sensitive method with either intact [4.3] or permethylated [4.2] oligosaccharides to analyze the non-reducing terminal linkage position when non-reducing terminal neutral sugars are linked to a penultimate amino sugar [4.2].

### **Experimental**

Oligosaccharides were synthesized as described in the chapter III, and characterized by  $^1\text{H}$  NMR. The trisaccharides were permethylated by the method of Ciucanu and Kerek [4.30] and dissolved in chloroform.

*FAB MS*- The FAB MS spectra were obtained on a Finnigan TSQ-70 triple quadrupole instrument using Xenon gas and an Ion Tech Saddle-Field FAB gun at 8-9 KeV.

*FAB MS/MS*- The CID studies were performed using 0.8 mTorr of argon as collision gas and varying the collision energy offset from -10 to -40 eV at 5 eV increments. Each permethylated oligosaccharide (3ug) was dissolved in 1 ul of glycerol on a copper probe tip and the spectra were scanned during 3 sec from m/z 200 to 700. For CID measurements four to eight spectra from m/z 50 to 750 were averaged taken as 5 second scans at each 5 eV collision energy increment.

*Molecular calculations*- Molecular calculations were performed on a DEC MicroVAX 3500 or an IBM-3090 using SYBYL (Tripos. Associates Inc., 1989) and specially modified MM2 (Indiana Univ., 1987) force field data and software for

carbohydrate molecules. The starting geometry of the disaccharide, cellobiose, was obtained from the Cambridge Structural Data base (Cambridge Crystallographic Data Center, 1990). Each O-methyl group replaced every hydroxyl group using the graphic portion of SYBYL software. Energy contour maps were made with TOPO and SURF programs from the SURFER package (Golden Software, Inc., Golden Co.).

### Results and Discussion

The FAB MS-CID-MS spectra of the methylated synthetic trisaccharides, G3 [gal $\beta$ 1->4glu $\beta$ 1->3glu], G4 [gal $\beta$ 1->4glu $\beta$ 1->4glu] and G6 [gal $\beta$ 1->4glu $\beta$ 1->6glu] are shown in Figure 4.1 and Figure 4.2 at both -20 eV and -40 eV collision energy offset, respectively. The spectra all show the same [M+H]<sup>+</sup> ion at m/z 659. The main fragmentation process common to all members of this set [4.1] involves cleavage of the internal glycosidic bonds which give fragment ions at m/z 423, m/z 219 and m/z 187 (Scheme 4.1). The exceptional glycosidic cleavage can probably be related to bond energies. In CID, vibronic energy absorbed from collision kinetic energy imparted to molecules and distributed among several modes including normal, bending, and rotation. In low energy CID experiments, sugar ring cleavages are of very low abundance while through-the-ring cleavage fragments are more apparent in high energy CID [4.13]. Also, hydroxyl group blocking by permethylation may stabilize the ring and restrict rotation of sugar rings. Vibronic normal and bend modes are strongly connected to rotation, thereby providing spectra with strong dependence on freedom of motion at the glycosidic bonds.



### Incrementing collision energy

Fragmentation patterns and ratios could be correlated with structural features. The survival rate of the molecular ion ( $m/z$  659) in compounds decreases according to linkage position as the collision offset increases. The relative intensities of the molecular ions with respect to the daughter ions in the neutral trisaccharide series at -40 eV collision offset and 0.8 mTorr argon were as follows:

methylated G6 (80%) > methylated G4 (40%) > methylated G3 (30%). We expected that the methylated G4, 1->4 linkage containing compound would be cleaved easier than the 1->3 linkage containing compound (methylated G3) because of the nearby methoxyl group on the C3 position and the bulky  $\text{CH}_2\text{OCH}_3$  group on C5 of the ring. This is opposite to the experimental observations of cleavage from amino-sugars. Unexpectedly, the 1->3 linkage shows the highest rate of cleavage in the neutral trisaccharides among the three linkages. This result corroborates the observations of Domon *et al.* [4.9] who utilized peracetylated linkage- isomeric disaccharides. Pare *et al.* [4.31] suggested that the oxygen lone pair also affects the steric hindrance around the glycosidic bond, but the specific effects of the lone pair are still controversial [4.31,4.32].

The major fragment ion at  $m/z$  423 is formed by loss of methylated glucose with cleavage of the glycosidic bond between the reducing saccharide and the internal glucose (Scheme 4.1). Subsequent loss of the methylated internal sugar or, more likely, loss of the reducing disaccharide with cleavage of the glycosidic bond between the non-reducing monosaccharide (with charge retention) and the internal glucose gives  $m/z$  219 (the molecular weight of a methylated monosaccharide). The  $m/z$  455 which is the molecular weight of a methylated disaccharide and protonated methoxyl group appeared in methylated G3 and methylated G4, but not in

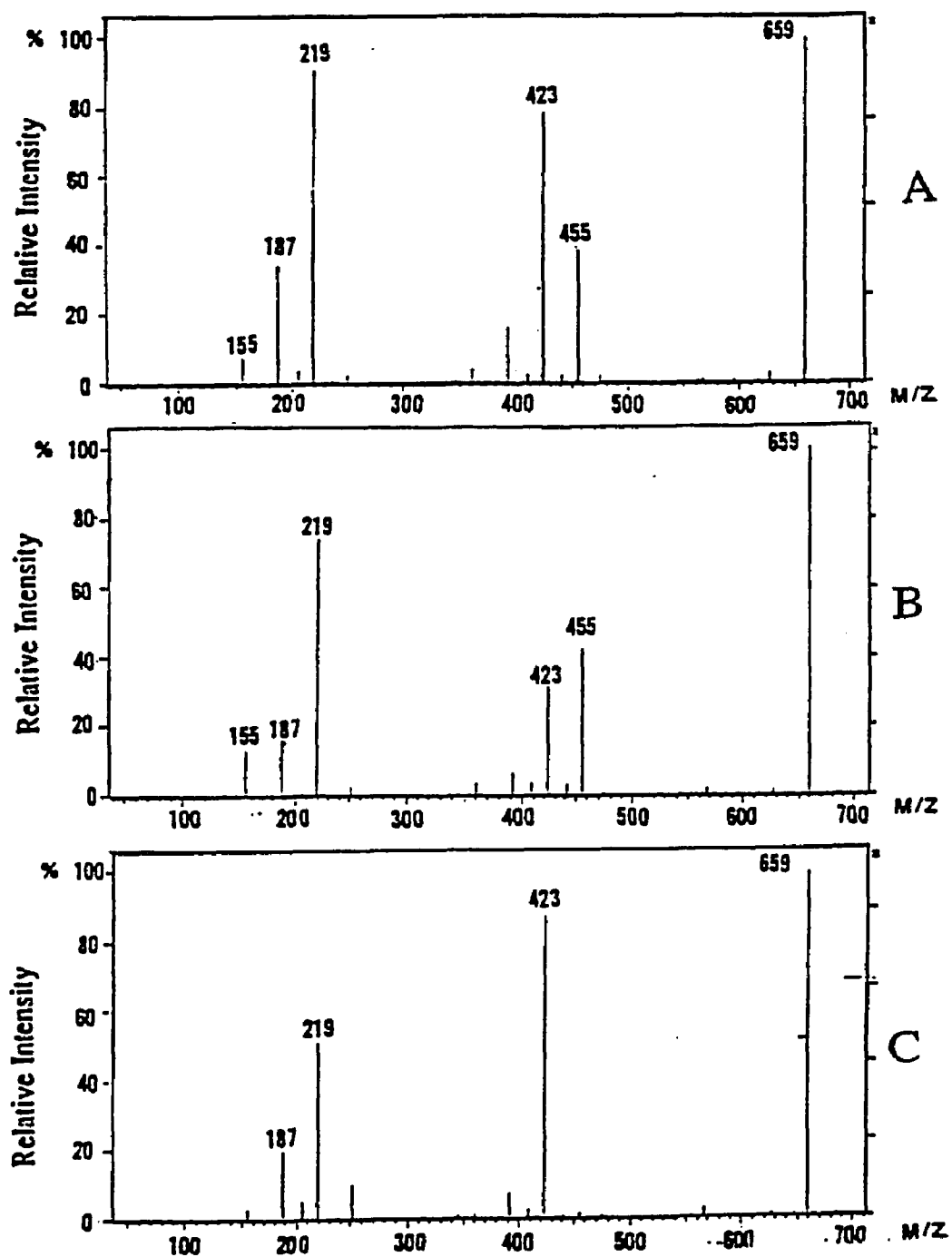


Fig. 4.1 FAB-MS-CAD-MS spectra of  $m/z$  659 for permethylated  $\text{Gal}_p(\beta 1-4)\text{Glu}_p(\beta 1-X)\text{Glu}_p$  at  $-20\text{eV}$  where X=3 (A), 4(B), or 6(C).

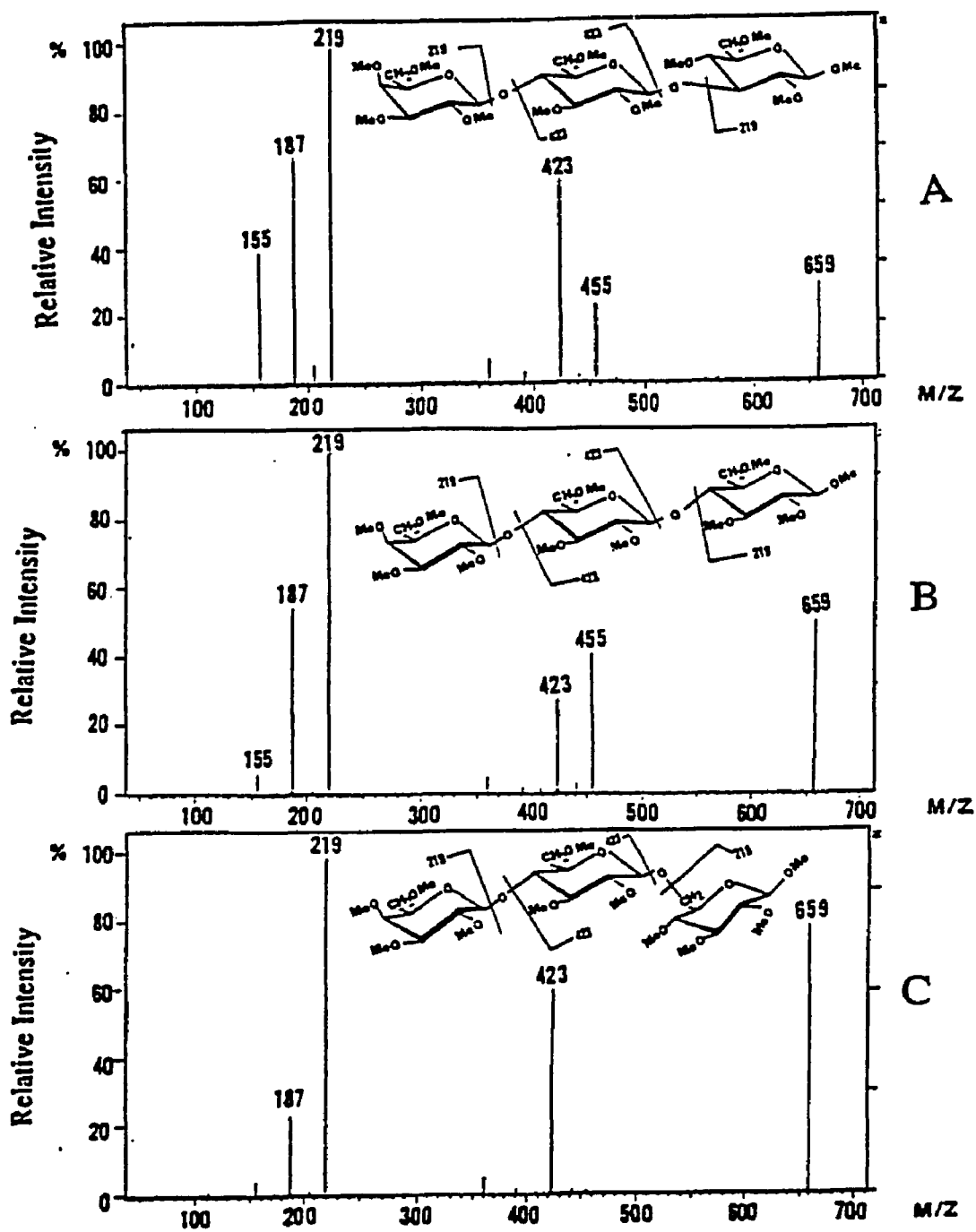
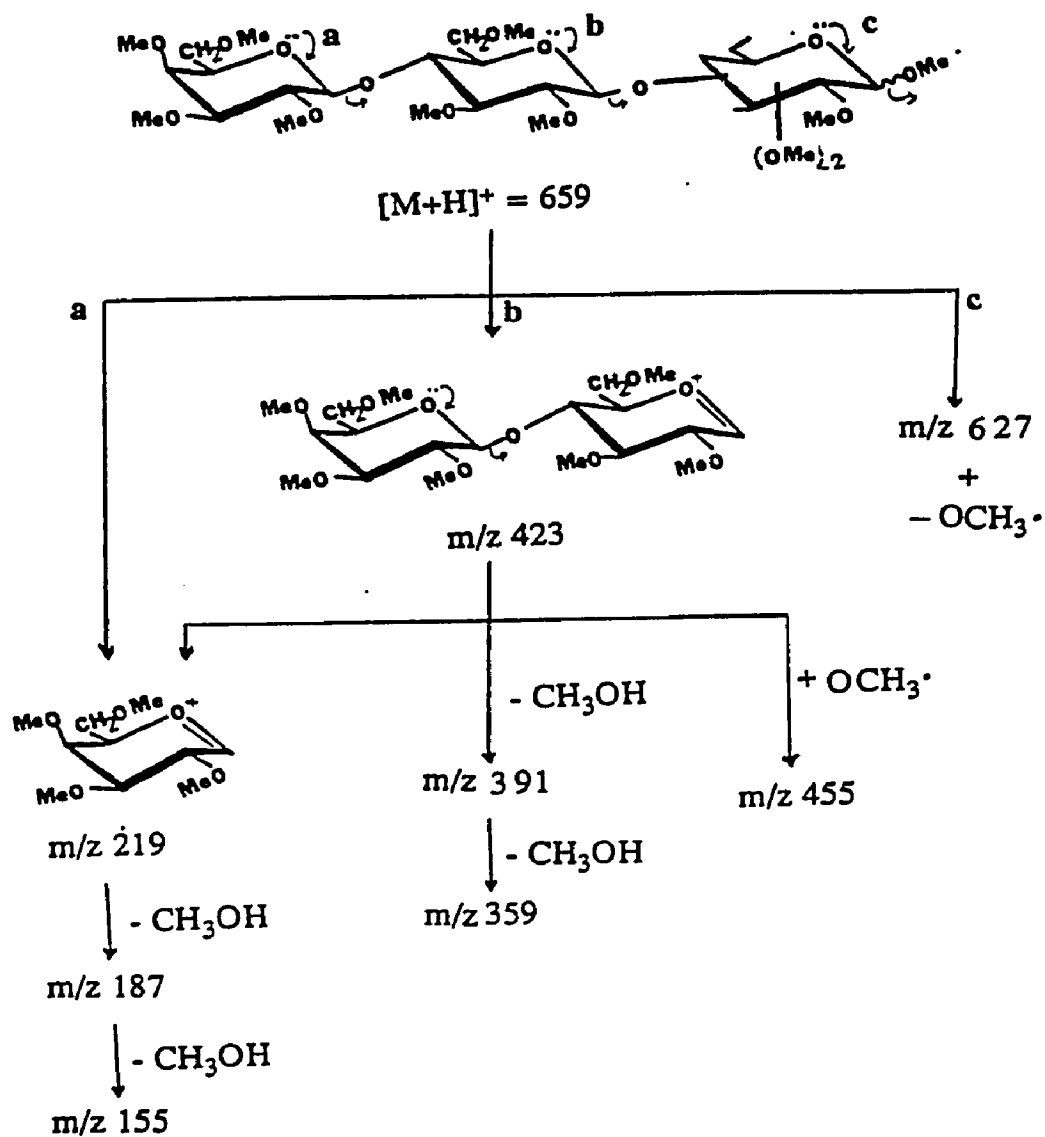


Fig.4.2 FAB-MS-CAD-MS spectra of m/z 659 for permethylated Gal<sub>p</sub>(β1-4)Glu<sub>p</sub>(β1-X)Glu<sub>p</sub> at -40eV where X=3 (A), 4(B), or 6(C).



Scheme 4.1 Possible fragment pathway of permethylated Gal<sub>p</sub>(β1-4)Glu<sub>p</sub>(β1-X)Glu<sub>p</sub> where X=3, 4, or 6.

methylated G6 (Figs. 4.1 and 4.2). The ratios  $m/z$  423/455 were switched when comparing methylated G3 and methylated G4 at several levels of collision offsets. The  $m/z$  455 also appeared from FAB MS/MS spectra of permethylated maltotriose and cellotriose (unpublished data).

#### Plot of collision energy vs. parent/daughter ratio

The unique relationship between the collision offset of FAB MS/MS experiment and the linkage position in the permethylated amino-sugar containing oligosaccharides was previously reported [4.2] to be helpful to depict the relative stability of the three different linkage positions. This relationship can be extended to the permethylated, neutral linkage-isomeric trisaccharides.

Figure 4.3 shows the plot of collision offset energy vs. major fragment ion/parent ion ratio. Since larger fragment ions generally reflect more characteristics of the original molecular structure, these ions may be used for identification purpose more readily than smaller fragment ions.

The relative intensity of the molecular ion shows the same linkage-dependent trend as the amino sugar-containing trisaccharides we studied earlier [4.2,4.3]. Methylated G3, the 1- $\rightarrow$ 3 linkage-containing trisaccharide, was cleaved more readily than the 1- $\rightarrow$ 4, or 1- $\rightarrow$ 6 linked trisaccharides, according to the slope across a gradient of collision energy. The ratio of  $m/z$  (219+423+455)/659 showed relative stability among the three linkage positions as follows: methylated G3 > methylated G4 > methylated G6. Our assumption about steric hindrance as a factor in CID-induced cleavage of oligosaccharides may be as important as ionic mechanisms.

Methylated amino sugar containing trisaccharides are good examples for suspecting an ionic effect to the cleavage events due to charge on the N-acetyl

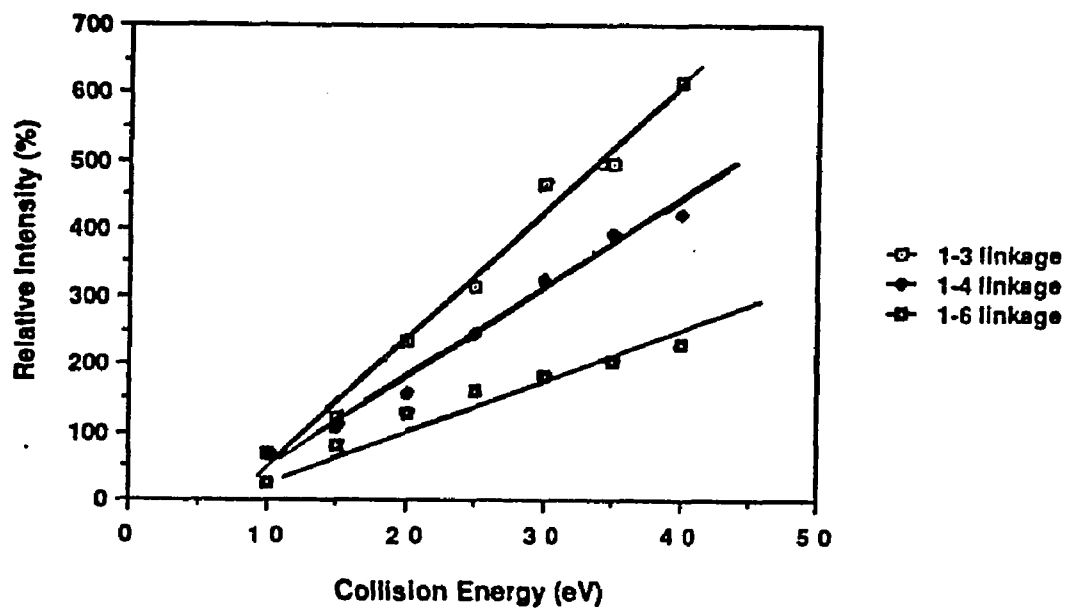


Fig. 4.3 Plot of collision offset vs. ion ratio in  $\text{Gal}_p(\beta 1-4)\text{Glu}_p(\beta 1-X)\text{Glu}_p$  where  $X=3$  (A), 4(B), or 6(C):  $m/z (219+423+455)/659$ .

group. Neutral trisaccharides (G3, G4, and G6), free from a dominant charge center, may provide credence for the effect of steric hindrance on saccharide cleavage events.

#### Molecular calculations

Molecular modeling of the methylated saccharides was performed to rationalize observed FAB MS/MS fragmentation ratios in the gas phase. The minimum energy structures and freedom of motion volumes near these minima were calculated below the bond-breaking energy for the permethylated glu $\beta$ 1- $\rightarrow$ Xglu series (where X=3,4, or 6).

Minimum energy structures were calculated on the basis of thermodynamic considerations that the most stable equilibrium state of a system is the one with the lowest free energy. It is the rationale of a combination of FAB MS/MS and molecular energy calculations that threshold energies imparted to oligosaccharide ions in collision cells of tandem mass spectrometers may give different patterns of fragmentation based on differential ability of isomers to absorb and dissipate vibrational energy [4.2-4.4]. Structures with more freedom of motion would more readily dissipate energy absorbed from collision events due to lowered probability of populating the reaction coordinate for glycosidic bond cleavage. Figure 4.4 shows the 2-D energy maps and 3-D energy wells derived from the MM2 calculations on permethylated neutral molecules. Permethylated G3, the most rigid isomer, generates the smallest volume (1.0), while permethylated G4 generates an intermediate value of 1.2, permethylated G6, being the most stable to collision induced dissociation among the three linkages, generates a much larger well (1.6). Previous comparison [4.2,4.3] of the volumes of rotational freedom for intact and methylated derivatives of aminosugar-containing oligosaccharide, showed much

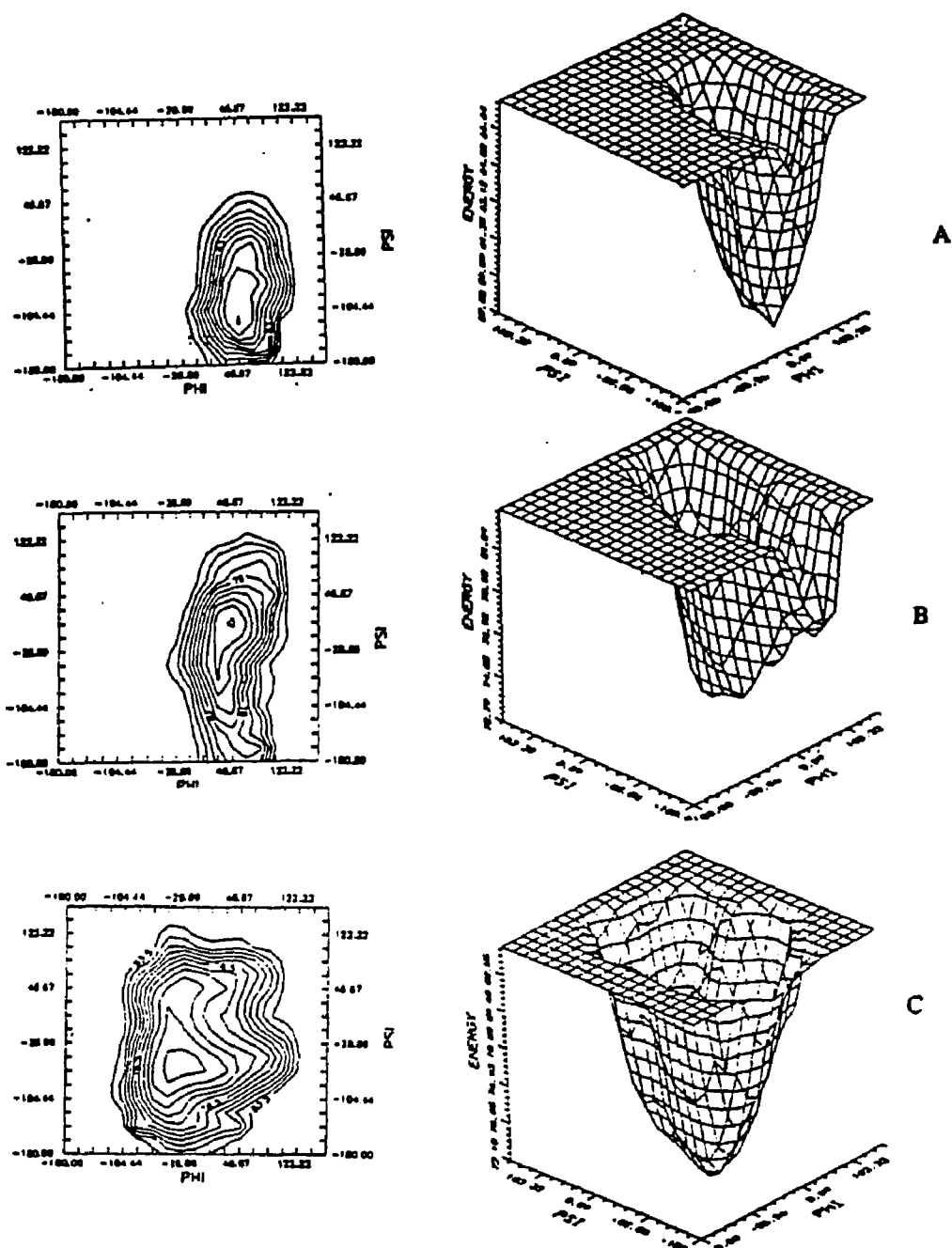


Fig. 4.4 The  $\phi$  and  $\psi$  plots of the total energies and energy wells derived from the MM2(87) calculation of permethylated Gal ( $\beta 1-4$ )Glu ( $\beta 1-X$ )Glu, where  $X=3$  (A), 4(B), or 6(C). (The drawings were made with the SURF program of SURFER from Golden software.)



smaller volumes (about 5 times smaller than intact saccharides) for the latter due to greater steric hindrance caused by the methyl groups. Here, Comparison of the energy well volumes of methylated amino-sugar containing and methylated neutral oligosaccharides, showed smaller volumes for the latter due to greater steric hindrance caused by lone pairs attached to oxygen. This situation is in accord with the FAB MS/MS data that same levels of survival rates of molecular ions (30% in 1->3 linkage, 40% in 1->4 linkage, and 80% in 1->6 linkage) appeared at -60 eV in amino-sugar containing trisaccharides, and -40 eV in neutral trisaccharides.

## References

- 4.1. E. Yoon and R.A. Laine, submitted (1991).
- 4.2. R.A. Laine, E. Yoon E, T.J. Mahier, S.A. Abbas, B. de Lappe, R.K. Jain and K.L. Matta *Biological Mass Spectrometry*, **20**, 505 (1991).
- 4.3. R.A. Laine, K.M. Pamidimukkala, A.D. French, R.W. Hall, S.A. Abbas, R.K. Jain, and K.L. Matta, *J. Am. Chem. Soc.* **110**, 6931 (1988).
- 4.4. R.A. Laine, *Methods in Enzymol.* **179**, 157 (1989).
- 4.5. S.A. Carr, V.N. Reinhold, B.N. Green, and J.R. Hass, *Biomed. Environ. Mass Spectrom.* **12**, 288 (1985).
- 4.6. D. Garozzo, K.M. Giuffrida, G. Impallomeni, A. Ballistreri, and C. Montaudou, *Anal. Chem.* **62**, 279 (1990).
- 4.7. F.W. Crow, K.B. Tomer, J.S. Looker and M.L. Gross, *Anal. Biochem.* **155**, 286 (1986).
- 4.8. E.G. deJong, W. Heerma, J. Haverkamp and J.P. Kamerling, (1979) *Biomed. Mass Spectrom.* **6**, 72.
- 4.9. B.M. Domon, D.R. Mueller, W. Blum, and W.J. Richter, *Org. Mass Spectrom.* **24**, 357 (1989).
- 4.10. D.R. Mueller, B.M. Domon, W. Blum, F. Rashdorf, and W.J. Richter, *Biomed. Environ. Mass Spectrom.* **15**, 441 (1988).
- 4.11. D.R. Mueller, B. Domon, W.J. Richter, *Adv. in Mass Spectrom.* **118**, 1309 (1989).
- 4.12. D.R. Mueller, B. Domon, and W.J. Richter, *Methods in Enzymology*, **193**, 607 (1990).
- 4.13. B.M. Domon, D.R. Mueller, and W.J. Richter, *Biomed. Environ. Mass Spectrom.* **19**, 390 (1990).
- 4.14. J.E. Thomas-Oates, and A. Dell, *Biochem. Soc. Trans.* **17**, 243 (1989).
- 4.15. A. Dell *Adv. Carbohydr. Chem. Biochem.* **45**, 19 (1987).
- 4.16. H. Egge, and J. Peter-Katalinic, *Mass Spectrometry Review* **6**, 331 (1987).
- 4.17. K.-A. Karlsson, *FEBS Lett.* **32**, 317 (1973).

- 4.18. A. Dell, N.H. Carman, P.R. Tillar and J.E. Thomas- Oates, (1988) *Biomed. Environ. Mass Spectrometry*, **16** 19.
- 4.19. C.C.Sweeley and N.A. Nunez, *Annu. Rev. Biochem.* **54**,756 (1985).
- 4.20. A. Kobata, K. Yamashita and S. Takasaki, *Methods in Enzymol.***138**, 884 (1987).
- 4.21. N.K. Kochekov and O.S. Chizhov, *Adv. Carbohydr. Chem. Biochem.* **21**, 39 (1966).
- 4.22. J. Karkkainen, *Carbohydr. Res.* **17**, 1 (1971).
- 4.23 E.G. deJong, W. Heerma and C.A. Sicherer, (1979) *Biomed. Mass Spectrometry* **6**, 242.
- 4.24. E.G. deJong, W. Heerma, Dijkstra (1980) *Biomed. Mass Spectrom.* **7** 127.
- 4.25. W.T. Wang, N.C. LeDomne, Jr.B. Ackerman and C.C. Sweeley, *Anal. Biochem.* **141**, 366 (1984).
- 4.26. G.R. Her, S. Santikarn, V.N. Reinhold and J.C. Williams, *J. Carbohydr. Chem.* **6**, 129 (1987).
- 4.27. B.L. Gillece-Castro, S.J. Fisher, A.L. Tarentino, D.L. Peterson and A.L. Burlingame, *Arch. Biochem. Biophys.* **256**,194 (1987).
- 4.28. A. Dell, J.E. Oates, H.R. Morris, H. Egge, *Int. J. Mass Spectrom. Ion Phys.*, **465**, 415 (1983).
- 4.29. E.A. Nothnagel, M. McNeil, P. Albersheim and A. Dell, *Plant Physiol.* **71**, 916 (1983).
- 4.30. I. Ciucanu, and F. Kerek, *Carbohydr. Res.* **131**, 209 (1984).
- 4.31. J.R.J. Pare, K. Jankowski and J.W. ApSimon, *Advances in Heterocyclic Chemistry*, **42**, 335 (1987).
- 4.32. G.W. Small and M.K. McIntyre, *Anal. Chem.***61**,666 (1989).

### **Future Work**

This dissertation introduces the simplified method of identification of the linkage position of carbohydrates using FAB-MS-CID-MS combined with molecular modeling. Also, a faster way for synthesis of a series of trisaccharides was reported.

Although the link between the FAB-MS-CID-MS and molecular modeling was a worthwhile approach to distinguish linkage position of carbohydrates, it needs further work to apply this study to biologically active glycoconjugates. Some specific linkages such as 1->3 linkage between HexNAc and Hexose (Chapter 2) and 1->6 linkage between Hexose and Hexose (Chapter 4) gave diagnostic signals which could be used directly to identify these linkage positions. While other linkages could be determined using survival rates of molecular ions or major fragment ions at each collision energy level. In order to apply this method to the biologically active components, general criteria for linkage determination are required at optimized conditions of derivatization, ionization and collision.

It will be possible by creating a database with a number of sets of synthetic isomeric oligosaccharides. The enzyme-assisted synthetic method mentioned in Chapter 2 will accelerate the synthesis of test isomeric oligosaccharides to form a database.

In Chapter 3, four novel trisaccharides were synthesized using lactose synthase-assistance. In order to synthesize a series of linkage isomeric trisaccharides using loose acceptor specificity of lactose synthase, several substrates (laminaribiose, cellobiose and gentiobiose as  $\beta$ -linkage-containing substrates and nigerose, maltose and isomaltose as  $\alpha$ -linkage-containing substrates) as well as conditions by varying

the pH (pH 5.0, 6.0, 7.0, 8.4 and 9.0), temperature (30°C, 37°C and 50 °C), incubation time (1 hr, 3 hr, 1 day, 3 days and 4 days) and in the presence or on the absence of  $\alpha$ -lactoalbumin.

After trying several combination of above conditions, four novel compounds were obtained from the substrates, laminaribiose, cellobiose, gentiobiose and maltose at pH 6.0, 37°, 3 days incubation and in the presence of  $\alpha$ -lactoalbumin. The pH condition was the key factor to obtain these trisaccharides. No trisaccharide was obtained at any other pH levels except pH 6.0. At pH 6.0, other conditions such as temperature, incubation time and  $\alpha$ -lactoalbumin, influenced the amounts of products.

The four novel compounds resulting from the enzyme synthesis were used as models (Chapter 4) to determine the linkage positions using FAB-MS-CID-MS. Also these compounds may be interesting acceptors for other transferase to synthesize biologically active trisaccharides such as fuc( $\alpha$ 1->3)glu(X)glu and sialyl( $\alpha$ 2->3)glu(X)glu, where X = X= $\beta$ 1->3,  $\beta$ 1->4,  $\beta$ 1->6 and  $\alpha$ 1->4.

The molecular modeling used in Chapters 2 and 4, is part of a growing body of carbohydrate structural information. Although FAB MS/MS was dealing with protonated or cationized ions, the modeling calculations used in this dissertation were performed on neutral molecules. Drs. A.D. French and N.L. Allinger are considering the further revised version of MM2 program to include charged, or ionized molecules. After inclusion of protonated or charged groups in the molecular modeling, the modeling study will give more clearly predictable FAB MS/MS fragmentation pathways.

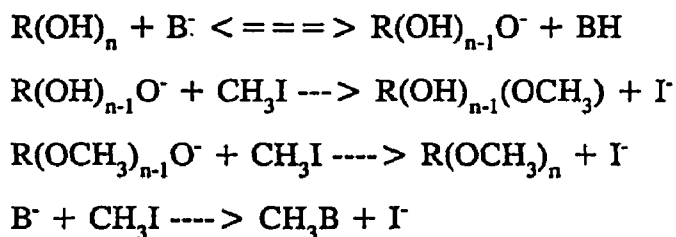
The negative FAB MS/MS of the synthesized set of neutral trisaccharides will be performed to obtain specific fragmentation patterns according to different glycosidic linkage position between glucose containing reducing end and intermediate glucose. The anomeric hydroxyl of reducing end of the oligosaccharide is considered more acidic with respect to the remaining hydroxyl groups in sugar. Thus, once the negative charge is localized at the saccharide reducing end, it may help produce different fragmentation patterns in low-energy FAB MS/MS and distinguish the linkage position between glucose containing reducing end and adjacent glucose.

## Appendix

### Permethylation method of Ciucanu and Kerek

The method [A.1] is rapid and gives high yields (98 +/- 2 %) without the formation of the non-sugar products that are characteristic of the earlier Hakomoli method [A.2].

The methylation of carbohydrates occurs through continuous, base (B)-catalyzed ionization of the hydroxyl groups followed by reaction with the methylating agent such as CH<sub>3</sub>I.



The trisaccharide sample (5 mg) was dissolved in methylsulphoxide (0.5 ml). Then, finely powdered NaOH (20 mg) and methyl iodide (1 ml) were added to the sample solution. Each mixture was stirred (100 r.p.m.) for 6 min in a closed vial at 25°C. Water (1 ml) and chloroform (1 ml) were then added and the chloroform layer was washed with water (3 X 10 ml) and dried under nitrogen gas.

### **Experimental procedure of MM2 calculation [A.3]**

MM2 calculations were performed to rationalize the fragmentation ratio from FAB MS/MS of sample trisaccharides. Calculations were performed in this dissertation without necessity for consideration of solvent effects because the mass spectral experiments were performed in a vacuum.

1. the first step: The first step in the MM2 calculations was determination of the interatomic distances, bond angles and torsional angles in the starting geometry made by SYBYL program.

2. Calculation of an initial steric energy: Then the values obtained were used in the different potential function expressions [A.4] to calculate an initial steric energy, which was simply the sum of various potential energies calculated for all bonds, bond angles, torsional angles, nonbonded pairs of atoms and so forth in the molecule.

3. Optimization: The MM2 program uses a block diagonal Newton-Raphson optimization [A.5]. Once the optimization had converged, the program printed the final steric energy and optimized geometry.

4. Calculation of dihedral driver option:

Procedure 2 and 3 were repeated at each 20° increment of phi and psi torsional angles from -180° to 160°.



**References**

- A.1. I. Ciucanu, and F. Kerek, *Carbohydr. Res.* **131**, 209 (1984).
- A.2. S Hakomori , *J. Biochem. (Tokyo)* **55**, 205 (1964).
- A.3. A.D French, V.H. Tran and S. Perez, *Computer Modeling Carbohydrate Molecules*, 191-212, (ed. by A.D. French and J.W. Brady), American Chemical Society, Washington D.C. (1989).
- A.4. J.-H. Lii and N.L. Allinger, *MM2 Program (QCPE 543)*, University of Georgia (1987).
- A.5. T. Clark, *A Handbook of Computational Chemistry: A Practical Guide to Chemical Structure and Energy Calculations*. 12-92, John Wiley & Sons (1985).

## Vita

Eunsun Yoo Yoon was born in Inchon, Korea, on May 11, 1960. She was admitted to the Yonsei University, Seoul, Korea, from which she obtained a B.S. degree in Food and Nutrition. She obtained a M.S. degree with emphasis in Nutritional Biochemistry in 1985. She then married Inmo Yoon in January, 1986 and had a daughter, Suhyoung Yoon, in December, 1986. She then came to Louisiana State University to pursue a graduate education in January, 1987. She is a member of the Honor Society of Phi Kappa Phi, Phi Lambda Upsilon Honorary Chemistry Society, and is currently a candidate for the degree of Doctor of Philosophy in the Department of Biochemistry of Louisiana State University.

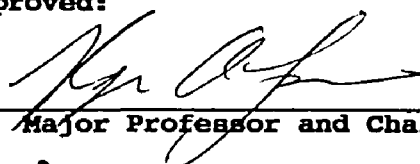
DOCTORAL EXAMINATION AND DISSERTATION REPORT

**Candidate:** Yoon, Eunsun Yoo

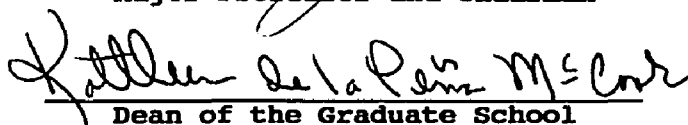
**Major Field:** Biochemistry

**Title of Dissertation:** Structure of Synthetic Oligo-  
saccharides by Tandem Mass Spectrometry

**Approved:**

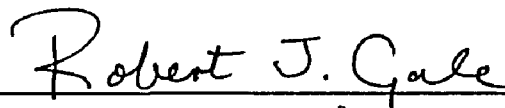


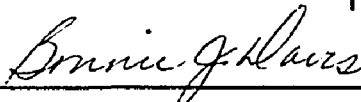
Major Professor and Chairman

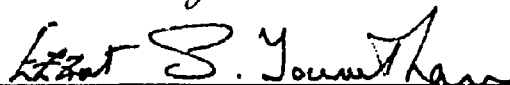


Dean of the Graduate School

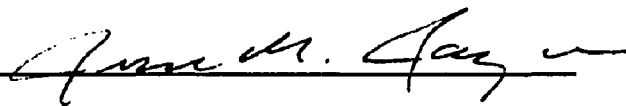
**EXAMINING COMMITTEE:**











**Date of Examination:**

November 7, 1991